1-14-2013 12:00 AM

Change in pore size distribution of compacted soil layers and its effect on solute breakthrough curves

Sara Karimi
The University of Western Ontario

Supervisor
Dr. Ernest Yanful
The University of Western Ontario

Graduate Program in Civil and Environmental Engineering
A thesis submitted in partial fulfillment of the requirements for the degree in Master of Engineering Science

Change in pore size distribution of compacted soil layers and its effect on solute breakthrough curves

(Spine title: Pore size distribution of glass beads-kaolinite mixtures and its effect on sodium and chloride breakthrough curves)

(Thesis format: Monograph)

By

Sara Karimi

Graduate Program in Civil and Environmental Engineering

A thesis submitted in partial fulfillment
of the requirements for the degree of
Master of Engineering Science

THE UNIVERSITY OF WESTERN ONTARIO

School of Graduate and Postdoctoral Studies

CERTIFICATE OF EXAMINATION

Supervisor

Dr. Ernest Yanful

Supervisory Committee

Examiners

Dr. Tim A. Newson

Dr. Abouzar Sadrekarimi

Dr. Amarjeet Bassi

The thesis by

Sara Karimi

entitled:

Change in pore size distribution of compacted soil layers and its effect on solute breakthrough curves

is accepted in partial fulfillment of the

requirements for the degree of

Master of Engineering Science

Date_____

Chair of the Thesis Examination Board

Abstract

It is often useful to predict contaminant migration from waste containment systems, such as landfills, as part of the assessment of the overall impact of such systems on the receptor environment. In many instances, material properties, for example, those of the liner, are assumed to be constant. This study was conducted to evaluate the accuracy of considering constant material and transport parameters in the modelling of sodium and chloride breakthrough curves through a compacted soil layer using the commercial software, Pollute v.7. Experiments were conducted with three different mixtures of glass beads and varying amounts of kaolinite (30, 40 and 50% by weight). The base line hydraulic conductivity K of the samples was established using distilled water as permeant. The observed values of K were $8.2X10^{-11}$ m/s, $1.28X10^{-10}$ m/s and $1.48X10^{-10}$ m/s for the 30, 40 and 50% kaolinite, respectively. These values did not change when the permeant was changed from distilled water to 0.04 M NaCl Effective diffusion coefficient of 3.5-8.5 x 10^{-10} m^2/s was obtained for sodium and 1.9-4 x 10^{-10} m^2/s for chloride. These results also showed that diffusion of both ions in the soils was affected by the percentage of clay fraction. The greater the amount of clay, the lower the diffusion coefficient obtained. Moreover, the diffusion coefficient of sodium was approximately two times that of chloride and this trend was visually apparent from the shape of the breakthrough curves for Na^+ and Cl^-. Modelling with constant porosity overestimated the concentration of both ions. The pore size distribution of each mixture was determined from mercury intrusion porosimetry testing before and after hydraulic conductivity test. The results showed a decrease of 24%, 13% and 12% in the porosity of the 30, 40 and 50% kaolinite mixture. Sensitivity analysis carried out by decreasing the porosity of the mixture by these percentages did not alter breakthrough curves noticeably. On the other hand, sensitivity analysis based on changes in the distribution coefficient and diffusion coefficient showed a considerable change in model outputs. It was concluded that although the porosity changed during hydraulic conductivity test, it did not eliminate the discrepancy between experimental results and modelling results, In fact, the model was found to be more sensitive to change in diffusion coefficient and distribution coefficient. Therefore, more studies are required to monitor these parameters during hydraulic conductivity testing.

Keywords: diffusion coefficient, distribution coefficient, porosity, breakthrough curve, pore size distribution, mercury intrusion porosimetry

Acknowledgement

I owe my deepest gratitude to my supervisor, Dr. Ernest Yanful, for all his support, guidance and encouragement from the initial steps to final levels. This work would not have been possible without his advice and unsurpassed knowledge. I am grateful for his continuous support and encouragement in many respects other than research as well. I am also indebted to laboratory technician, Tim Stephens, for his assistance in almost all the tests. I will never forget how patient and kind he is. I would like to thank other laboratory staff, Wilbert Logan and Melodie Richards, for their help during hydraulic conductivity test.

Very special thanks to administrative staff of civil and environmental engineering department, Whitney Barrett, Stephanie Laurance, Cynthia Quintus and Connie Walters for their kindness and support. I would also like to thank Paul Sheller, procurement Coordinator of engineering store.

Words fail me to express my deepest appreciation to Navid Hatami, for being the best friend ever; he was always a constant source of support and encouragement. He supported me in all and every single step of this work from getting admission from university until submitting this thesis. I will always remember all he did for me. My sincere thanks also go to my friends, Venkateswara Reddy Kandlakuti, Naemeh Naghavi and Behrang Dadfar who were always willing to listen to me, stand by me and help me to overcome the difficulties of this way.

I would like to dedicate this thesis to my parents, my sister and brother and my best friend, Navid. Without their unending support and unconditional love, I could not have completed my graduate study.

Table of Contents

Abstract iii

Acknowledgements iv

List of Tables vii

List of Figures viii

List of Symbols ix

Introduction 1

1.1. Problem Definition 1

1.2. Objectives of Study 4

1.3. Scope of Thesis 4

1.4. Thesis Outline 5

Literature Review 6

2.1. Waste Generation 6

2.2. Waste Management 7

2.3. Modern Landfill 8

2.4. Waste Stabilization 9

2.5. Leachate Generation and Composition 12

2.6. Effects of Leachates 14

2.6.1. Clayey Soil 14

2.6.2. Groundwater 15

2.7. Contaminant Transport Mechanism through a Liner 16

2.8. Contaminant Transport Modelling Approach 18

Materials and Methods 28

3.1. Materials 28

3.2. Methods 28

3.2.1 Cation Exchange Capacity (CEC) 29

3.2.2 Hydraulic Conductivity Test 30

3.2.3 Batch Sorption Tests 37

3.2.4 Diffusion Tests 40

3.2.5 Water Samples Analysis 43

3.2.5.1 Solution Analysis for Cations 43

3.2.5.2 Solution Analysis for Chloride 43

3.2.6 Mercury Porosimetery Test 44

3.2.6.1 Freeze Drying 45
3.2.6.2 Mercury Intrusion 46
3.2.7 Computer Modelling 48
Results and Discussion 54
4.1. Soil Properties 54
4.2. Column Diffusion Test 58
4.3. Batch Sorption Studies 58
4.4. Hydraulic Conductivity 62
4.5. Effluent pH 70
4.6. Effluent Electrical Conductivity 70
4.7. Solute Breakthrough Curves 73
4.8. Mercury Porosimetry Analysis 78
Conclusion and Recommendations 85
5.1. Conclusion 85
5.2. Recommendations for Future Studies 86
References 87
Appendix A 95
Appendix B 99

List of Tables

Table 2.1: Range of concentration of Basic Parameters in MSW Landfill Leachate 22
Table 2.2: Heavy metals concentration in landfill leachate (Adopted from Renou 2008) 24
Table 2.3: Landfill leachate classification based on age (Adopted from Renou 2008) 24
Table 2.4: Selected leachate flow and transport models ithin landfills 25

Table 3.1: Physical Data of Glass Beads 52
Table 3.2: Chemical Composition/Heavy Metal Content of Glass Beads 53
Table 3.3: Sodium Chloride Specifications 53

Table 4.1: Physical properties of glass beads-kaoline mixtures used in study 55
Table 4.2: Chemical Properties of soils in this study 57
Table 4.3: Distribution coefficient, diffusion coefficient and retardation factor of solutes 60
Table 4.4: Soil Samples Properties in Hydraulic conductivity Test 64

List of Figures

Figure 2.1: Composition of solid waste in different countries (OECD 2008) 20
Figure 2.2: Different methods contribution to municipal solid waste disposal in different countries 21
Figure 2.3: Typical modern sanitary landfill cross section 21

Figure 3.1: Different part of the fixed-wall hydraulic conductivity cell 49
Figure 3.2: Set up of hydraulic conductivity test 49
Figure 3.3: Schematic of hydraulic conductivity cell cross-section 50
Figure 3.4: Schematic of diffusion cell 51
Figure 3.5: Diffusion test set up 51
Figure 3.6: schematic of IC instrumentation 52

Figure 4.1: Atterberg limits for different glass beads-Kaolinite mixtures 56
Figure 4.2: Compaction curves for glass beads-Kaolinite mixtures 56
Figure 4.3: Hydrometer analysis for kaolinite 57
Figure 4.4: Batch equilibrium test results for Sodium 61
Figure 4.5: Batch equilibrium test results for Chloride 61
Figure 4.6: Variation in hydraulic conductivity of G80K20 64
Figure 4.7: Variation in hydraulic conductivity of G70K30 65
Figure 4.8: Variation in hydraulic conductivity of G60K40 66
Figure 4.9: Variation in hydraulic conductivity of G50K50 67
Figure 4.10: Turbidity in G80K20 effluent 68
Figure 4.11: Segregation of kaolinite and glass beads in G80K20 68
Figure 4.12: Settlement versus pore volumes during testing 69
Figure 4.13: pH curves versus net pore volumes 71
Figure 4.14: Variation in relative effluent electrical conductivity during permeation of soils with NaCl .. 72
Figure 4.15: Sodium breakthrough curves 75
Figure 4.16: Chloride breakthrough curves 77
Figure 4.17: Cumulative Intrusion versus Pore size 80
Figure 4.18: Sodium breakthrough curves (Adjusted porosity) 81
Figure 4.19: Sodium Breakthrough Curves (Adjusted Darcy velocity) 84
Figure 4. 20: Sodium breakthrough curves (Sensitivity analysis) 84

List of Symbols

A	Activity of soil
α	Dispersivity
BOD	Biochemical oxygen demand
C	Solute concentration
C_b	Background concentration of species in a soil
C_i	Initial concentration
C_e	Effluent concentration
C_t	Species concentration in the source solution at time t
CEC	Cation exchange capacity
COD	Chemical oxygen demand
D	Coefficient of hydrodynamic dispersion
D_e	Effective diffusion coefficient
D_m	Coefficient of mechanical dispersion
$erfc$	Complementary error function
K_d	Distribution coefficient
M	Molar concentration of a solution
MIP	Mercury intrusion porosimetry
MSW	Municipal solid waste
N_{pv}	Number of pore volumes
ρ	Dry density
PI	Plasticity index
pH	Log_{10}(Hydrogen ion concentration)
q	Darcy velocity
R	Retardation factor of contaminant species
S_0	Dissolution degree

Chapter1

Introduction

1.1. Problem Definition

Our society consumes and discards a diverse range of materials in the course of a wide range of activities. The processes of accelerated population growth and urbanization translate into a greater volume of wastes generated since urban population tends to have higher incomes, so there will be higher rate of goods consumption and eventually higher generation of waste compared to rural populations (OECD 2004).

In the past the waste used to be disposed of by dumping in uncontrolled landfills which had adverse impact on local environment and human health. These damages include methane production and greenhouse gas emission through anaerobic decaying of waste which can reach explosive concentration and release to the atmosphere, leading to global warming problems and threat to human health. Landfill leachate generation is another environmental hazard. Leachate may form from moisture within the landfill itself, but the main source of landfill leachate is natural precipitation, which filters down through the landfill and aids bacteria in the decomposition process. Depending on what is in the landfill, this liquid (leachate) can carry with it metals, alkaline, acid and organic materials and may be dangerously toxic. In the past, this contaminated water was not well managed and was allowed to leak into the adjacent environments and threatened groundwater and surface streams, making water supplies unsafe for human and wildlife. Some of these older sites are still in use and are sources of pollution.

However currently the 3Rs concept – Reduce, Reuse, and Recycle – are being employed in municipal solid waste management, but there are often still residual materials left over requiring

treatment or disposal. Internationally, about 70% of MSW is disposed of in landfills (OECD, 2001; Zacarias-Farah and Geyer-Allely, 2003). At this point, it is important to minimize the human health and environmental effects by managing waste in an environmentally sound manner. Sanitary landfilling is a preferred management option for the disposal of solid urban waste. The use of sanitary landfills is widely accepted in many parts of the world because based on comparative studies completed in some countries; it is the most economical option among the various alternative disposal methods (Lema et al., 1988). Moreover, sanitary landfills allow decomposition of most solid wastes under more or less controlled conditions, until their final transformation into relatively inert, stabilized materials (Tatsi et al., 2002). Modern landfills are often designed to prevent liquid from leaching out and entering the environment. In addition, many new landfills collect harmful landfill gas emissions and convert them to energy (USEPA 2012). In fact, they are designed and located in a way to minimize both social and environmental impacts. To achieve this goal, a waste containment system which acts as a barrier to the outside environment is required. The top barrier in the containment system is the landfill cover which will not be discussed here as it is outside the scope of this study. The other barrier is the landfill liner located at the base and sides which should have a minimum permeability and thickness, depending on the type of the waste allowed to be deposited in the site. Liners are constructed from natural clay or composite materials that have some important advantages over natural liners (Giroud and Bonaparte 1989; Giroud et al. 1992; Daniel 1993; Rowe et al. 1995; Van Impe 1998). However, the use of these kinds of liners has several problems such as long-term durability and compatibility and sensitivity to stress cracking failure. The other problem is the high cost of geosynthetic materials procurement, especially for most developing countries that

have to import these materials. So, natural clayey soils are more cost-effective but need to be assessed adequately to make sure they are safe.

The compatibility of different types of clayey soil and municipal solid waste has been studied over the past years (Fernandez and Quigley 1985; Rowe et al. 1995; Thorton et al. 2000; Frempong et al. 2008) and there is a large database in the literature about it. Although sanitary landfills help to reduce the adverse impacts of leachate, the long-term performance operation of liners is still matter of concern. As stated in the USEPA Solid Waste Disposal Criteria (August 30, 1988a), the release of contaminants to the environment may be delayed but even the best liner and leachate collection system will eventually fail and the waste will represent a threat as long as it is in the landfill. Hence, future concerns of landfills should be taken into consideration to the greatest possible extent during the design of landfills. Soil and leachate properties, as well as soil-leachate interaction are used for modelling of contaminant transport through landfill liners to evaluate their long-term performance and efficiency. Although there are published data on modelling of solute breakthrough curves from different methods and their comparison with laboratory experiments in the literature, they all assume that soil properties are constant during the life of the landfill and none of them considers variable soil properties over time. The present study was undertaken to fill part of this gap and try to interpret the discrepancy between experimental breakthrough curves and model predictions observed in previous studies (Frempong and Yanful 2006).

1.2. Objectives of Study

As stated above, input data are considered constant during breakthrough curve modelling which may not be true and this assumption may result in underestimation or overestimation of the flux of contaminant that enters the environment in the long term and can considerably affect the landfill design consideration. In this study, the effective porosity as an effective parameter in breakthrough curve modelling is assessed; thus the objectives of study are to:

1) Establish experimental breakthrough curves of sodium and chloride through glass beads samples mixed with different amounts of kaolinite.
2) Model breakthrough curves of sodium and chloride with the commercial software, Pollute7 and compare with the experimental results.
3) Develop the pore size distribution graph versus time during the experiments and assess its effect on discrepancy between the experiment and modelling.
4) Assess the overall accuracy of maintaining constant properties over time during modelling.

1.3. Scope of Thesis

The following tasks were performed in the research:

1) Determination of soil properties before and after permeation with permeant
2) Determination of hydraulic conductivity of soils when permeated with sodium chloride solution
3) Performance of batch sorption and column diffusion tests to determine distribution coefficient and diffusion coefficient
4) Chemical analysis of effluents from permeation experiments

5) Modelling of sodium and chloride breakthrough curves obtained during hydraulic conductivity test

1.4. Thesis Outline

This thesis is divided into five chapters and two appendices. Chapter 1 is an introduction to this study which highlights its necessity and also includes its objectives and scope. Literature relevant to the research is reviewed and summarized in Chapter 2. A review is carried out on waste generation and disposal. Problems arising from landfilling as a common way of disposing of generated municipal solid waste are described and Contaminant transport mechanisms and factors that influence them are also discussed.

Chapter 3 deals with materials and methods adopted in the experiment and covers procedures for batch sorption, column diffusion and hydraulic conductivity tests and pore size distribution determination. The experimental results analysis, details of breakthrough curves modelling using Pollute7 and their comparison with experimental results are discussed in chapter 4. Chapter 5 (last chapter) presents the study conclusion and recommendations for future studies.

Chapter 2

Literature Review

2.1. Waste Generation

Municipal solid waste, commonly known as trash or garbage, is defined as material thrown away as unusable which originate from agricultural, commercial, domestic, industrial and institutional solid wastes (Ramachandra, 2009). As shown in Figure 2.1, waste composition varies widely in various regions and countries as it is very dependent on local condition such as socio-economic factors, geographic location and climate, level of industrialisation and also on method of reporting, classification and degree of recycling (OECD 2008). The global generated waste is about 1636 million tonnes per year and it continues to rise (OECD 2008; UNEP 2004) which can be partly related to changing patterns of consumption and population increase. In this regard, high-income countries also have higher waste production per capita compared to poorer countries. Lacoste and Chalmin (2006) showed that the United States of America generated the highest quantity of waste per capita among all western countries in 2004. This volume of waste is a major challenge for any society and proper management, which includes collection, transport, treatment and disposal, is required to handle it. Proper management is also important because It is also crucial as it reduces public safety risks, contributes to sustained economic activity, and enhances public welfare (United Nations Publication, 2011).

2.2. Waste Management

Nowadays, solid waste management is focused on developing environmentally sound methods of getting rid of trash. For example, solid waste is no longer dumped into oceans or in unlined landfills as it used to be the case. The main operating philosophy in most existing waste management programs is waste reduction, reusing, recycling and safe disposal (Fifth Environmental Action Programme, 1993-2000); however, management practices can differ for developed and developing countries and they also depend on waste composition. Figure 2.2 shows the contribution of different waste management methods in some countries around the world (European Commission 1997-2010; EPA 2009).

Waste reduction is defined as any process or techniques that result in preventing or reducing waste at its source (Crittenden and Kolaczkowski 1995) and it is both environmentally and economically beneficial. Reusing a product more than once or reusing it in another application extends its lifespan and therefore reduces the quantity of waste requiring treatment and disposal. So, there will be a saving in raw material and energy costs. Collection, separation, clean-up and processing of waste material to produce a new marketable product is recycling and can be done in the manufacturing process or at the consumer stage. According to OECD 2004, there has been a remarkable increase in the level of recycling throughout the world. Although these 3Rs have reduced the amount of waste, there are still some residuals that need to be disposed and the majority of them end up in landfills as a controlled system. Landfills are still widely accepted and used in many parts of the world because of financial advantages (Lema et al. 1988; El-fadel 1997) and suitability for a wide variety of wastes, especially in developing countries that do not have sufficient money to employ new costly methods. In spite of these advantages, sanitary landfill sites are

a source of some environmental concerns, such as greenhouse gas emissions, leaching of toxic compounds and land use pressures. To minimize the side effects of landfills, some regulation in their design and construction is generally imposed and the operation is controlled during the life of the landfill.

2.3. Modern Landfill

Landfills were built without engineering considerations, such as use of liners and leachate collection systems. During this period, the practice was to cover the waste in open dumps with soil to control negative consequences, such as vermin growth and odour. However, there were still two other main complications: first methane gas production through anaerobic decomposition of waste which leads to global warming and, also, the production of toxic leachate that threatened groundwater and surface water resources. Therefore, new standards and regulations for landfills operation were enacted in the United States of America in the 1970s leading to the development of sanitary landfills (United Nations Publication 2011). Modern engineered landfills are designed based on two basic principles, containment and attenuation. The protective lining have a minimum thickness and a maximum permeability in order to prevent leachate leakage and piping at the bottom of the landfill as leachate collection was part of the requirement of the enhanced design elements (Porter, 2002). Further engineering elements included the construction of collection ponds for the leachate treatment to remove pollutants to environmentally acceptable levels, installation of venting tubes to extract generated methane gas and waste burial on a daily basis. More recently, regulations in many countries have required these elements. A cross

section of a typical sanitary landfill is illustrated in Figure 2.3 (Environmentalists Every Day, 2012).

The construction and operational costs of sanitary landfills increased because of all these regulations and caused significant reduction of the total number of landfills in many countries. For example, in the United States the number of landfills reduced from about 20,000 in the early 1970s to barely 2,000 by 1998 (Porter, 2002). The high costs of modern landfills also meant open-dumps remained the main waste-disposal methods in some developing countries. Older landfill sites must be dug up, and a new impermeable liner must be installed, or the material must be moved to another site. However, even if this is done, the damage would have already been done and it may take a long time before the area can fully recover.

2.4. Waste Stabilization

The deposited waste undergoes a series of biological, physical and chemical processes as it decomposes and waste stabilization occurs in the following four phases (Christensen and Kjeldsen, 1995; Bozkurt et al., 2000):

(1) An initial aerobic phase

(2) An anaerobic acid phase

(3) An initial methanogenic phase

(4) A stable methanogenic phase

Also, an additional aerobic phase of decomposition was proposed by Bozkurt et al. (2000). Once the waste is very well decomposed, the diffusion rate of oxygen into the landfill may be

more than the depletion rate of microbial oxygen. Therefore, over time the anaerobic landfill is hypothesized to become an aerobic ecosystem.

During the aerobic phase, the oxygen present in the void space of buried waste is consumed rapidly and this results in carbon dioxide production. This reaction is exothermic and can result in waste temperature of up to 60°C (Farquhar and Rovers 1973). The waste typically is not at field capacity during the aerobic phase (Barlaz and Ham, 1993) and most produced leachate is from released moisture during compaction and also short-circuiting of precipitation through the buried refuse. Field capacity is the maximum moisture content that can be retained without downward percolation. As oxygen is not replenished once the refuse is covered, the aerobic phase lasts a few days. Due to the depletion of oxygen within the landfill, the waste becomes anaerobic and fermentation reactions occur. The major biodegradable constituents of MSW are cellulose and hemicellulose (Barlaz et al., 1989b) and their biodegradation is carried out by three groups of bacteria, these compounds are decomposed to methane and carbon dioxide in landfills under anaerobic conditions (Barlaz et al., 1990; Pohland and Harper, 1986; Bookter and Ham, 1982). In this phase the hydrolytic, fermentative, and acetogenic bacteria dominate and result in carboxylic acids accumulation, and pH decrease. The highest concentration of BOD and COD in the leachate is generally observed during the second phase (Barlaz and Ham, 1993; Reinhart and Grosh, 1998). The reported value for BOD:COD ratio in the acid phase is above 0.4 (Ehrig,1988) or 0.7 (Robinson, 1995). The leachate in this phase is chemically aggressive because of the acidic pH and will increase the solubility of many compounds (Kjeldsen 2002).

The third phase, initial methanogenic phase, starts when measurable amounts of methane are generated. During this phase, the accumulated acids in the previous phase are converted to

methane and carbon dioxide and the methane production rate increases (Christensen and Kjeldsen, 1989, Barlaz et al., 1989a). As acids are consumed, BOD and COD concentrations will decrease and pH will increase. The consumption of carboxylic acids causes a decrease in BOD to COD ratios. Methane production rate reaches its maximum and then drops after as carboxylic acids decrease and because carboxylic acids consumption is as rapid as their production, the BOD:COD ratio generally will fall below 0.1. In theory, after this phase, refuse decomposition will continue until no more degradation occurs and the landfill becomes aerobic.

The progress rate through these phases is dependent on the existing physical, chemical and microbiological conditions within the landfill (Pohland and Harper 1985; Reinhart and Grosh 1998). Some of the factors affecting refuse decomposition have been summarized in earlier studies (Barlaz et al., 1990; Christensen et al., 1992) and moisture content has most consistently been shown to affect the waste decomposition rate. It is generally accepted that refuse decomposition in arid climates progresses much slower than in regions that receive more than 50 to 100 cm of annual infiltration into the waste. As waste burial in landfills takes place over many years, different parts of the landfill can be in different decomposition stages. Therefore, leachate composition can vary throughout a landfill because of a strong relationship between the state of refuse decomposition and its associated leachate properties. An understanding of leachate composition is crucial for predictions of the long-term impacts of landfills (Kjeldsen et al. 2002).

2.5. Leachate Generation and Composition

Leachate is generated when the waste moisture content exceeds its field capacity and the magnitude of gravitational forces exceeds moisture holding forces which are surface tension and capillary pressure (El-Fadel et al. 1997). In leachate formation, soluble compounds which are generally encountered in the refuse at emplacement, or are formed in chemical and biological processes, are removed by the non-uniform and intermittent percolation of water through the refuse mass. Precipitation, irrigation and runoff are the primary sources of percolating water and cause infiltration through the landfill cover. Ground water intrusion, and to a lesser extent, the initial refuse moisture content can be sources of this free water as well and in smaller amount, waste decomposition due to microbial activity may also contribute to leachate formation (Public administration service 1970; El-Fadel et al. 1995). The factors that influence leachate generation can be divided in two groups. Those that contribute landfill moisture directly such as precipitation, irrigation, initial moisture content, groundwater intrusion, recirculation and refuse decomposition and other factors such as waste age, particle size distribution of waste, refuse density, settlement, cover and liner material affect moisture and leachate distribution within the landfill. Leachate generation prediction based on the knowledge of basic hydrological factors has been mathematically modelled. (Lema et al., 1988)

It has been shown that there is a large variation in leachate composition for different landfills and even for different parts of the same landfill (Robinson and Luo, 1991). There is a comprehensive discussion about controlling factors on leachate composition in the literature (Lu et al. 1985, Reinhart 1993, Qasim and Chiang 1994, Britz 1995, Robinson 1995, Reinhart and Grosh 1998 and Blight et al. 1999). Factors that are commonly known to affect

landfill leachate composition are site management and operational procedures such as refuse pre-treatment, irrigation, recirculation and liquid waste disposal; refuse characteristics such as waste age, waste composition and degree of waste stabilization Other factors include internal reactions such as biodegradation, speciation, dissolution, ion exchange, contact time, gas and heat generation and transportation (Hoeks and Harmsen, 1980; Parker and Williams, 1981; Harmen, 1983; Pohland et al., 1983, El-fadel et al. 1997). However, in particular, the leachate composition varies greatly depending on landfill age (Baig et al. 1999). MSW landfill leachate constituents can be divided into four groups:

- Dissolved organic matter, quantified as COD (Chemical Oxygen Demand) or TOC (Total Organic Carbon), volatile fatty acids (that accumulate during the acid phase of the waste stabilization, Christensen and Kjeldsen, 2002) and more refractory compounds such as fulvic-like and humic-like compounds.
- Inorganic macro-components: calcium (Ca^{2+}), magnesium (Mg^{2+}), sodium(Na^{+}), potassium (K^{+}), ammonium (NH_4^{+}), iron (Fe^{2+}), manganese (Mn^{2+}), chloride (Cl^{-}), sulfate (SO_4^{2-}) and bicarbonate (HCO_3^{-}).
- Heavy metals: cadmium (Cd^{2+}), chromium (Cr^{3+}), copper (Cu^{2+}), lead (Pb^{2+}), nickel (Ni^{2+}) and zinc (Zn^{2+}).
- Xenobiotic organic compounds (XOCs) originating from domestic or industrial chemicals and present in relatively low concentrations (usually less than 1 mg/L of individual compounds). Other compounds such as borate, sulfide, arsenate, selenate, barium, lithium, mercury, and cobalt may also be found in leachate at very low concentrations and are only of secondary importance (Kjeldsen et al. 1997).

Basic parameters like COD, BOD, the ratio BOD/COD, pH, suspended solids (SS), ammonium nitrogen (NH3-N), total Kjeldahl nitrogen (TKN) and heavy metals can usually represent the leachate characteristics (Renou et al. 2008). Tables 1 and 2 summarize the range of these parameters in landfill leachate. Although leachate composition may vary widely within four phases of waste evolution, three types of leachates- recent, intermediate and old- have been defined based on landfill age (Table 3, Chian, and DeWalle 1976). Dramatic change occurs in several parameters as the landfill stabilizes. For example, the pH value is low during the acid phase and the concentrations of many compounds are high, specifically easily degradable organic compounds, such as volatile fatty acids. However, in the stable methanogenic phase, the pH increases and the biological oxygen demand measured over 5 days divided by chemical oxygen demand (BOD_5/COD) which reflects the organic carbon degradability is lowered significantly (Ehrig, 1988). Hazardous constituents, such as volatile organic compounds and heavy metals are present in MSW leachate and the release of leachate to the groundwater can pose several risks to human health and to the environment.

2.6. Effects of Leachates

2.6.1. Clayey Soil

Various complex interactions can occur between clay minerals and landfill leachate constituents (Rowe, 1987) which are dependent on physical and chemical properties of both of them. The performance of clayey soils as liners can be affected by these interactions. The processes involved in these interactions include clay mineral transformations, cation exchange, adsorption and desorption. It has been shown that the crystal structure of smectitic

clays collapse and change to that of illite because of cation exchange with leachate constituents (Batchelder et al. 1996, 1997a & b). The illitic clay agglomeration and decrease in double layer thickness lead to an increase in clay hydraulic conductivity up to three orders of magnitude (Quigley et al. 1988). Batchelder et al (1997b) reported that the rate of structural change is dependent on the leachate ionic strength and reaction temperature. Solutions with relatively high ionic concentrations of landfill leachate cause crystals collapse in a few seconds and higher temperature also result in increase in the rate of reactions. Weaker solutions have a slower influence but they still run to completion. However, previously it was assumed that illitic clays did not react with leachates; more recent studies suggest that illitic and kaolinitic clays may also undergo structural changes such as fluctuation and dispersion at a slower pace (Joseph et al. 2001). There is a well-documented study of landfill leachate impacts on clayey soils in the literature (Mitchell 1993; Cancelli et al. 1995; Rowe et al. 1995; Batchelder et al. 1997).

2.6.2. Groundwater

Once leachate is formed and reaches the bottom of landfill it can move through the liner to subsurface formation. Groundwater is a main source of drinking water in many countries and the release of pollutants from landfill leachate poses a risk to groundwater if not controlled adequately (Ikem et al. 2002). Additionally, the contamination can continue to move through the groundwater and finally reach where it discharges (streams, wetlands and lakes) and may lead to loss of aquatic life and change in local ecosystem. Leachate impacts on groundwater continue to raise concern and have been widely investigated (Kjelsen et al., 2002; Ahmed and Sulaiman, 2001; Fatta et al., 1999; Bjerg et al., 1995; Robinson and Gronow, 1992;

Cariera and Masciopinto, 1998; Loizidou and Kapetanios, 1993; Gallorini et al., 1993; Khan et al., 1990; Kunkle and Shade, 1976).

Municipal solid waste leachates contain a wide range of inorganic compounds and also volatile organic compounds (VOCs) at lower concentrations (Rowe, 1998; Foose 1997). It has been shown that the transport of volatile organic compounds generally is more critical than the transport of inorganic compounds (e.g. toxic heavy metals) as VOCs are generally toxic at lower concentrations than many inorganic compounds and they diffuse readily through geomembrane polymers (Park & Nibras, 1993, Park et al., 1996, Brown & Thomas, 1998, Haxo & Lahey, 1988, Mueller et al., 1998, Friedman, 1988, Foose et al., 2001 and Kile et al., 1995). Moreover, the organic compounds and heavy metals may be toxic, corrosive, flammable, reactive and carcinogenic (Slack et al.2005). Accordingly, the liner system is one of the most crucial elements of a modern engineered landfill which should prevent or minimize the migration of contaminants into surrounding soil and groundwater.

2.7. Contaminant Transport Mechanism through a Liner

The movement of contaminants through a porous medium occurs through three mechanisms. Advection is the transportation of dissolved contaminants by flowing groundwater at its average linear velocity and is governed by Darcy's Law, with the Darcy flux, v_a, given by:

$$v_a = -ki \qquad (2.1)$$

Where k is the hydraulic conductivity (permeability coefficient) and i is the hydraulic gradient, which is often controlled by the level of mounded leachate on the landfill liner (Rowe 2005). As the mass of contaminant flows through the medium, the solute spreads due to variation in magnitude and direction of local velocity and this movement away from the

mass because of the deflection is dispersion. The second mechanism, diffusion, is the movement of contaminants from an area of high concentration to one of low concentration and can happen in the absence of any bulk air or water movement. Diffusive transport is generally governed by Fick's laws, with the diffusive flux f given by:

$$f = - Ddc/dz \qquad (2.2)$$

Where D is the diffusion coefficient and dc/dz is the concentration gradient. The apparent contaminant diffusion through a porous media is a complicated process that involves molecular diffusion because of concentration gradient. However, it is also influenced by other parameters such as the complex tortuosity of the porous media, osmotic flow, electrical imbalance, and possible anion exclusion (Rowe et al. 2004). Although early concerns about clay liners focused on their hydraulic conductivity and their ability to limit contaminant migration by advection (Daniel, 1984; Anderson et al., 1985, Fernandez and Quigley, 1988), later research showed that a clay liner with acceptable hydraulic conductivity can be constructed if construction is done carefully. Some previous studies have suggested that municipal solid waste landfill leachate does not influence the hydraulic conductivity of clayey liners detrimentally (Bowders and Daniel, 1987; Yanful et al., 1990; Kim et al., 2001; Berger et al., 2002; Kalbe et al., 2002). It has also been shown that in well-built liner systems, the dominant contaminant transport mode is via diffusion and considering the leakage rate as the only mode of migration may be misleading (Crooks and Quigley, 1984; Shackelford, 1990; Rowe et al., 1995; Kim et al., 2001; Foose et al., 2002; Kalbe et al., 2002). In many practical situations, the one dimensional contaminant transport of a single reactive solute in a porous medium involves solving the following equation by applying appropriate boundary and initial conditions (Rowe et al., 2004):

$$n\frac{\delta c}{\delta t} = nD_e\frac{\delta^2 c}{\delta Z^2} - \rho_d K_d\frac{\delta c}{\delta Z} \qquad (2.3)$$

Where c is the contaminant concentration at depth z and time t, n is the effective porosity, D_e is the effective diffusion coefficient, ρ_d is the dry density, and K_d is the partitioning coefficient. Biodegradation of organic wastes generate heat which can influence the liner temperature and consequently the contaminant transport as both K_d and D_e are dependent on temperature.

In addition, retardation mechanisms that include dilution, sorption, precipitation, volatilization, radioactive and biological decay, may affect contaminant transport through a clay liner. Sorption is defined as contaminant removal from solution by solid matter (e.g. clay particles or organic matter) and can be further divided into adsorption and absorption. The former refers to adhesion of contaminant to the surface of a solid while the latter implies a more or less uniform penetration of the solid by a contaminant. As discharged leachate from landfills is the primary source of the organic and inorganic contaminants release to surrounding environment, an understanding of processes and factors controlling the release and migration of these contaminants in the landfill is essential.

2.8. Contaminant Transport Modelling Approach

Transport mechanisms of contaminants through a liner are individually well understood and can be reasonably modelled in a laboratory but their interactions in a landfill are still not well understood (El-Fadel et al. 1997b) and are associated with a high degree of uncertainty (Bou-Zeid 2004). Numerous studies have been conducted to investigate pollutant mobility through landfill liners (Foose et al., 2002; Kalbe et al., 2002; Baun et al., 2003; Edil, 2003; Lo et al., 2004; Haijian et al., 2009; Chalermtanant et al., 2009; Lu et al., 2011) and the analytical

solution for the transport equation based on the modelled system properties for a wide range of flow and transport problems such as one, two or three dimensional, transient and steady state transport, saturated or non-saturated state in a fractured or non-fractured medium have been developed, however, none of them can simulate these processes in a reasonable degree of scientific certainty because of inadequate field data and, also, because of insufficient understanding of the biochemical transformation and biodegradation processes. Numerical methods based on the finite difference or finite element techniques are commonly used to solve the transport equations, especially for non-homogenous systems with complicated geologic properties; descriptive summary of selected models is presented in Table 2.4.

An inherent assumption in these models is that landfill condition and input parameters remain uniformly constant which is unlikely as landfill undergoes physical, chemical and biological interactions during its operation and after closure (El-Fadel 1997). Developing a comprehensive, integrated model would lead to a better understanding of a landfill environment and consequently a better control of its negative environmental effects can be achieved. Several software packages, such as EnviroScape, Migrate and Multimed for Windows, have been developed which simulate contaminant migration in a porous medium based on properties of leachate and ecosystem. The software used in the current study was Pollute which has been utilized in landfill design and remediation industry for over fifteen years and the designs that can be considered range from simple systems on a natural clayey aquitard to composite liners, multiple barriers and multiple aquifers. This program implements a one and a half dimensional solution to the advection-dispersion equation. Unlike finite element and finite difference formulations, POLLUTEv7 does not require a time-marching procedure, and thus involves relatively little computational effort

while also avoiding the numerical problems of alternate approaches. In addition to advective-dispersive transport, POLLUTEv7 can consider non-linear sorption, radioactive and biological decay, transport through fractures, passive sinks, phase changes and time-varying properties.

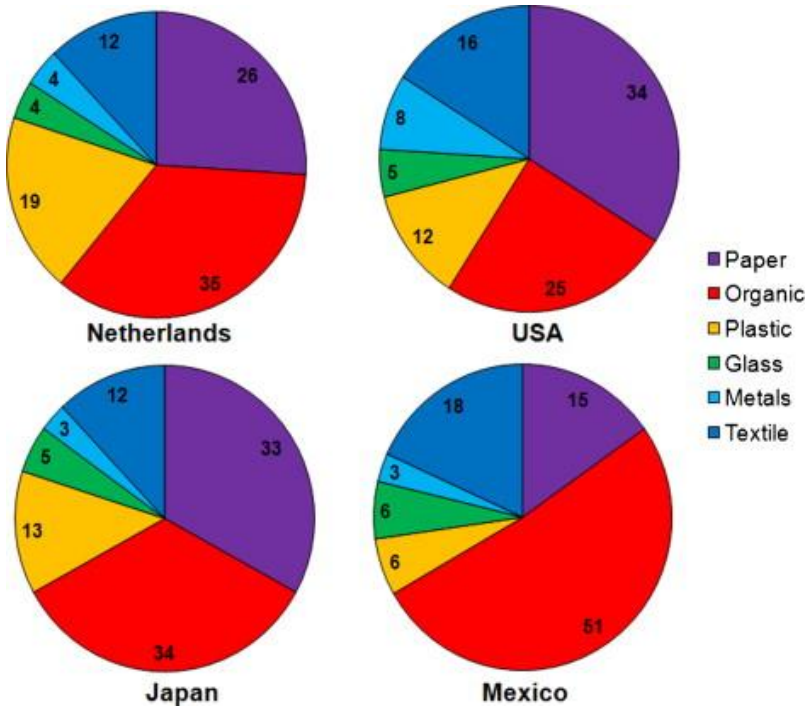

Figure 2.1: Composition of solid waste in different countries (OECD 2008)

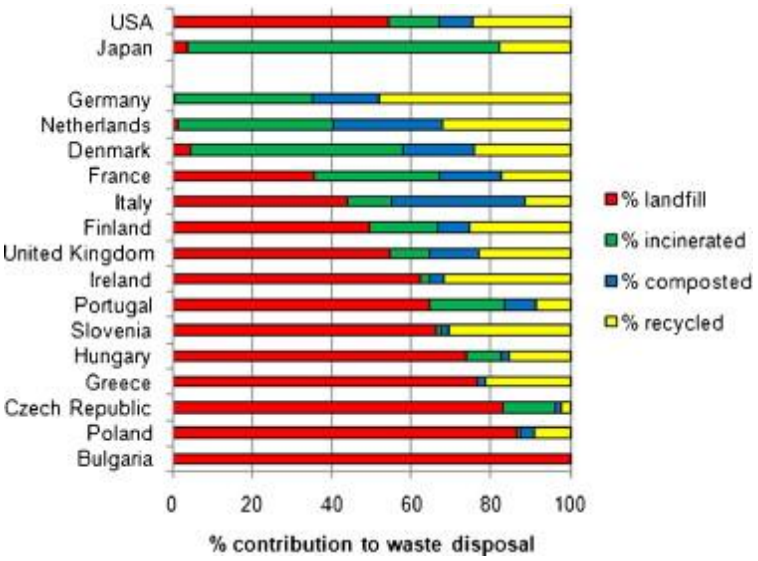

Figure 2.2: Different methods contribution to municipal solid waste disposal in different countries (European commission 1997-2010; EPA 2009).

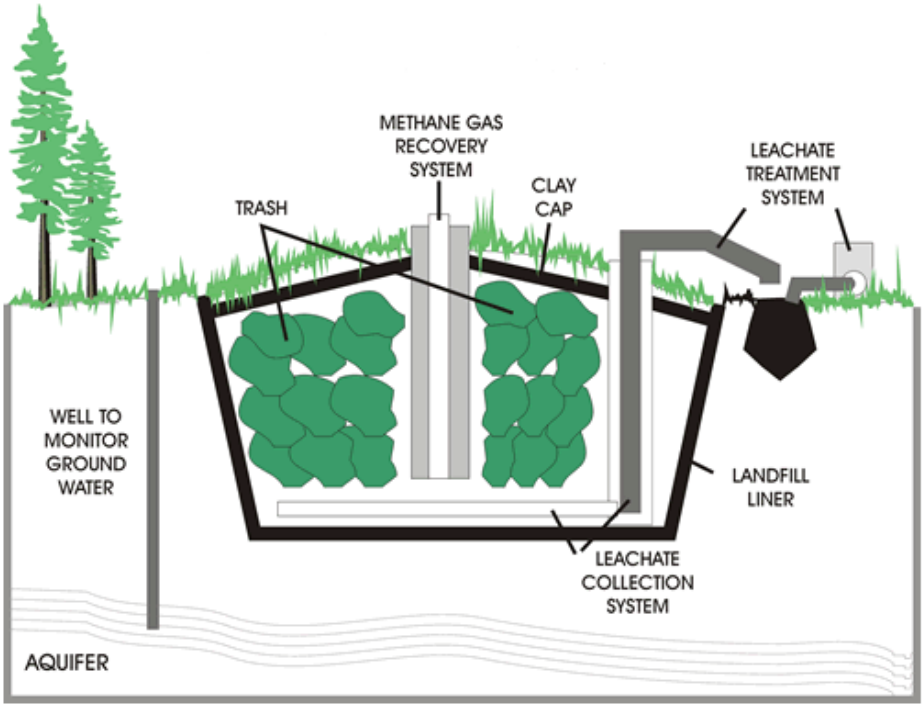

Figure 2.3: Typical modern sanitary landfill cross section

Table 2.1: Range of concentration of Basic parameters in MSW landfill leachate (Adopted from Renou 2008)

Age	Landfill site	COD	BOD	BOD/COD	pH	SS	TKN	NH_3-N	Reference
Y	Canada	13,800	9660	0.7	5.8	–	212	42	Henry et al.1987
Y	Canada	1870	90	0.05	6.58	–	75	10	
Y	China, Hong Kong	15,700	4200	0.27	7.7	–	–	2,260	Lau et al. 2001
Y	China, Hong Kong	17,000	7300	0.43	7.0–8.3	>5000	3,200	3,000	Lo 1996
Y		13,000	5000	0.38	6.8–9.1	2000	11,000	11,000	
Y		50,000	22,000	0.44	7.8–9.0	2000	13,000	13,000	
Y	China, Mainland	1900–3180	3700–8890	0.36–0.51	7.4–8.5	–	–	630–1,800	Wang and Shen 2000
Y	Greece	70,900	26,800	0.38	6.2	950	3,400	3,100	Tatsi et al. 2003
Y	Italy	19,900	4000	0.2	8	–	–	3,917	Palma et al. 2002
Y	Italy	10,540	2300	0.22	8.2	1666	–	5,210	Lopez et al.2004
Y	South Korea	24,400	10,800	0.44	7.3	2400	1,766	1,682	J.-H. Im et al. 2001
Y	Turkey	16,200–20,000	10,800–11,000	0.55–0.67	7.3–7.8	–	–	1,120–2,500	Timur and Ozturk 1999
		35,000–50,000	21,000–25,000	0.5–0.6	5.6–7.0	–	–	2,020	
Y	Turkey	35,000–50,000	21,000–25,000	0.5–0.6	5.6–7.0	2630–3930	2,370	2,020	Ozturk et al. 2003
Y	Turkey	10,750–18,420	6380–9660	0.52–0.59	7.7–8.2	1013–1540	–	1,946–2,002	Ceçen and Aktas 2004
MA	Canada	3210–9190	–	–	6.9–9.0	–	–	–	Kennedy and Lentz 2000
MA	China	5800	430	0.07	7.6	–	–	–	Wang et al. 2002
MA	China, Hong Kong	7439	1436	0.19	8.22	784	–	–	Li and Zhao 2001
MA	Germany	3180	1060	0.33	–	–	1,135	884	Baumgarten and Seyfried 1996

Age	Landfill site	COD	BOD	BOD/COD	pH	SS	TKN	NH_3-N	Reference
MA	Germany	4000	800	0.2	–	–	–	800	Dijk and Roncken 1997
MA	Greece	5350	1050	0.2	7.9	480	1,100	940	Tatsi et al. 2003
MA	Italy	5050	1270	0.25	8.38	–	1,670	1,330	Frascari et al. 2004
MA	Italy	3840	1200	0.31	8	–	–	–	Chianese et al. 1999
MA	Poland	1180	331	0.28	8	–	–	743	Bohdziewicz et al. 2001
MA	Taiwan	6500	500	0.08	8.1	–	–	5,500	Wu et al. 2004
MA	Turkey	9500	–	–	8.15	–	1,450	1,270	Kargi and Pamukoglu 2003
O	Brazil	3460	150	0.04	8.2	–	–	800	Silva et al. 2004
O	Estonia	2170	800	0.37	11.5	–	–	–	Orupold et al. 2000
O	Finland	556	62	0.11	–	–	192	159	Hoilijoki et al. 2000
O	Finland	340–920	84	0.09–0.25	7.1–7.6	–	–	330–560	Marttinen et al. 2002
O	France	500	7.1	0.01	7.5	130	540	430	Trebouet et al. 1999
O	France	100	3	0.03	7.7	13–1480	5–960	0.2	Tabet et al. 2002
O	France	1930	–	–	7	–	–	295	Gourdon et al. 1989
O	Malaysia	1533–2580	48–105	0.03–0.04	7.5–9.4	159–233	–	–	Aziz et al. 2004
O	South Korea	1409	62	0.04	8.57	404	141	1,522	Cho et al. 2002
O	Turkey	10,000	–	–	8.6	1600	1,680	1,590	Uygur and Kargi 2004

Y: young; MA: medium age; O: old; all values except pH and BOD/COD are in mg L^{-1}

Table 2.2: Heavy metals concentration in landfill leachate (Adopted from Renou 2008)

Age	Landfill site	Fe	Mn	Ba	Cu	Al	Si	Reference
Y	Italy	2.7	0.04	–	–	–	–	Lopez et al. 2004
MA	Canada	1.28–4.90	0.028–1.541	0.006–0.164	–	<0.02–0.92	3.72–10.48	Kennedy and Lentz 2000
MA	Hong Kong	3.811	0.182	–	0.12	–	–	Li and Zhao 2001
MA	South Korea	76	16.4	–	0.78	–	–	J.-H. Im et al. 2001
MA	Spain	7.45	0.17	–	0.26	–	–	Rivas et al. 2003
O	Brazil	5.5	0.2	–	0.08	<1	–	Silva et al. 2004
O	France	26	0.13	0.15	0.005–0.04	2	<5	Tabet et al. 2009
O	Malaysia	4.1–19.5	15.5	–	–	–	–	Aziz et al. 2004
O	South Korea	–	0.298	–	0.031	–	–	Cho et al. 2002

Y: young; MA: medium age; O: old; all values are in mg L−1.

Table 2.3: Landfill leachate classification based on age (Adopted from Renou 2008)

	Recent	Intermediate	Old
Age (years)	<5	5–10	>10
pH	6.5	6.5–7.5	>7.5
COD (mg L^{-1})	>10,000	4000–10,000	<4000
BOD_5/COD	>0.3	0.1–0.3	<0.1
Organic compounds	80% volatile fat acids (VFA)	5–30% VFA + humic and fulvic acids	Humic and fulvic acids
Heavy metals	Low–medium		Low
Biodegradability	Important	Medium	Low

Table 2.4: Selected leachate flow and transport models within landfills

Reference	Model Description
Fuller et al. 1979	Adopted an existing analytical solution to predict the movement of Cd, Ni and Zn using parameters from disturbed soil columns and municipal solid waste leachate. The model described the effect of longitudinal diffusion in labarotary columns where, unlike in landfills, chemical and physical parameters are well controlled.
Straub, 1980; Strub and Lynch, 1982	Applied numerical models to water flow and contaminant transport, dissolution and decay in unsaturated sanitary landfills. The model application is limited to simulating the production and removal of organic substrates.
Bernades, 1984	Developed a model describing fixation of heavy metals in the co-disposal of industrial sludge with domestic solid waste. The model suffers from a lack of real values for its inputs parameters.
Korfiatis, 1984 Korfiatis *et al.*, 1984	Analyzed leachate flow through refuse of a laboratory column using the theory of unsaturated flow through porous media. Leachate quality and solute transport were not modelled.
Demetracopoulos *et al.*, 1982, 1984, 1986, 1987	Based on the work of Korfiatis *et al.* and Erdogan, they improved numerical techniques to simulate leachate generation and transport through solid waste landfills. No comparison with actual field data was presented.
Papadopulos, 1988	Developed a mathematical model to simulate the transport of a single chemical species in solid waste to the landfill boundary based on the simultaneous flow of gas and water in unsaturated porous media. Development of this model discontinued prior to complete validation and no results simulating field or laboratory data were reported.
Noble *et al.*, 1989	Developed a one-dimensional finite difference model (FULLFILL) to evaluate moisture transport and distribution in landfills. Experiments were conducted in conjunction with this modelling effort to obtain calibration data.
Lu and Bai, 1991	Developed a mathematical model to simulate leaching from solid waste landfills. The model suffers from need of many parameters that are usually are not readily available at landfill sites. Indeed, a sensitivity analysis showed that at least eight parameters strongly affect the model simulations.
Al-soufi, 1991	Developed a three-dimensional model to simulate water and solute movement through the soil and applied the model at a landfill site. Although the model provides a comprehensive framework to model leachate behaviour in landfills, it suffers from the need of many parameters that are not usually readily available at landfill sites.
Findikakis and Ng, 1991	Combined the HELP model with the three-dimensional ground water flow and transport model, and a tidal circulation model to estimate percolation rates in a landfill, analyze subsurface flow and contaminant transport under the landfill and its immediate vicinity, and simulate the

Reference	Model Description
	transport and dilution of leachate discharge from the landfill in the harbour due to tidal circulation and dispersion. The application of this model is site specific and depends on the estimation of many parameters. It illustrates however, the usefulness of combining existing models to simulate leachate behaviour.
Reinhart *et al.*, 1991	Used the Vadose Zone interactive processes (VIP) model to simulate the fate of organic constituents co-disposed in municipal refuse landfill. Although the model reportedly provided a good fit with column data, its application is limited due to the uncertainty associated with its input parameters, particularly at actual landfill sites.
Krom *et al*., 1991	Applied the model VS2D to help explain observed measurements and simulate the effect of proposed waste disposal solutions. The model does not account for leachate quality.
Vincent *et al.*, 1991	Presented a model to describe the leachate flow, chemical transport and biodegradation in landfills. The model was used to simulate experimental data. The authors recommended the incorporation of additional processes to describe physcio-chemical reactions in landfill. Additional experiment work was being pursued to refine the basic biological and physcio-chemical components of the model
Batchelor, 1992	Developed a numerical model that describes leaching from solidified/stabilized wastes by simulating chemical and physical mechanisms. The model addresses only leachate quality. It does not simulate leachate quantity or moisture routing. The model was applied to simulate data from laboratory leach tests.
Al-Yousfi, 1992	Developed a model (PITTLEACH-2) to simulate leachate quantity and quality, as well as biogas generation, at sanitary landfills. The uncertainty associated with parameter estimation was not addressed.
Ahmed, 1992 Ahmed *et al.*, 1990	Presented two-dimensional unsteady state Flow Investigation for Landfill Leachate (FILL) to describe the leachate flow process in a landfill. Although the model reportedly provided a good simulate with field data, its application is limited to quantifying the amount of the leachate and does not address leachate quality.
Ballestero and de Castro, 1993	Presented a one-dimensional model that simulates the generation of landfill leachate due to large precipitation events. Although the model reportedly provides good predictions of landfill leachate behaviour, the authors recognized the limitations and the difficulty in obtaining the hydraulic properties of the landfill layers. The uncertainty associated with estimating other model parameters was not addressed. Leachate quality was also not simulated in this modelling effort.
Khanbilvardi and Ahmed, 1993; Khanbilvardi et al., 1992, 1995	Compare results obtained by the FILL model with other models; HELP, EPA water-balance model, and Darcy's law. The FILL model reportedly indicated a lower value of leachate outflow compared to the values obtained by the other models. Although the FILL model may better represent the field conditions, it is not clear which model provides better estimates because of the uncertainties associated in its parameters.

Reference	Model Description
	Leachate quality was not addressed in this modelling effort.
Riester, 1994	Presented a numerical model that includes three-dimensional moisture transport coupled with two-dimensional surface runoff and one-dimensional liner flow. The model was used to simulate leachate production and contaminant transport, and gas generations at existing landfills.
Gonullu, 1994	Presented analytical models of organic and inorganic contaminants in leachate. The models were used to simulate experimental data form laboratory columns. The parameters for the analytical solutions were estimated by simulating experimental data. Moisture routing was not modelled.
Piotrowski, J. J., 1995	Developed a two dimensional finite element model to examine the effects of anisotropic conditions on moisture distribution within a landfill. Leachate flow was simulated as unsaturated flow in porous media. The model consistently underestimated peak leachate generation measurements which were attributed to the smoothing of the input precipitation data were conducted to eliminate numerical oscillations.

- Adopted from: : M. El-Fadel, A. N. Findikakis & J. O. Leckie, "Modeling Leachate Generation and Transport in Solid Waste Landfills", , Environmental Technology, 18:7, 669-686 (1997)

Chapter 3

Materials and Methods

3.1. Materials

The tested specimens in this study included different mixtures of glass beads and kaolinite. The glass beads were obtained from Jaygo Incorporated (Union, New Jersey). Approximately 93% of the particles was in the range of 100 to 200 (μm), 5% was larger than 200 μm and 2% smaller than 90 (μm). The bulk density was 1519 (kg/m^3). The physical characteristics and chemical composition of the glass beads provided by the manufacturer are presented in Tables 3.1 and 3.2.

The powdered kaolinite ($Al_2Si_2O_5(OH)_4$) was purchased from Ward's Natural Science Establishment Incorporated (St. Catharines, Ontario). Kaolinite commonly forms as a secondary product of the weathering or hydrothermal alteration of aluminum silicates, particularly feldspar, and it is a main constituent of kaolin. According to the manufacturer, the specific gravity of the kaolinite is 2.6.The as-received product was white with brown or grey staining likely due to the presence of minor impurities.

Sodium chloride which was used to make the sodium chloride solutions was reagent grade a purity of at least 99% and met the American Chemical Society (ACS) specification. Its constituents are presented in Table 3.3.

3.2. Methods

Standard geotechnical methods were used to characterize the samples for water content, particle size distribution, Atterberg limits, specific gravity and compaction parameters (maximum dry

density and optimum water content) according to American Society for Testing and Materials (ASTM). The as-received soluble salt concentrations of glass beads and kaolinite were determined by washing the samples with deionized, dstilled or mega pure water with a 1:100 soil:water ratio.

3.2.1 Cation Exchange Capacity (CEC)

The C.E.C of kaolinite was determined using the potassium and ammonium acetate exchange method. To prepare ammonium acetate solution, 10 g of ammonium acetate was dissolved in 500 mL of mega pure water to give a concentration of approximately 0.12 mol/L. The measured pH of this solution was 7 to 8 which ensured enough ammonium (NH_4^+) existed to displace ions held in the exchange sites. Potassium solution was made by dissolving 9.5 g of potassium chloride in 500 mL of mega pure water to make a 0.12 mol/L solution. For the extraction of exchangeable cations, exactly150 mL of ammonium acetate solution was added to 1.5 g of air-dried soil in a plastic centrifuge bottle. The bottles were then capped and shaken overnight using the wrist-action shaker. After 24 hours of shaking, the bottles were centrifuged at 5000 rpm for 20 mins to separate solid particles from solution. The supernatant was filtered through a 0.45 micron syringe filter into a Nalgene sample bottle for storage and subsequent determination of cation concentration using inductively-coupled plasma-optical emission spectroscopy (ICP-OES). A similar procedure was followed for the extraction of cations by the potassium solution. The following equation was used to calculate the CEC value of the four major cations which are sodium, calcium, potassium and magnesium:

CEC = [(cation concentration in ppm) x (volume of extract g) x 100 g of soil]/[(cation molecular weight/cation valence x 1000) x (soil dry weight in g)] (3.1)

The four calculated values were added together and the soluble salt concentrations were subtracted from this value to determine the exchangeable cation concentrations.

3.2.2 Hydraulic Conductivity Test

There are several variations of hydraulic conductivity test cells available for laboratory testing of soil samples which can be divided into two main categories, rigid-wall permeameters and flexible-wall cells. The advantages and disadvantages of each group are discussed in the literature (Zimmie, 198; Daniel et al. 1986). Rigid-wall cells are easier to use and less expensive than flexible-wall cells but on the other hand it is always possible to have sidewall leakage as a result of reduction in boundary stress and this leakage is difficult to quantify. Therefore an increase in hydraulic conductivity due to side-wall leakage cannot be determined and there will be overestimation in hydraulic conductivity. The flexible-wall permeameter virtually eliminates this problem; it also decreases testing time as fairly rapid saturation of samples is possible by applying back pressure and the saturation of sample can be confirmed by measuring the B value. However, high cost of flexible-wall equipment, complexity of the test and membrane integrity in sample permeation with special chemicals or waste liquid is three main disadvantages of this device. The importance of the project that hydraulic conductivity is desired for, best simulation of field condition, time and budget limitation are some of the factors that must be considered before choosing the appropriate laboratory device.

In the present study, a constant-flow permeameter was used to permeate different mixture of kaolinite and glass beads with three pore volumes of distilled water and subsequently with several pore volumes of sodium chloride solutions. The fixed-wall, constant- flow rate permeameter generates a constant flow rate through all specimens by a triaxial loading frame driving four piston-syringes system containing permeant. The main components of the compression machine are a gear box, a motor and two stainless steel syringes holder. Each syringe has a capacity of 65 mL and can travel at velocities within the range 1.48 x 10^{-2} mL/s to 5.92 x 10^{-6} mL/s. This wide range is possible due to the possibility of selecting different size of gears in two gear locations and controlling the motor speed at each selected position. Prior to the test, an estimate of soil hydraulic conductivity was made according to Kozeny-Carman formula (Carrier W.D., 2003).

$$k = 1.99 * 10^4 \left(\frac{1}{S_0^2}\right)\left[\frac{e^3}{1+e}\right] \qquad [For\ 20°C] \qquad (3.2)$$

Where,

S_0= specific surface area per unit volume of particles (1/cm); and

e= void ratio.

Based on the estimated hydraulic conductivity, the speed of the flow pump motor was selected so that the flow pump could deliver permeant at the desirable flow rate and generate the acceptable head difference. The constant flow rate induces head drop across the sample used along with flow rate and sample area to calculate the hydraulic conductivity of the soil sample according to Darcy's law; this procedure is extensively described by Olsen (1966). Pressure transducers were used to measure the pressure in permeant influent and the effluent pressure was kept at atmospheric pressure. The equipment consisted of eight cylindrical stainless steel moulds with

5.38 cm inner diameter and 7 cm height. To seal the contact between the cylinders and aluminum plates, both ends of the cylinder are machined to contain Viton O-rings. The fluid outlet which is connected to the cell base is for collection of effluent for chemical analysis. There are two ports on the top of the cell, one for fluid inlet which is also used as the pressure transducer mount and the other one for escape of air during filling of the fluid chamber. Appropriate spring and supporting ring assembly are placed on top of the sample to prevent swelling of specimen during permeation. The assembled cell is held together by four threaded and sleeved rods which are attached to the lower stainless steel plate. Filter papers are placed between soil sample and porous stones. A photo of the assembled device showing the various parts of the equipment are illustrated in Figure 3.1 and Figure 3.2, respectively. Figure 3.3 shows a cross-section of the cell assembly.

Four different mixtures were prepared by mixing sufficient air-dried glass beads with different amounts of powdered kaolinite. The samples were named G80K20, G70K30, G60K40, G50K50 while G stands for glass beads and K for kaolinite and the following numbers denote their percentage portion. In accordance with standard procedure for construction of compacted clay liners for waste containment (Shackelford and Redmond, 1995; Steiakakis et al., 2012), each sample was mixed with water to achieve a water content of approximately 2% wet of optimum in order to minimize the hydraulic conductivity and obtain a fairly homogeneous distribution of voids within the material. After wetting and mixing the samples to the desired water content, the soils were placed in double-sealed plastic bags and were allowed to hydrate for several days in order to promote uniform water content before compaction. O-rings were added to the cell body and the cell was placed on a Plexiglas plate, a fine porous stone with 0.2 cm thickness was placed in the cell bottom and a filter paper was added on top of the disk. The hydrated samples

were removed from the plastic bags and compacted in fixed-wall permeameter cells in three equal layers by tamping each layer with 30 blows. According to the test instruction the compaction should be done by Harvard miniature test but the mixture of 20% kaolinite and 80% glass beads was too loose, the foot penetrated through the soil layer resulting in excessive penetration and displacing the soil upward around the spring loaded tamping foot and compaction by this method was impossible. Therefore, hand tamping was used instead.

After compacting the final layer, the thickness of the sample was reduced to approximately 2 cm by trimming the soil with a T-shaped trimmer and the trimming was used to determine the moisture content. A short sample length was desired in order to reduce both testing time and volume changes of sample during permeation. The compacted soil was weighed with the porous stone and filter paper to calculate the degree of saturation, dry density and porosity. Another filter paper was placed on top of the sample and a coarse porous stone was added to it.

The cell base was located on aluminum A frame support and the assembled cell was placed on the base. The compacted soil was then confined under a vertical stress of 42.5 kPa to simulate the static stress on a liner below a landfill with an approximate waste height of 10 m and waste density of 482 kg/m^3. The bulk density of municipal solid waste is highly variable depending on the applied pressure. If a final soil cover is considered, the range of total landfill density can change from about 420 kg/m^3 for a poorly compacted landfill to as high as 1000 kg/m^3 for a landfill where thin layers of waste are compacted (Vesilind et al., 2002). This stress was applied by using two 40mm length spring with 3.0 mm porous stone. The spring constant produces a stress of 2.36 kPa per spring per millimetre of spring compression. To ensure that there will be no air trapped in the cell after tightening the cell top, the cell was filled to the brim with distilled water. A dial gauge was adjusted on the top center of the sample to measure the consolidation

due to the static stress caused by spring-loading device. Dial gauge readings were recorded at specific time intervals to generate a consolidation graph. The cell was left to sit overnight and the final dial gauge reading was taken before starting the permeation. The syringes filled with distilled water were located in the compression machine and the pressure transducers were connected to them. Details of pressure transducers calibration are presented in Appendix A. As air bubbles reduce hydraulic conductivity and cause error in the measured value, they should be completely removed from the syringes and also from the cylindrical cells. By driving the plungers, all attached lines to the syringes bled permeant at the outlet and all the air was expelled. After connecting the lines to the inlet port on top of the cell, the samples were loaded by hand loading until permeant overflowed from the measuring rod port which ensured no air bubble was in the fluid chamber. After finger tightening of the nuts around the measuring rods, the test was started.

Each test specimen was permeated with distilled water for three days in order to obtain the base hydraulic conductivity of each sample and also flush excess soluble salts from the samples in order to minimize background concentration effect on the result. Permeating with distilled water helped to minimize the introduction of additional ions into the soil pore water. After about 3 pore volumes the test was stopped, the solution in the syringes were refilled with 0.04 M sodium chloride solution and then the test was continued.

The imposed flow rate of permeation was 1.18×10^{-4} mL/s for both distilled water and sodium chloride solution. The identical volumetric flow rate for flushing with distilled water minimized the differences between sample properties before NaCl permeation. The produced pressures of this flow rate were lower than the maximum reading of the pressure transducers (600 kPa) while the gradients were high enough to pass a reasonable number of pore volumes of the permeant in

a reasonable time frame. The hydraulic head, hydraulic gradient and hydraulic conductivity were calculated based on following equations.

$$\Delta h_p = \frac{P_u}{\gamma} \qquad (3.3)$$

Where,

Δh_p = Differential pressure head across soil sample

P_u= Differential pressure across soil measured by the pressure transducer which were acquired continuously with GEN2000 Version 1.45, data acquisition and control software for Microsoft Windows (Sciemetric Instruments Inc. 1996).

γ = Unit weight of permeant.

The hydraulic gradient, i, was calculated from the relationship:

$$i = \frac{\Delta h_p}{L} \qquad (3.4)$$

Where,

i = hydraulic gradient; and

L = Length of compacted soil sample.

The pore volumes of permeant passed, PV, during the hydraulic conductivity test was determined as follows:

$$PV = \frac{qt}{V_v} \qquad (3.5)$$

PV = Number of pore volumes of permeant flow;

q = Volumetric flow rate;

t = time of flow; and

V_v = Volume of voids in compacted soil sample

The hydraulic conductivity of the compacted soil sample, k, was computed from the well-known Darcy's law:

$$k = \frac{q}{iA} \quad (3.6)$$

Where,

q = Volumetric flow rate, mL/s;

A = Cross sectional area of the sample (cm^2)

i= Hydraulic gradient;

High-density polyethylene bottles were sealed to the outlet tube of each cell to collect the effluent. These bottles were periodically replaced with new ones to collect effluent for analysis.

During the test room temperature, effluent pH and electrical conductivity were monitored simultaneously to assist in the result interpretation. Room temperature was measured by an OMEGA temperature data logger (OM-EL-USB-1-LCD). The pH of solutions was determined with an Orion Model 410A pH meter with a gel electrode and a HACH conductivity meter (HQ 30d) was used to measure the conductivity of them.

3.2.3 Batch Sorption Tests

Sorption testing may be conducted either as a column test or as a batch operation. In the batch test, a quantity of adsorbent is mixed with a specific amount of solution and the mixture is kept for agitating for a convenient period of time and the separation of the supernant is accomplished by filtering, centrifuging or decanting. In a column test, however, the solution is allowed to percolate through a column of soil, so transient flow takes place and porosity and density of compacted soils are more representative of field conditions. Although column testing is considered to simulate field conditions better; the batch test is usually adopted to determine distribution coefficient of species because of the relatively short time involved in the test procedure (Shackelford 1994).

Different parameters such as soil: solution ratio, the moisture content of the adsorbent, method of mixing, contact time, and the composition and concentration of competitive specimen in the solution can affect the capacity of a soil to adsorb an inorganic specimen from an aqueous solution (Barrow 1978; Barrow and Shaw 1979; Roy et al. 1991).

In the present study, batch sorption test was performed according to the specified procedure in ASTM D4646-03 (2008) to determine the sorption affinity of sodium chloride by unconsolidated kaolinite-glass beads mixtures. This test method allows a rapid index of a geomedium's sorption affinity for given specimen. Duration of this test is 24 hours which is used to make the test convenient and to minimize microbial degradation that can be a problem in longer time procedures. It is believed that this method is useful for all stable and non-volatile inorganic and organic constituents. The distribution coefficient, K_d, is the ratio of the concentration of sodium and chloride sorbed on the soil from the sodium chloride solutions to its concentration in solution. The dissolution degree, S_o, is a measure of the extent to which sodium and chloride

were dissolved from each of the soils by the sodium chloride permeant. Depending on the solute sorption behaviour and geomedia characteristics, dissimilar K_d value smay be obtained when different initial solute concentrations are used and this results in a nonlinear sorption curve but if solute concentrations are sufficiently low or properties of particular solute-sorbent combination result in K_d values independent of the solute concentration, linear sorption curve may be obtained.

Prior to the sorption tests, representative samples of each mixture were air-dried. Four different initial concentrations of sodium chloride, 0.04, 0.03, 0.02 and 0.01 molar, were prepared to see how the distribution coefficient of sodium and chloride changed based on initial solute concentration. Exactly 10 (g) of air-dried soil was placed in 250 mL wide-mouth centrifuge bottles and 200 millilitres of sodium chloride solution was added to obtain a soil: solution ratio of 1:20. The bottles were placed in a wrist-action shaker and agitated continuously for 24 hours at 160 r/min at room temperature (22±5 °C). At the end of shaking, the bottles were removed from the shaker and were centrifuged at 7000 rpm for 20 minutes to separate the solution phase from the solid phase. Sufficient amount of the supernatant from each bottle was filtered through a 0.45- µm pore size filter into high density polyethylene bottle. The bottles were kept in a cold room at 4±2 °C for inductively coupled plasma (ICP) and ion chromatography analysis (IC). Three replicates were prepared for each sample. Samples of blank (solute solution without a geomedium) were taken through all steps to check the initial concentrations of source solutions and to assess the compatibility of this method and the solute of interest.

The distribution coefficient, K_d in mg/L, and dissolution degree, S_0 in mL/g, of each chemical species of interest was calculated as follow:

$$k_d = \frac{(C_i - C_f) * V}{(C_f) * M} \quad (3.7)$$

$$S_0 = \frac{(C_f - C_i) * M}{(C_i) * V} \quad (3.8)$$

Where,

C_i= Initial concentration of species in solution (mg/L);

C_f= Concentration of species in decanted solution at the end of test (mg/L);

V= Volume of solution used (mL); and

M= Mass of soil expressed on an oven-dried basis (g).

As contaminants are percolating through porous media, some of the chemical species in soil have the potential to retard or even immobilize the solutes (Domenico and Schwartz 1998). The retardation factor, a dimensionless number, provides a measure of the capacity of a particular adsorbent to sorb solutes that yield in solute attenuation during contaminant movement,

$$R = 1 + \frac{\rho k_d}{n} \quad (3.9)$$

Where,

R = Retardation factor of contaminant species

ρ = Density of the soil (g/cm3);

n = Porosity of the soil; and

k_d= Distribution coefficient (mL/g).

For non-reactive or non-adsorbing solutes, k_d=0, therefore R=1, while for reactive (adsorbing) solutes, k_d>0, hence R>1. The sorption parameters including distribution coefficient, k_d, and retardation factor, R, for ionic species of interest are used as input parameters for contaminant migration modelling.

3.2.4 Diffusion Tests

Where the hydraulic conductivity of a barrier is very low and (or) the hydraulic gradient is negligible, diffusion which is movement of contaminants from points of high chemical concentration to points of low chemical concentration, is the dominant contaminant transport mechanism. The diffusion coefficient (D) and distribution coefficient become the controlling parameters. These two parameters are generally determined by doing column test in which a source solution containing single salt is placed on top of a soil layer and the source constituents are allowed to migrate through the soil by diffusion. According to Freeze and Cherry (1979), the following one-dimensional equation can be used to predict the diffusive transport of a single solute in a saturated porous medium:

$$\frac{\partial C}{\partial t} = D\frac{\partial^2 C}{\partial z^2} - \frac{\rho K}{n}\frac{\partial C}{\partial z} \qquad (3.10)$$

Where,

C= Solute concentration in depth z (mg/L);

t= Time of flow (s)

z= Distance from contaminant source in direction of flow (m);

K= Distribution coefficient of the solute (mL/g);

ρ= Dry density of the soil (gr/cm^3);

D = Coefficient of hydrodynamic dispersion (m^2/s);

n = Porosity of soil (-)

Hydrodynamic dispersion is due to the combination of mechanical dispersion which is a physical mechanism and effective diffusion as a chemical mechanism.

$$D= D_e+ D_m \qquad (3.11)$$

The mechanical dispersion is a function of seepage velocity and can be expressed by the following equation:

$$D_m= \alpha v \qquad (3.12)$$

Where,

α= Dispersivity (m)

v= Seepage or groundwater velocity (m/s)

Hydraulic conductivity is low in most liners and hydraulic gradient in a diffusion test is also negligible because of the small height of solution on top of the soil liner, so mechanical dispersion can be ignored and the hydrodynamic dispersion is essentially equal to the effective molecular diffusion:

$$D= D_e \qquad (3.13)$$

In this study, the diffusion test was conducted to determine the diffusion coefficient and distribution coefficient of sodium and chloride. The test apparatus used to perform the test were the same cells used in the hydraulic conductivity test. They consisted of cylindrical stainless-steel cells with inside diameter of 5.4 cm and height of 7 cm, which were placed on a stainless-steel base and had a top cap with two ports on it. One port, 6 mm in diameter, was located in the center of the cap and was for holding a stainless steel rod with a triangular paddle attached to it. The rod was attached to a low RPM hobby gear motors which rotated the stirrer at 7 rpm when it was connected to a 12-volt battery. Continuous mixing of the solution at this low speed was in order to maintain a uniform concentration throughout the source reservoir. The other port, 9 mm in diameter, was for interval sampling of 0.1 mL of source solution to monitor solute concentration during the test. This port was closed with a screwed cap except for periodic sampling. A schematic diagram and a photo of whole assembly are shown in Figure 3.4 and Figure 3.5, respectively.

The soil samples were mixed to a water content of 2% above the optimum moisture content and were allowed to cure for 24 hours in sealed plastic bags, and were then compacted in diffusion cells in three layers. They were trimmed to height of 4 cm and a 3 cm height of 0.04 M sodium chloride solution was placed on top of the soil. Prior to the start of the test, the test duration was estimated approximately using POLLUTEv7, a commercial computer program that implements a solution to the one-dimensional advection-dispersion equation (Rowe et al. 1994), along with relevant soil parameters and published values of diffusion coefficient and distribution coefficient of sodium and chloride.

During the test, 0.1 mL of the solutions from different cells were taken by pipette and as this volume was not sufficient for analysis, it was first diluted and stored in high-density

polyethylene bottles. The measured data were corrected for dilution. At the end of the tests, the cells were disassembled and the solution was carefully poured out, and a sample was taken for ion analysis. The samples were extruded and cut to 4 layers of equal thickness. Part of each soil slice was sampled for moisture content determination and the other part was squeezed with a pneumatic porewater squeezer to obtain soil porewater for chemical analysis. Graphs of source solution concentration versus time and pore water concentration versus depth were established from the experimental data. POLLUTEv7 was used to best-fit a theoretical curve to the experimental graphs by and it was done through changing both diffusion coefficient and distribution coefficient while keeping other parameters constant. The combination of diffusion coefficient and distribution coefficient that gave the best fit was chosen as the experimentally determined values for these two parameters.

3.2.5 Water Samples Analysis

3.2.5.1 Solution Analysis for Cations

The concentrations of four major cations including, sodium, calcium, potassium and magnesium in permeants, effluents were measured using Inductively Coupled Plasma Optical Emission Spectrometry (ICP-OES). All the samples were filtered through 0.45 µm Acrodisc syringe filters and where their volumes were not enough for analysis, they were diluted with deionized, distilled water and the dilution factor was considered in calculation.

3.2.5.2 Solution Analysis for Chloride

Chloride (Cl^-), the only anion that was considered in the study, was measured by ion chromatography using a Waters 430 Conductivity detector, Waters IC-Pak A Column and a

Borate/Glauconate eluent. This consisted of stainless steel anion columns that separate and quantify ions at ppb levels. Before starting the analysis, the samples were filtered and then diluted with de-ionized distilled (mega pure) water (18 mega ohm), which was drawn and used in the preparation of standards as well. This was done to minimize accidental contamination. Appropriate sample dilution, prior to injection into the column, was undertaken with fresh mega pure (18 mega ohm) water to prevent the salt precipitation in the column due to the injection of samples with high concentrations of ions. Filtration was undertaken to prevent clogging of the analytical column system or its peripherals and excessive pressure build-up due to the particulates in the samples. The samples were introduced into the IC-Pak A via VISP sample injector. The recommended flow rate of 1.2mL/min was used to inject the samples and the pressure was 2413 kPa, which did not exceed the recommended pressure of 6894 kPa. A schematic of instrumentation of this method is illustrated in Figure 3.6.

3.2.6 Mercury Porosimetery Test

Mercury intrusion porosimetery (MIP) testing was done on specimens before and after the hydraulic conductivity tests to see how the pore distribution changed during the permeation. As it was impossible to perform the pre-hydraulic conductivity MIP test on the main samples, the same procedure described in section 3.2.2 was followed to prepare identical samples. Soil mixtures prepared at 2% above the optimum water content were compacted in conductivity cells and trimmed to obtain a 2-cm thick soil layer. The sample was confined under a vertical stress of 42.5 kPa for 24 hours. After one day, the distilled water was poured out and the sample was carefully extruded from the cell and part of it was taken for porosimetry testing.

3.2.6.1 Freeze Drying

Prior to MIP test, all moisture must be removed from the soil as the soil moisture can produce errors in the pore size measurement since it is incompressible even at the high pressures applied for mercury porosimetry. One of the requirements for mercury porosimetry is a constant volume drying process. Among air-drying, oven-drying and freeze-drying procedures, freeze drying is the best practical method as it causes the least amount of soil shrinkage and minimizes the soil structure disturbance (Zimmie and Almaleh, 1976). Vacuum freeze drying, which includes rapid freezing of specimen and subsequent application of vacuum, removes the moisture by the process of sublimation and elimination of the surface tension forces caused by air-water menisci.

Wet soil samples were cut into 1 cm cubes and were placed in a special cage consisting of stainless steel wire and aluminum screen. Three cubes of each mixture were prepared because of possible problems with sample cracking during freeze drying. To avoid formation of ice crystals that can disturb the soil structure, the samples should freeze rapidly at a temperature below -130 °C (Gillott 1969). Liquefied gases, usually liquid nitrogen, must be used to attain the low temperature. A Dewar flask, suitable for cryogenic liquids, was filled with the liquid nitrogen provided from Physics Department at the University and was placed under a fume hood. If the samples are placed in nitrogen directly, bubbling may occur as a result of heat transfer; hence the samples become surrounded by a thermally insulating layer of gas and the freezing process may be retarded. Samples can be immersed directly in an intermediate cooling liquid like iso-pentane cooled by liquid nitrogen (Rowe, 1960). Therefore, another appropriate container was immersed in liquid nitrogen to be cooled. The container was filled with pentane to about 3/4 full and was re-immersed in liquid nitrogen. Once the pentane was cooled, the sample holder assembly was placed in it for about one minute and it was continuously moved during immersion to prevent it

from freezing to the pentane container. After freezing, the samples were quickly placed in a vacuum desiccator and the desiccator was attached to a vacuum pump for 24 hours. After disconnecting the desiccator from pump, the samples were removed and were stored in small glass jars containing a few grams of silica gel desiccant in the bottom to prevent them from absorbing moisture from air.

3.2.6.2 Mercury Intrusion

The mercury porosimery test was performed with AutoPore IV 9500 Mercury Porosimeter, a 227527 kPa a porosimeter, which covers the pore diameter range from approximately 360 to 0.005 µm and has four built-in low-pressure ports and two high-pressure chambers.

Prior to analyzing the samples, the freeze-dried samples were weighed and then loaded in the appropriate penetrometer. To start the test, a sample information file including sample information, analysis conditions and penetrometer properties was created using the relevant software. The loaded penetrometer was installed in the low pressure port. The first phase of low pressure analysis is the gas evacuation from the penetrometer and after that the penetrometer is backfilled automatically with mercury. The second phase of low-pressure analysis is data collection at pressures up to 345 kPa. The pore diameter in this stage is in range of 360 to 3.6 µm. Once the low pressure analysis is complete, the penetrometer is removed from the low pressure port and is installed in a high pressure port which collects the data at pressures up to 227527 kPa.

The volume of mercury which remains in the penetrometer is used in the calculation of pore volume. This volume is measured by the determination of the penetrometer's electrical

capacitance which changes with length of mercury in the penetrometer. First, the penetrometer is full of mercury because of initial backfill but mercury moves into the sample's pores as pressure increases and vacates the stem (intrusion), in fact intrusion of different size pores occurs at different pressures, the smaller the pore, the greater pressure is required to move mercury in it. The decrease of mercury length in the stem of the penetrometer causes reduction in the penetrometer's capacitance reduction. Auto Pore IV software converts the measurements of penetrometer's capacitance to intruded volume of mercury. The basis of mercury porosimetry is capillary law, governing liquid penetration into small pores, which is expressed by the Washburn equation. As mercury has high surface tension and is also non-wetting to most materials, this equation can be used to calculate the pore diameter into which mercury intrudes at a given pressure.

$$D = -\left(\frac{1}{P}\right) 4\gamma \cos\varphi \qquad (3.14)$$

Where,

D= Pore diameter;

P= Applied pressure;

ɣ= Surface tension;

φ= Contact angel

The value of surface tension of mercury which was used in this experiment is 485 dynes/cm, however in general it varies with purity. In the present study, the contact angle between mercury and soil pore was considered to be 130 degrees.

3.2.7 Computer Modelling

The hydraulic conductivity testing was modelled by Pollute v.7 which provides a solution to the advection–dispersion equation for solutes:

$$\frac{\partial C}{\partial t} = \frac{D_e}{R}\frac{\partial^2 C}{\partial z^2} - \frac{v_s}{R}\frac{\partial C}{\partial z} \qquad (3.15)$$

The top boundary condition in the hydraulic conductivity test was modelled as a constant concentration and the bottom boundary was modelled as fixed outflow velocity, since the sample was placed on a porous stone as a permeable layer (aquifer) with a fixed outflow velocity. The other software inputs were:

1. Darcy velocity;
2. One 0.02m- thick soil layer with 4 soil sub-layers;
3. Soil porosity and dry density;
4. Initial trial effective diffusion and dispersion coefficients for sodium and chloride, subsequently varied until the best value for the experimental data was obtained;
5. Constant concentration in the source solution;
6. Base outflow velocity;
7. Background concentration throughout the sample thickness for the solute of interest; and
8. Depth and time of interest at which solute concentrations were required.

Figure 3.1: Different part of the fixed-wall hydraulic conductivity cell

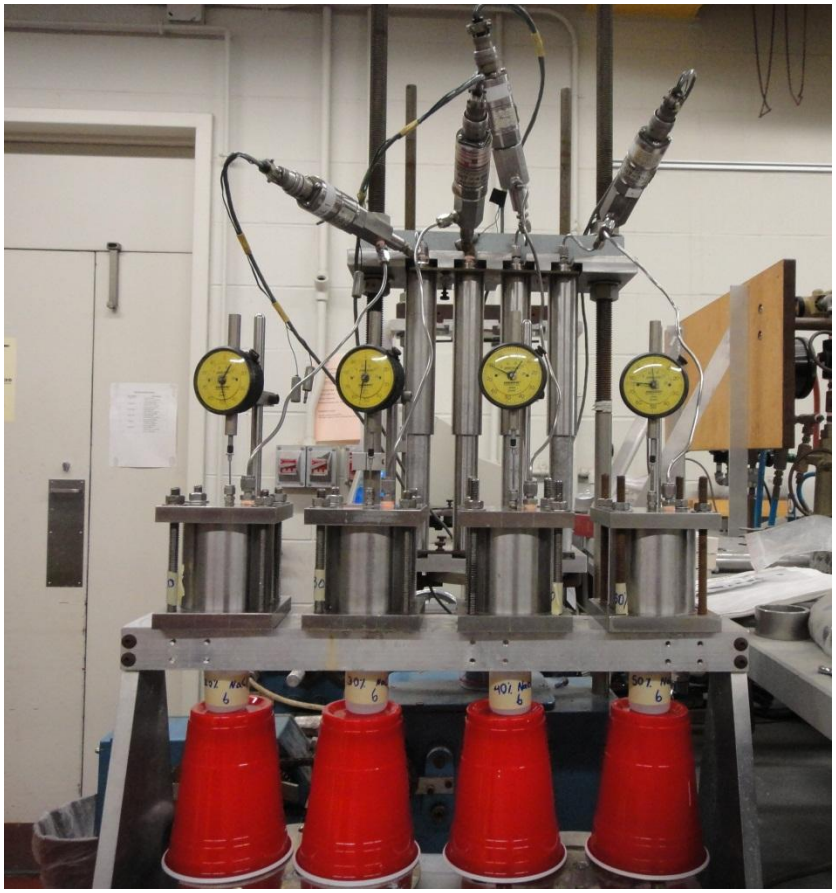

Figure 3.2: Set up of hydraulic conductivity test

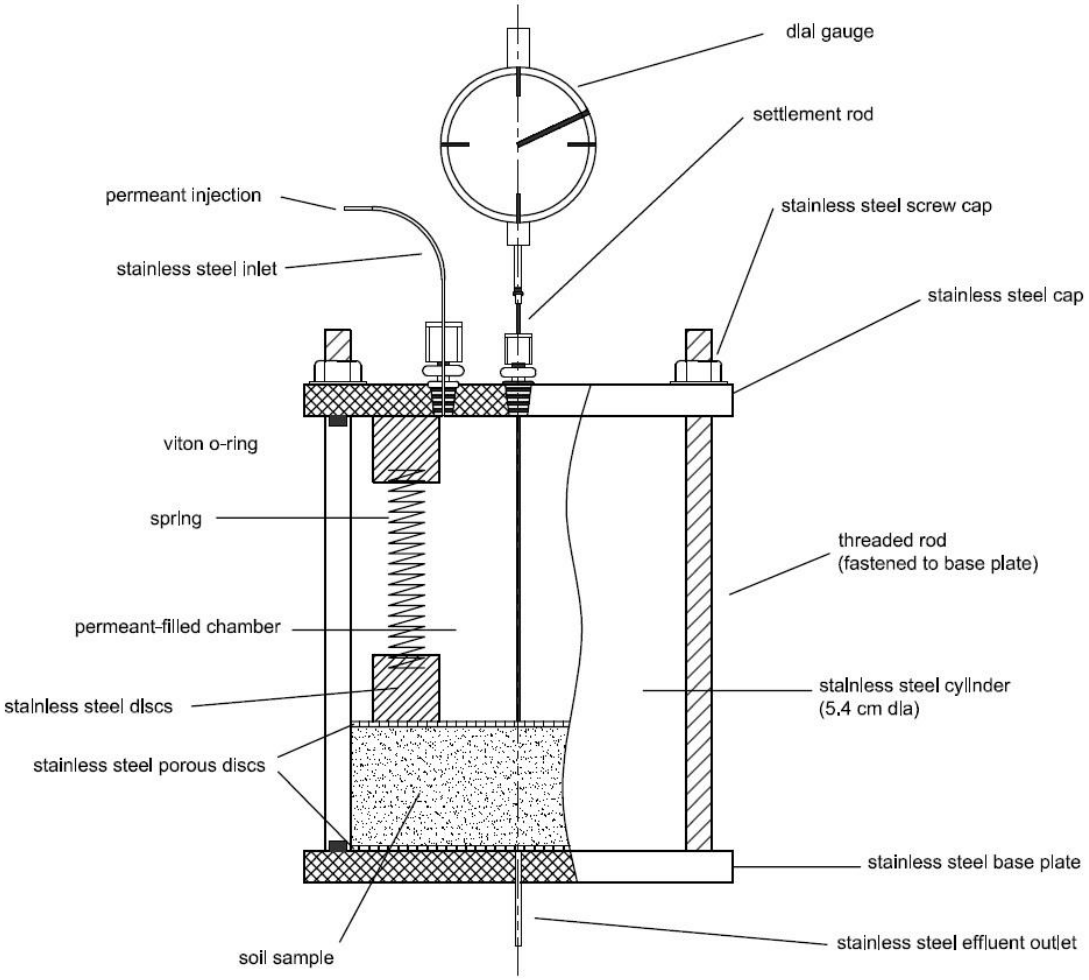

Figure 3.3: Schematic of hydraulic conductivity cell cross-section

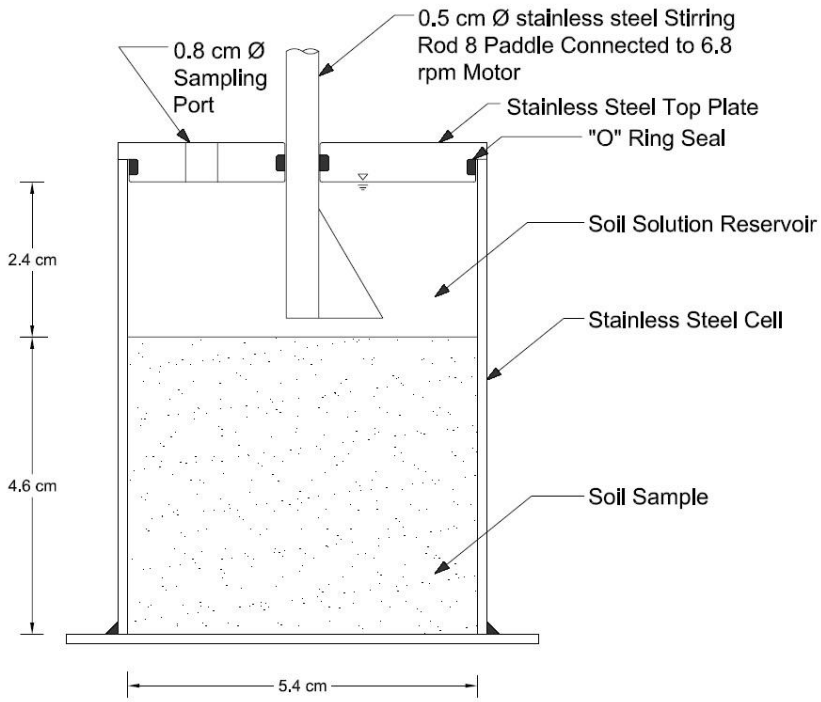

Figure 3.4: Schematic of diffusion cell

Figure 3.5: Diffusion test set up

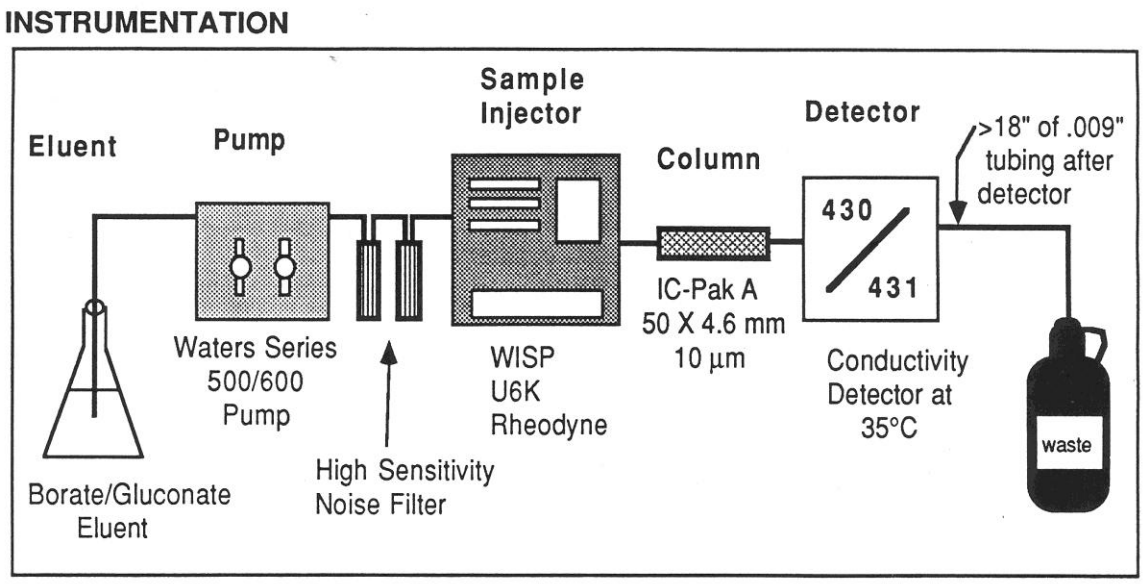

Figure 3.6: Schematic of IC instrumentation

Table 3.1: Physical data of glass Beads

Property	*Value*	*Unit*
Melting point	1446	°C
Softening point (Littleton point)	734	°C
Transformation temperature	549	°C
Specific thermal conductivity	1.129	W/Km
Coefficient of expansion	9.05	10^6 (1/K)
Specific thermal capacity	1.329	KJ/Kg K
Refractive index	1.5188	-
Young's-Modulus	63	Gpa
Hardness according to Mohs	≥ 6	-
*Specific weight**	2.5	Kg/dm^3
Roundness (ratio of axis)	≥ 80	%

* Test with pyknometer according DIN ISO 787-10

Table 3.2: Chemical composition/heavy metal content of glass beads

Property	*Value*	*Unit*
SiO_2	72.5	MA.- %
Al_2O_3	0.58	MA.- %
Fe_2O_3	0.11	MA.- %
TiO_2	0.04	MA.- %
K_2O	0.21	MA.- %
Na_2O	13	MA.- %
CaO	9.06	MA.- %
MgO	4.22	MA.- %
PbO	< 0.01	MA.- %
BaO	< 0.01	MA.- %
ZnO	< 0.01	MA.- %
As_2O_3	< 0.01	MA.- %
Sb_2O_3	0.02	MA.- %
SO_3	0.12	MA.- %
SrO	< 0.01	MA.- %
ZrO_2	0.01	MA.- %
B_2O_3	< 0.01	MA.- %

Table 3. 3: Sodium-Chloride specifications

Property	Value
Assay	99.0% NaCl min
pH of 5% solution at 25 °C	5.0- 9.0
Insoluble matter	0.005% max
Iodide (I)	0.002% max
Bromide (B)	0.01% max
Chlorate and Nitrate (as NO_3)	0.003% max
Phosphate (PO_4)	5 ppm max
Sulfate (SO_4)	0.004% max
Barium (Ba)	Passes test
Heavy metals (as Pb)	5 ppm max
Iron (Fe)	2 ppm max
Calcium (Ca)	0.002% max
Magnesium (Mg)	0.001% max
Potassium (K)	0.005% max

Chapter 4

Results AND Discussion

4.1. Soil Properties

The physical properties of the different glass beads-kaolinite mixtures are presented in Table 4.1. The Casagrande device was used to determine the liquid limit of the soil samples by means of the flow curve method. Plasticity index was determined as the difference between the liquid and plastic limits. The liquid limit of the mixtures increases from 11.9% for a mixture with 20 percent clay to approximately 30% as the weight concentration of clay reaches 50 percent but, as evident from Figure 4.1 it does not increase exactly proportionally with the addition of clay which is consistent with previous research (Sivapullaiah and Sridharan, 1985). Moreover, the addition of clay shows an increase in plasticity index, that is, the range of moisture content over which the soil is in a plastic condition.

Compaction curves for the mixtures are presented in Figure 4.2. As expected, on the dry side of the optimum moisture content, density increases with adding water due to particles lubrication with a larger water film around them resulting in a denser configuration (Holtz and Kovacs, 1981) while in the wet side of the optimum moisture content, the water particles replace soil particles. Therefore, the density will decrease. The maximum dry density decreases from 2.01 g/cm^3 to 1.78 g/cm^3 as the kaolinite amount increases from 20 to 50 percent as a result of lower particle density of water compared to soil particles. The specific gravity of G80K20 was measured to be 2.52 and there was no notable increase in this parameter due to the addition of kaolinite to mixtures.

The hydrometer analysis for kaolinite is presented in Figure 4.3. The data show that 60 percent of the kaolinite used in this research is finer than 0.002 mm. Therefore the clay size percentage in G80K20, G70K30, G60K40, G50K50 were 12%, 18%, 24% and 30% respectively. From the classification scheme for soil activity proposed by Head (1980), all four mixtures may be classified as inactive soils since their activity is less than 0.75.

Table 4.2 shows the soluble salts and exchangeable cations of glass beads and kaolinite. As it can be concluded the glass beads would not generally contribute to the cation exchange capacity of the mixture. Moreover, the cation exchange capacity of kaolinite was measured to be 2.46 meq/100g, which is close to the published value of 2.62 meq/100 g for pure kaolin (Ghosh and Bhattacharyya, 2002).

Table 4.1: Physical properties of glass beads-kaoline mixtures used in study

Property	Reference	Value			
		G80K20	G70K30	G60K40	G50K50
Specific Gravity	ASTM D 854	2.52	2.53	2.54	2.55
Liquid Limit (%)	ASTM D 4318	11.9	17.2	25.1	29.7
Plastic Limit (%)	ASTM D 4318	10.6	12.6	15.3	16.6
Plasticity Index (%)	ASTM D 4318	1.3	4.6	9.8	13.1
Kaolinite Particle Sizes:					
%Silt (0.002 to 0.074 mm)	ASTM D 422	8	12	16	20
%Clay (Clay < 0.002 mm)	ASTM D 422	12	18	24	30
Activity		0.11	0.26	0.41	0.44
Maximum Dry Unit Weight (g/cm^3)	ASTM D 698(A)	2.01	1.98	1.86	1.78
Optimum Water Content (%)	ASTM D 698(A)	8.5	11.5	14.8	17.8

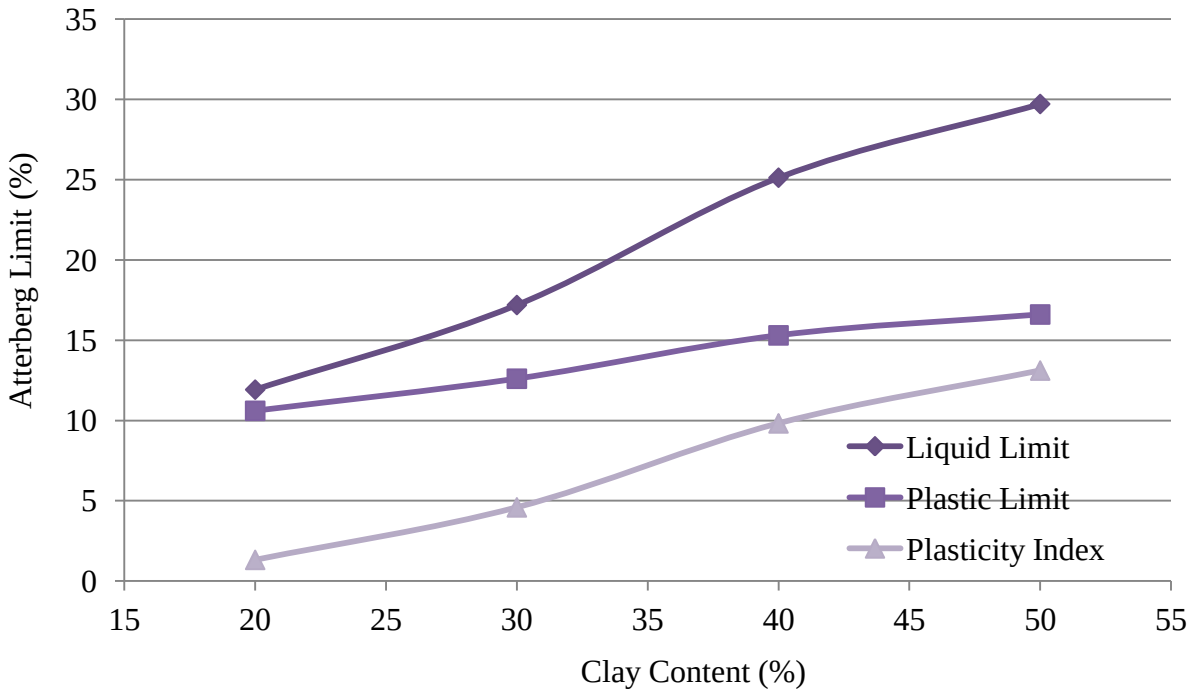

Figure 4.1: Atterberg limits for different glass beads-Kaolinite mixtures

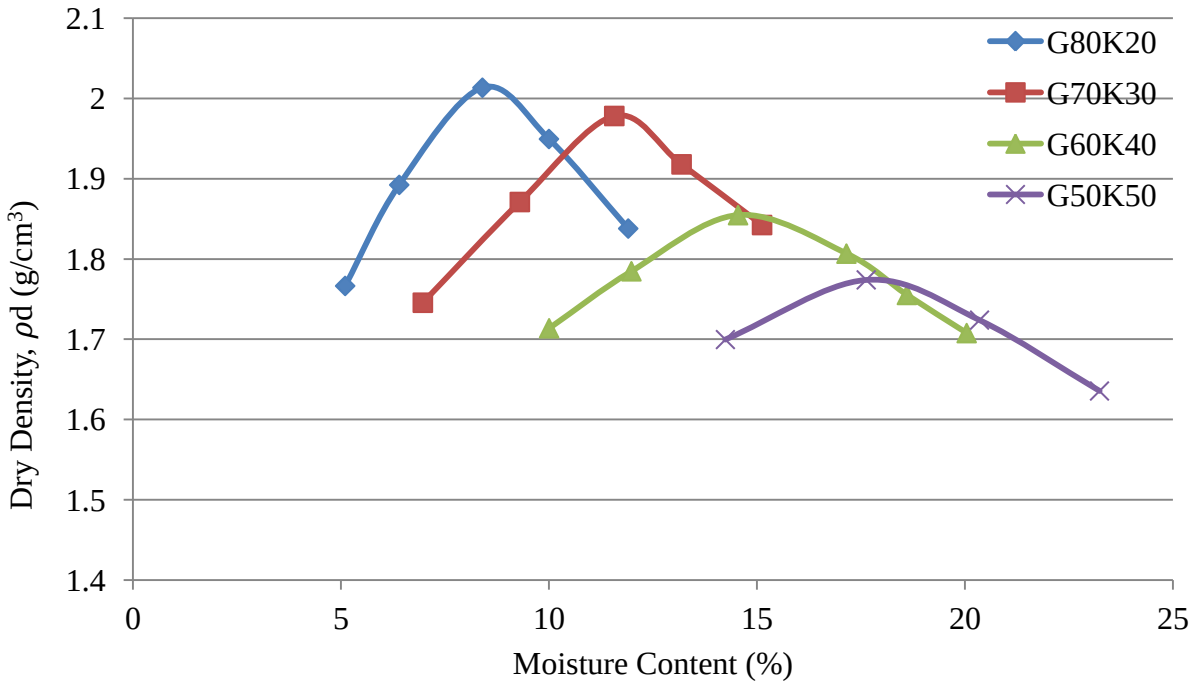

Figure 4.2: Compaction curves for glass beads-Kaolinite mixtures

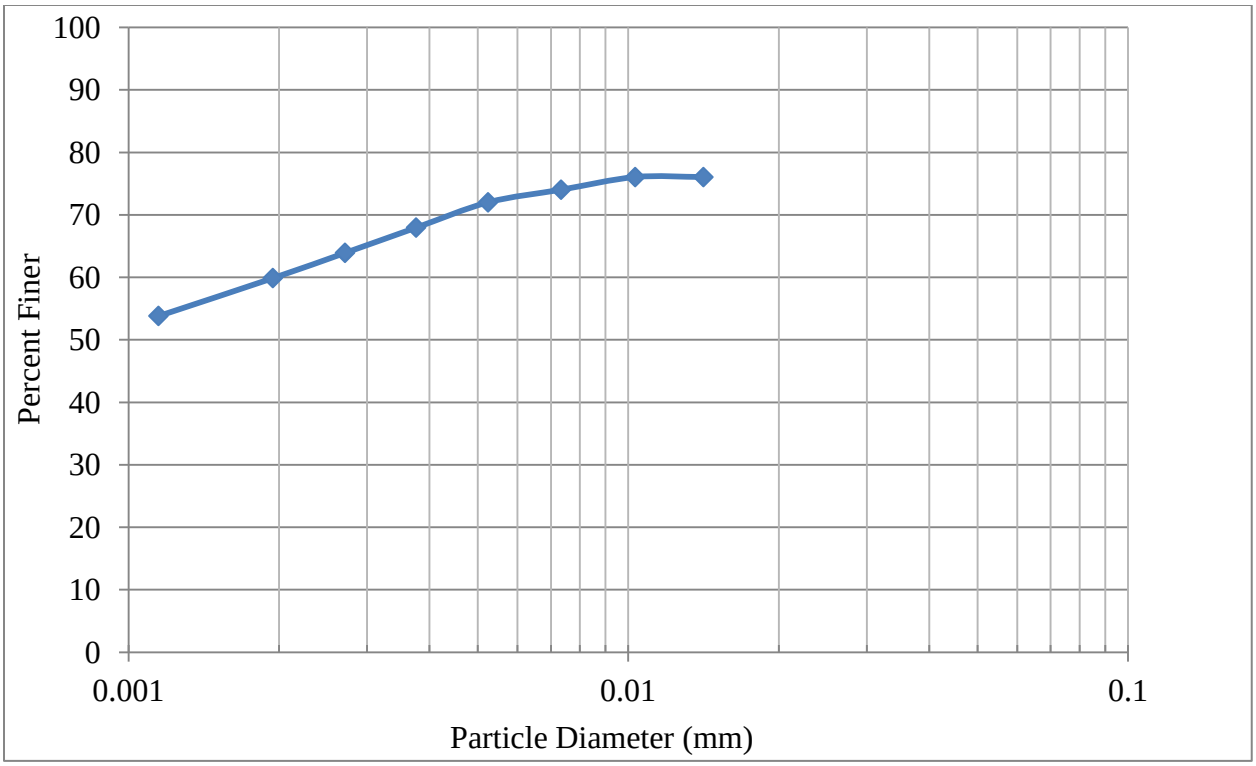

Figure 4.3: Hydrometer analysis for kaolinite

Table 4.2: Chemical properties of soils in this study

Species	Soluble Salts		Exchangeable Cations	
	Glass Beads	Kaolinite	Glass Beads	Kaolinite
	mg/L (meq/100g)		meq/100g	
Barium	< 0.01 (<0.01)	0.035 (<0.01)	< 0.01	< 0.01
Calcium	0.89 (0.45)	1.07 (0.53)	< 0.01	1.59
Iron	0.022 (<0.01)	0.22 (0.077)	< 0.01	< 0.01
Potassium	0.062 (0. 016)	0.4 (0.10)	< 0.01	<0.01
Magnesium	0.31 (0.25)	0.30 (0.25)	< 0.01	0.72
Manganese	<0.01 (<0.01)	0.02 (<0.01)	< 0.01	<0.01
Sodium	1.91 (0.83)	0.82 (0.36)	< 0.01	0.14
Cation Exchange Capacity, CEC (meq/100 g)			2.45	

4.2. Column Diffusion Test

The diffusion test ran for 10 days but as the pore water which was squeezed from four different sections of the soil sample at the end of the test was not enough for determination of sodium and chloride concentrations, establishing of concentration graph versus depth of the soil was impossible. Therefore, the diffusion coefficient and distribution coefficient were determined based on literature values and on solute breakthrough curves obtained from hydraulic conductivity test. The final selected values of the two parameters were within the range of previously reported values (D. shackelford and L. Redmond, 1995) and they provided a good fit to the experimental curves.

4.3. Batch Sorption Studies

Distribution coefficient obtained from batch tests and other soil parameters used in retardation factor calculation are presented in Table 4.3. According to Figure 4.4 and Figure 4.5, the sorption of solutes follows a linear isotherm in the range of concentrations considered in the present study, so the retardation factors were calculated from following equation:

$$R = 1 + \frac{\rho K_d}{n}$$

Where;

ρ= Dry density of the soil (g/cm^3)

n= Soil porosity

K_d= Distribution coefficient (mL/g)

The data indicate that the measured distribution coefficients from batch tests are lower than those back calculated using the commercial software POLLUTE (Rowe and Booker, 1975). This is consistent with results of earlier studies which found that experimental distribution coefficients obtained from batch tests in clayey soils were lower than values determined from diffusion tests (Barone et al. 1992; Myrand et al. 1992). This can be attributed to the lower ratio of soil to solution in batch test and, also, to the difference between no flow condition in batch test relative to transient condition in column test (Cherry et al. 1984). As the dry density and porosity of the samples were not similar, it was not expected to see same trend in distribution coefficients and retardation factors calculated from distribution coefficients. Moreover, adding kaolinite to the mixture resulted in an increase in the distribution coefficient of sodium as a result of increase in soil cation exchange capacity. However, the distribution coefficient of chloride was not affected by the addition of clay. The retardation factors for sodium and chloride are greater than one in all three samples which was expected for sodium because of cation exchange capacity (CEC) of the kaolinite but generally the chloride ion is assumed to be non-adsorbing solute which implies a distribution coefficient equal to zero and a retardation factor of 1. However, there is another study in the literature which found retardation factor greater than 1 for chloride, but the reason has not yet been investigated. The retardation factor of chloride is smaller than sodium which is consistent with preferential adsorption of Na^+ relative to Cl^- (Shackelford and Redmond, 1995).

The observed diffusion coefficients for sodium and chloride in the present study were in the range of 1.9×10^{-10} m^2/s to 8.5×10^{-10} m^2/s for the different glass beads-kaolinite mixtures. These observations suggest diffusion of both ions in the soils was affected by the percentage of clay fraction. The greater the amount of clay, the lower the diffusion coefficient obtained, which is consistent with classical advection-dispersion theory showing that diffusion coefficient increases

as the seepage velocity increases (Freeze and Cherry 1979). Moreover, the diffusion coefficient of sodium is approximately two times that of chloride. This trend is visually apparent from the shape of the breakthrough curves for Na^+ and Cl^- presented later in this chapter which shows greater dispersion of sodium relative to chloride. Cherry et al. (1984) that the dispersion of reactive solutes (R>1) is generally greater than that of nonreactive solutes (R=1) but as both sodium and chloride were determined to be reactive in this study, this reason probably cannot account for the observed discrepancy in ions dispersion.

Table 4.3: Distribution coefficient, diffusion coefficient and retardation factor of solutes

Soil		Solute	K_d (mL/g)		R	D_e ($*10^{-10}$ m^2/s)
			Batch Test	Model		
G70K30		Na	0.56	1.08	9.4	8.5
	ρ= 1.91(g/cm^3)	Cl	0.06	0.4	4.1	4
	n= 0.247					
G60K40		Na	0.68	1.23	8.9	6.26
	ρ= 1.82 (g/cm^3)	Cl	0.1	0.4	3.6	3.5
	n= 0.282					
G50K50		Na	0.77	1.31	7.8	3.5
	ρ= 1.71 (g/cm^3)	Cl	0.12	0.4	3.1	1.9
	n= 0.328					

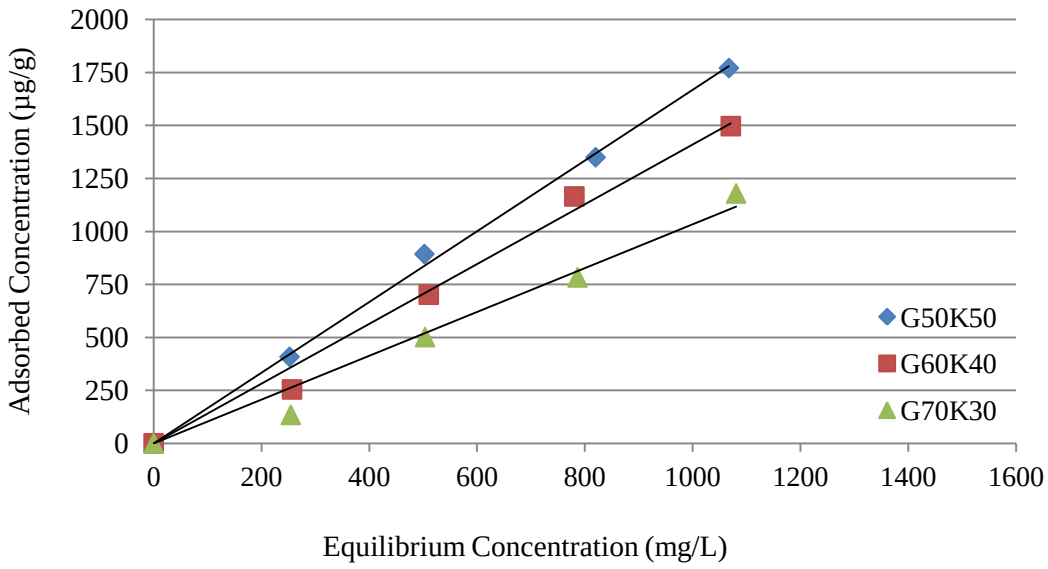

Figure 4.4: Batch equilibrium test results for Sodium

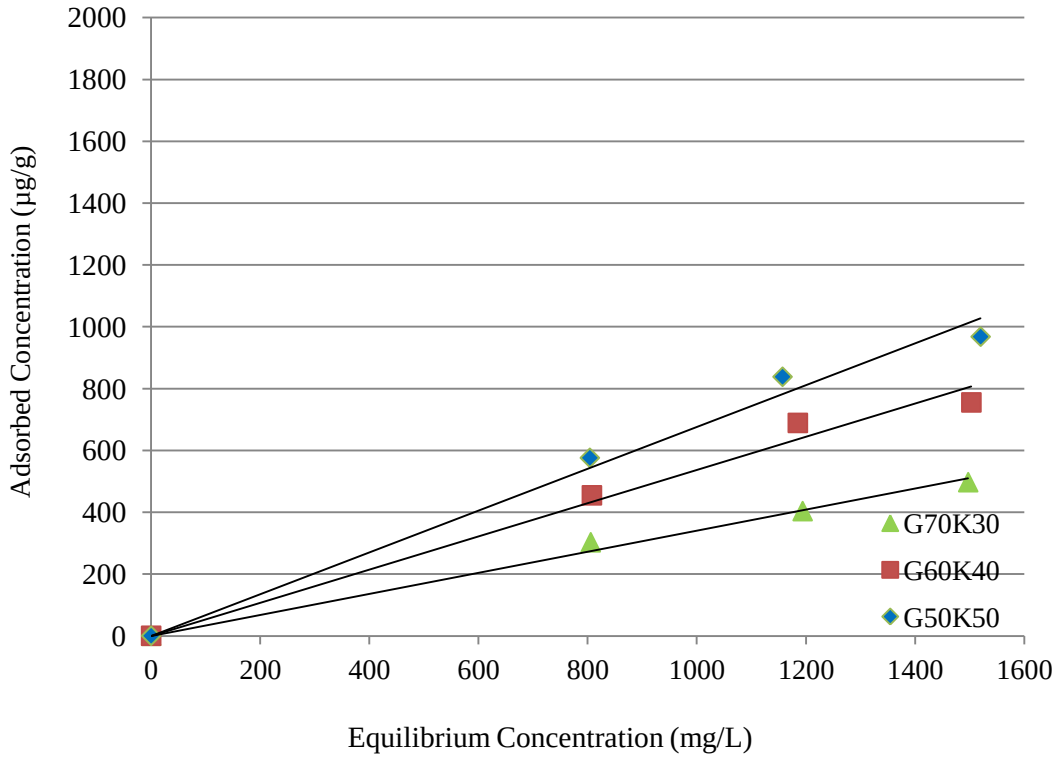

Figure 4.5: Batch equilibrium test results for Chloride

4.4. Hydraulic Conductivity

The hydraulic conductivity of different mixtures as well as temperature versus net pore volume of soils is shown in Figure 4.6 to Figure 4.9. It is clear from Figure 4.6, that for the soil containing 80 percent glass beads and 20 percent kaolinite, there was fluctuation in hydraulic conductivity up to approximately 6 pore volumes due likely to the segregation of kaolinite and glass beads, which was confirmed by the presence of kaolinite particles in the effluent during this period, as illustrated in the photographs in Figures 4.10 and 4.11 taken at the end of the hydraulic conductivity tests. The rather murky colour of the effluent in the middle bottle of Figure 4.10 shows dispersion and removal of kaolinite particles from the mixture likely via side-wall leakage. Figure 4.11 shows clear separation of kaolinite particles and glass beads. An attempt was made to minimize or prevent sidewall leaking by lightly greasing inside of the cell on top of the soil sample with vacuum grease, but this did not prevent the leaching of clay particles from the 80% glass beads-20% kaolinite mixture (G80K20) under the imposed hydraulic gradient. After several trials, it was concluded that it was not possible to obtain a mixture that was homogeneous enough to yield a reliable hydraulic conductivity value for G80K20; this mixture was therefore eliminated from the study and no further measurements were carried out.

The test results from the other mixtures show a slight decrease in hydraulic conductivity from the beginning to the point of distilled water permeation, which is likely because of seepage settlement and subsequent consolidation of samples. As shown in the settlement-pore volume graphs in Figures 4.12 (a) to 4.12 (c), during flushing stage there was 0.23 mm, 0.15 mm and 0.15 mm settlement in G70K30, G60K40 and G50K50, respectively. The measuring rods were tightened during permeation to prevent leakage and dial gauge readings were taken only during refilling of syringes. The total measured settlements of samples were 0.21 to 0.29 mm.

From the experimental results it can be concluded that the introduction of sodium chloride solution did not change the measured hydraulic conductivity of the three glass beads-kaolinite mixtures. Apparently the higher ionic strength of the 0.04 M NaCl relative to distilled water was not large enough to result in particle rearrangement, flocculation and ultimately higher hydraulic conductivity in the presence of induced effective stresses in the soil samples (Mitchell 1993; Shackelford 1994a). However, the hydraulic conductivity of all samples increased after the third refill of syringes as a result of higher temperature. Increase in temperature results in decrease in viscosity of water, which can contribute greatly to an increase in hydraulic conductivity of soil (Cho et al., 1999).

After passing approximately 17 pore volumes of NaCl solution through G70K30, its final hydraulic conductivity was 8.2 $x10^{-11}$ m/s at a hydraulic gradient equal of 628 whereas passing 15 pore volumes of the solution through G60K40 and G50K50 resulted in final hydraulic conductivity of $1.28*10^{-10}$ m/s and $1.48*10^{-10}$ m/s at a hydraulic gradient of 408 and 347, respectively. The higher hydraulic conductivity in the mixture with 50 percent kaolinite relative to the two other samples may be partly explained by the lower dry density and larger porosity of this mixture. The properties of the samples obtained at the start of the hydraulic conductivity tests are presented in Table 4.4.

Table 4.4: Soil samples properties in hydraulic conductivity test

Property	Unit	Value		
		G70K30	G60K40	G50K50
Sample thickness	(cm)	2	2	2
Sample volume	(cm^3)	45.8	45.8	45.8
Volume of solid	(cm^3)	34.5	32.9	30.8
Volume of pore	(cm^3)	11.3	12.9	15.0
Void ratio	(-)	0.33	0.39	0.49
Porosity	(-)	0.25	0.28	0.33
Water Content	(%)	13.4	16.5	19.5
Dry density	(g/cm^3)	1.91	1.82	1.71
Degree of saturation	(%)	100.0	100.0	95.8

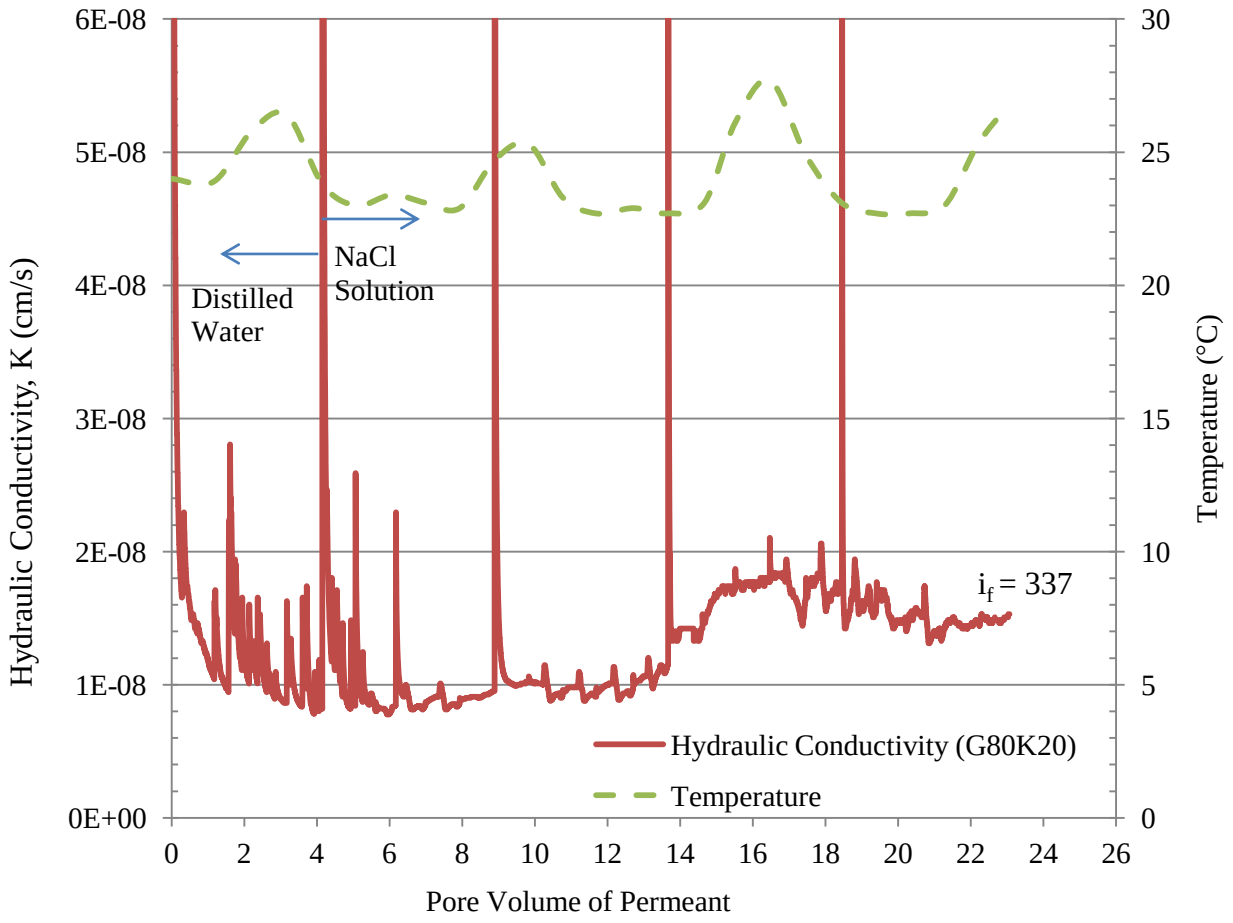

Figure 4.6: Variation in hydraulic conductivity of G80K20

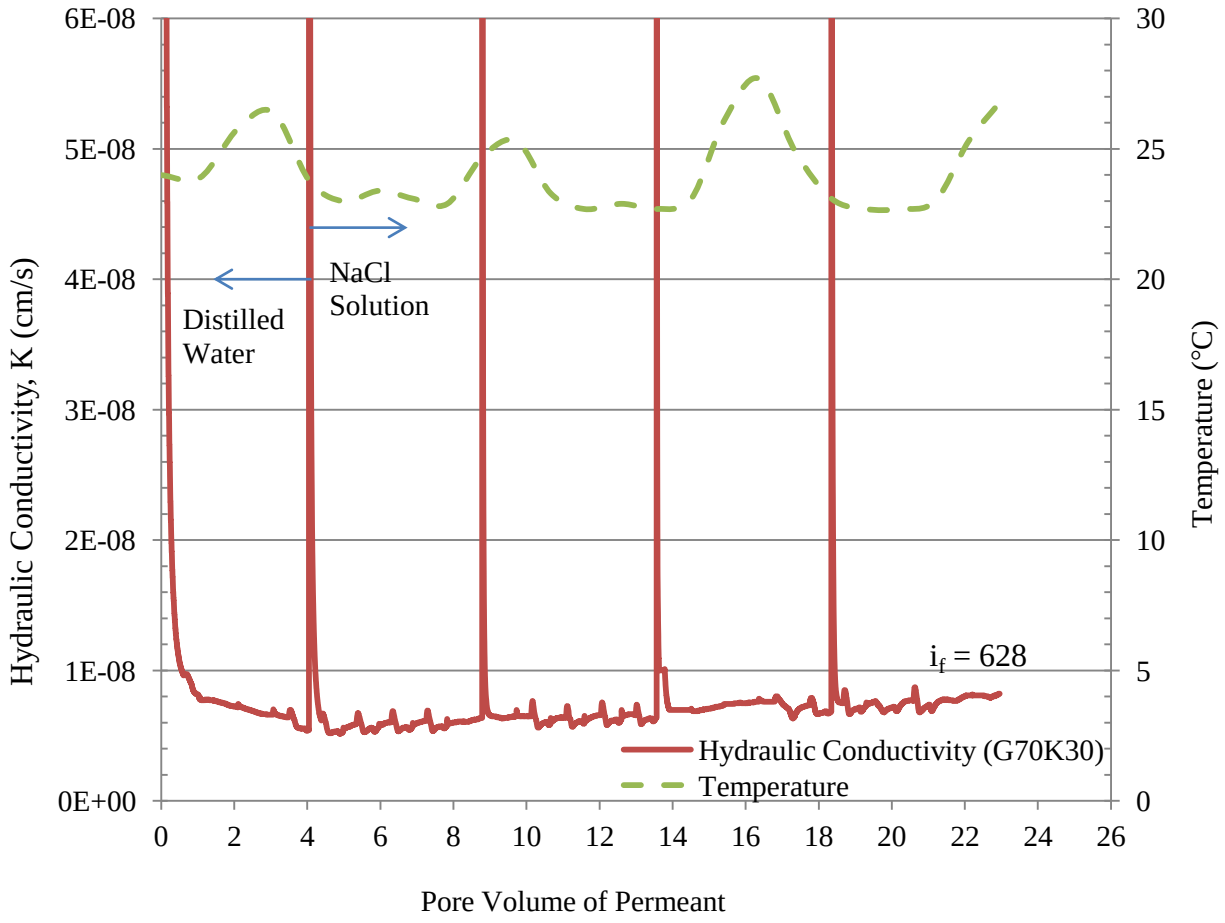

Figure 4.7: Variation in hydraulic conductivity of G70K30

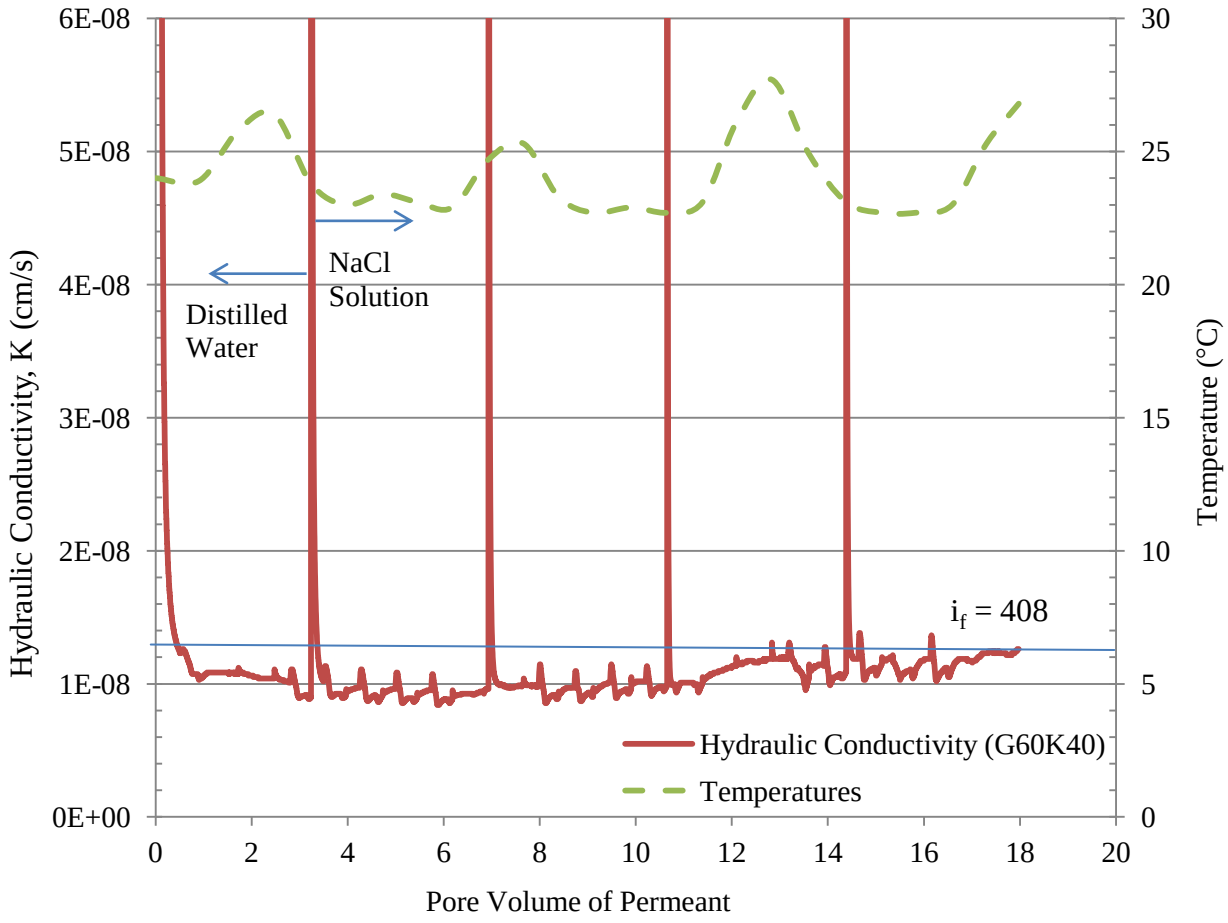

Figure 4.8: Variation in hydraulic conductivity of G60K40

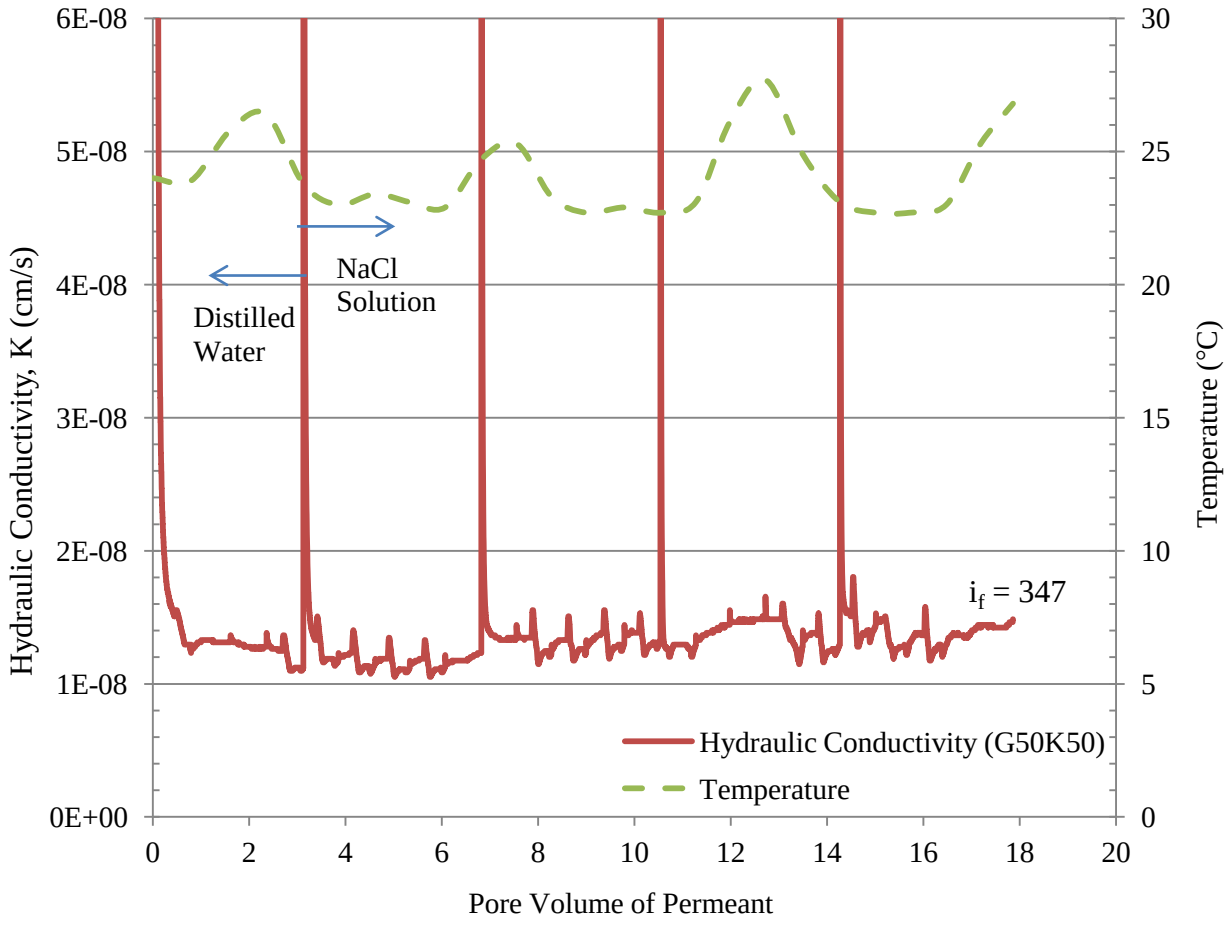

Figure 4.9: Variation in hydraulic conductivity of G50K50

Figure 4.10: Turbidity in G80K20 effluent

Figure 4.11: Segregation of kaolinite and glass beads in G80K20

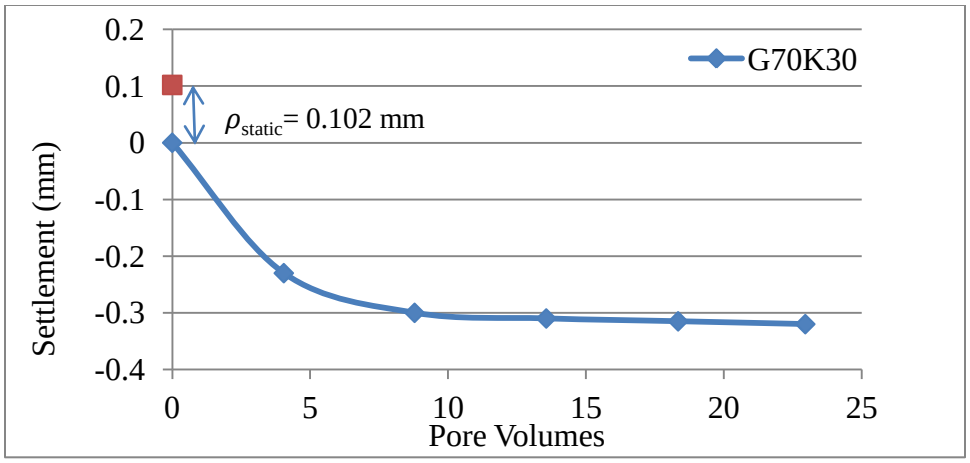

(a)

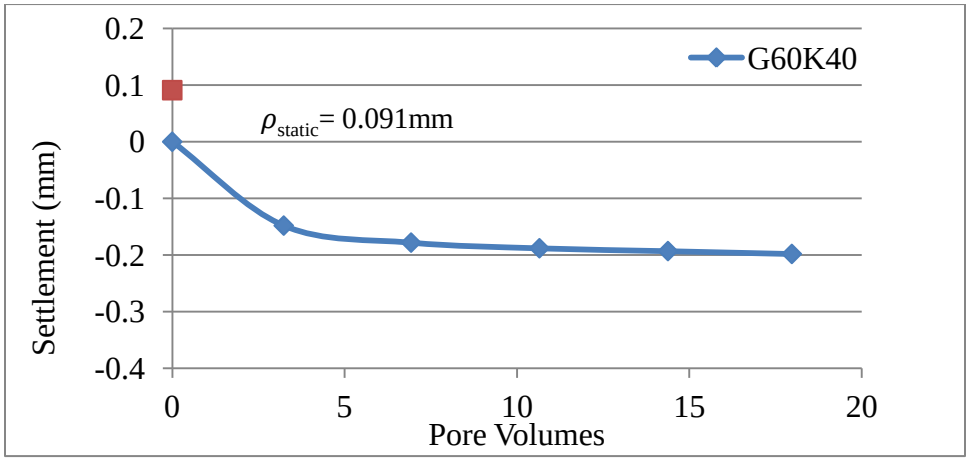

(b)

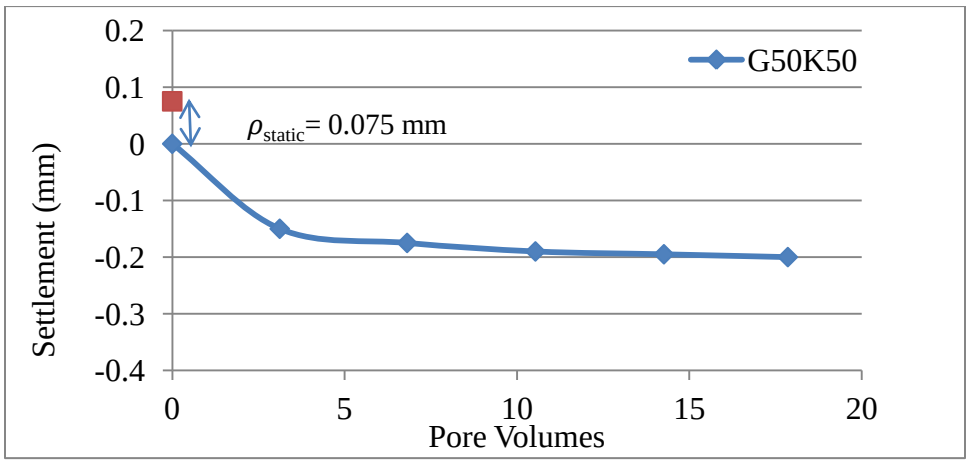

(c)

Figure 4.12: Settlement versus pore volumes during testing

4.5. Effluent pH

The measured pH of the effluents from the hydraulic conductivity cells is illustrated in Figure 4.13 (a) to (c). Although there are some differences in the results, the general trend is approximately the same. The pH values stabilized after a few pore volumes and decreased slightly, in comparison to the pH observed during the distilled water permeation stage. A decrease in pH following NaCl permeation may be attributed to the replacement of hydrogen ions (H^+) attached to exposed hydroxyls on the kaolinite clay particle surface by sodium ions (Na^+) present in the permeant. Ion exchange likely did not occur during permeation with distilled water because very few ions are present in distilled water (Shackelford and Redmond, 1995). There was no subsequent increase in pH which indicated minimal ion exchange during the test.

4.6. Effluent Electrical Conductivity

Figure 4.14 shows a plot of the measured electrical conductivity of the effluent relative to the initial conductivity of the sodium chloride solution. As indicated by the graphs, the general trend is the same for all three specimens: a decrease in electrical conductivity during distlled water permeation and an increase following the introduction of NaCl solution. The initial decrease is because of the reduction of soluble salts concentration in the samples pore water. But, as the concentration of ions, specifically Na^+ and Cl^-, increased in the effluent, the EC/EC_0 increased and finally reached a value of unity after 17 pore volumes of permeation of G70K30 with NaCl solution and passing of approximately 15 pore volumes of solution through the other two samples. Shackelford and Redmond (1995) reported that electrical conductivity of the effluent reaches half of the initial value (EC/EC_0= 0.5) usually after about one pore volume of permeant flow but this was not observed in the present study. No definite conclusions regarding the migration of nonreactive and reactive solutes may be drawn from the electrical conductivity

measurements. However, the trend in solute breakthrough curves is expected to be similar to that of electricial conductivity (EC).

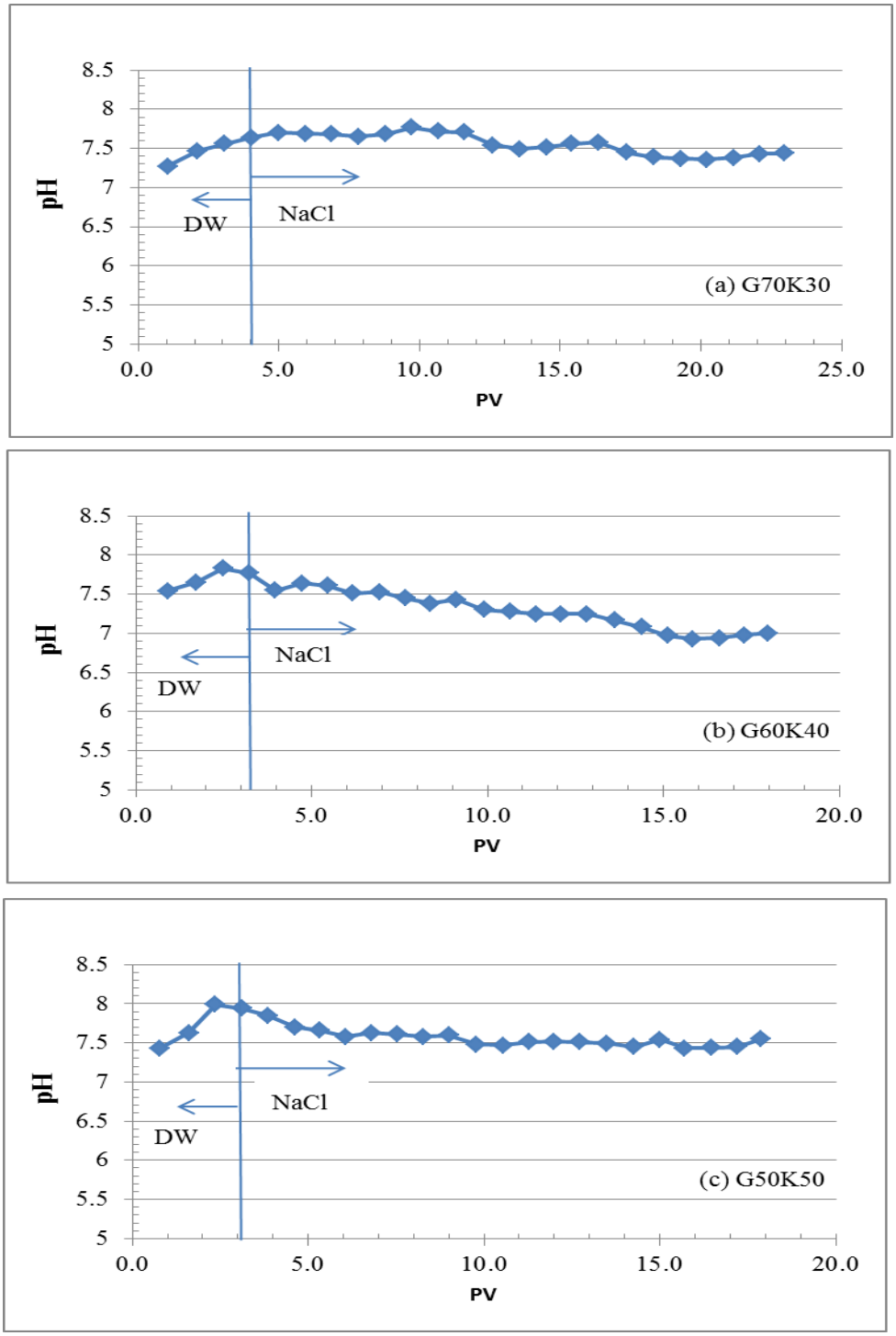

Figure 4.13: pH curves versus net pore volumes

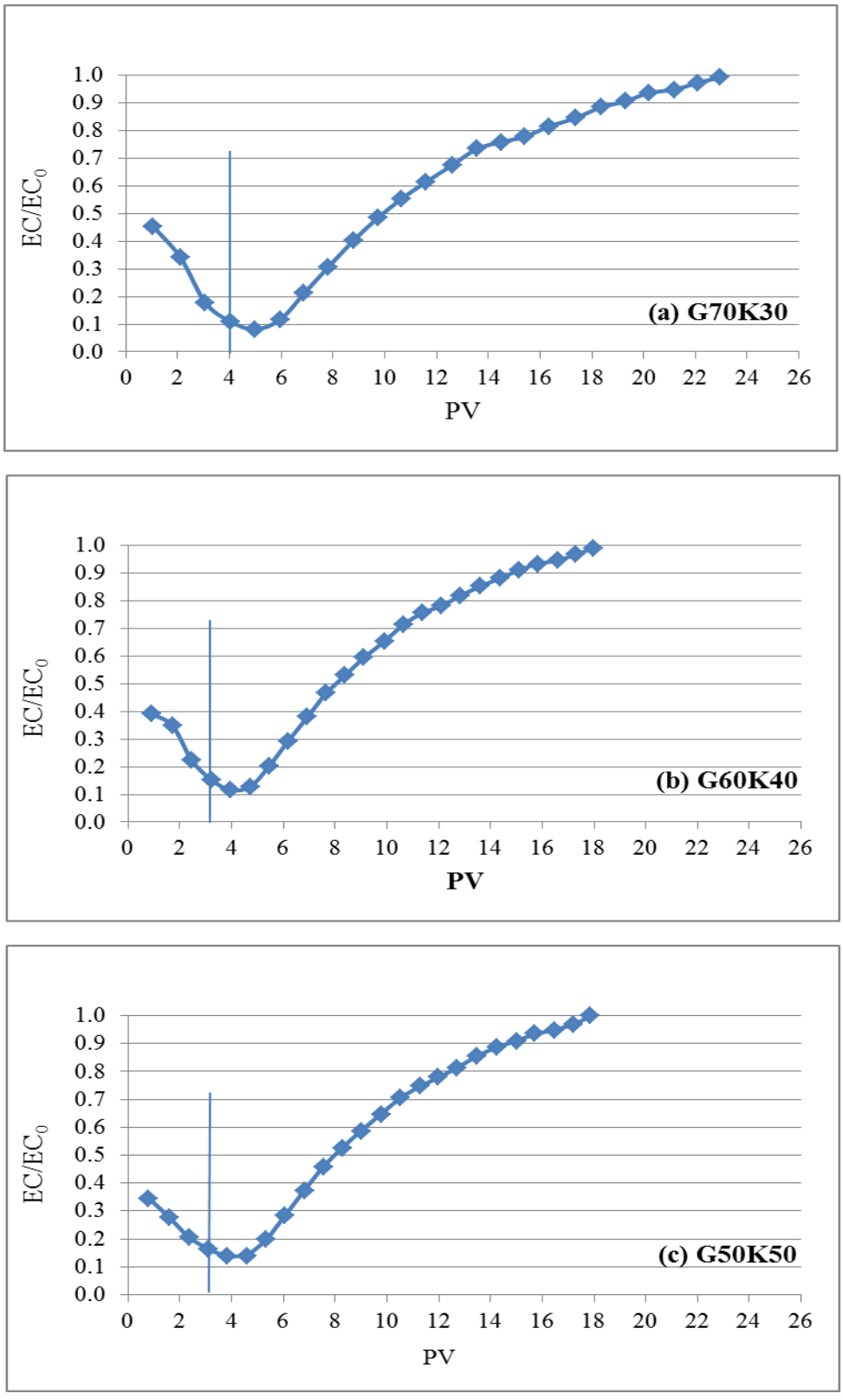

Figure 4.14: Variation in relative effluent electrical conductivity (EC) during permeation of soils with NaCl solution

4.7. Solute Breakthrough Curves

The measured sodium and chloride concentrations in the effluent from the three cells are presented in Figures 4.15 (a) to 4.15 (c) and Figures 4.16 (a) to 4.16 (c). There was a significant decrease in sodium concentration in all samples during permeation with water which was reflected in the measured electrical conductivity noted in the previous section. The as- received glass beads was found to contain sodium ions. During the permeation of the compacted samples with distilled water, sodium was washed out and its concentration reached 69.9 mg/L, 112.7 mg/L and 98.6 mg/L for G70K30, G60K40 and G50K50, respectively. A decrease in chloride concentration likely occurred, however, as the initial value in the samples were not high, the decrease was not noticeable.

The best-fit values of distribution coefficient and diffusion coefficient along with other soil parameters were used as input in the commercial software Pollute7 (Rowe and Booker, 1995) to model the breakthrough curves for sodium and chloride. The results show that there is a good agreement between modelling and experimental results during early stages of hydraulic conductivity testing with NaCl solution for sodium. However, after a few pore volumes (5 PV) of permeation with NaCl solution, the predicted concentrations for sodium exceeded the experimental values for a considerable number of pore volumes.

Moreover, regardless of the soil mixture, the effluent chloride concentration was overestimated by the model after approximately three pore volumes of sodium chloride permeation. The difference between the experimental and modelling results may be attributed to processes that

may have occurred during the hydraulic conductivity tests and were likely not considered in the modelling.

One of the possibilities could be a change in soil pore size distribution and porosity during permeation, which results in a different Darcy velocity. In this study, the pore size distribution of compacted samples were determined by mercury intrusion porosimetry (MIP) test at the start and end of the hydraulic conductivity tests, to evaluate how permeation affected the pore structure of the mixtures.

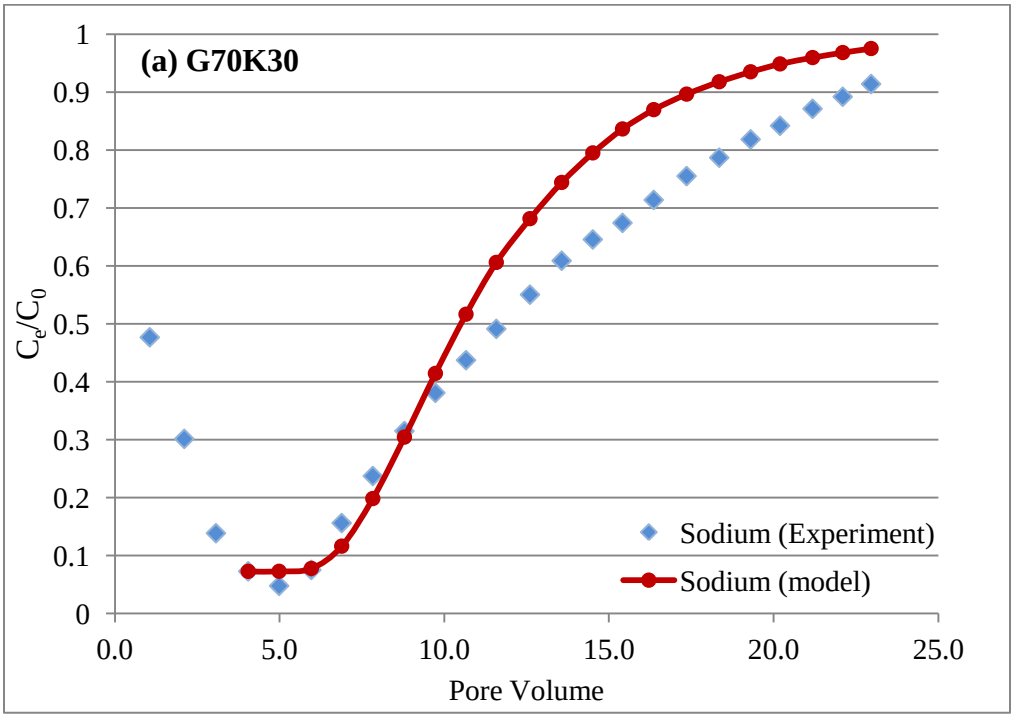

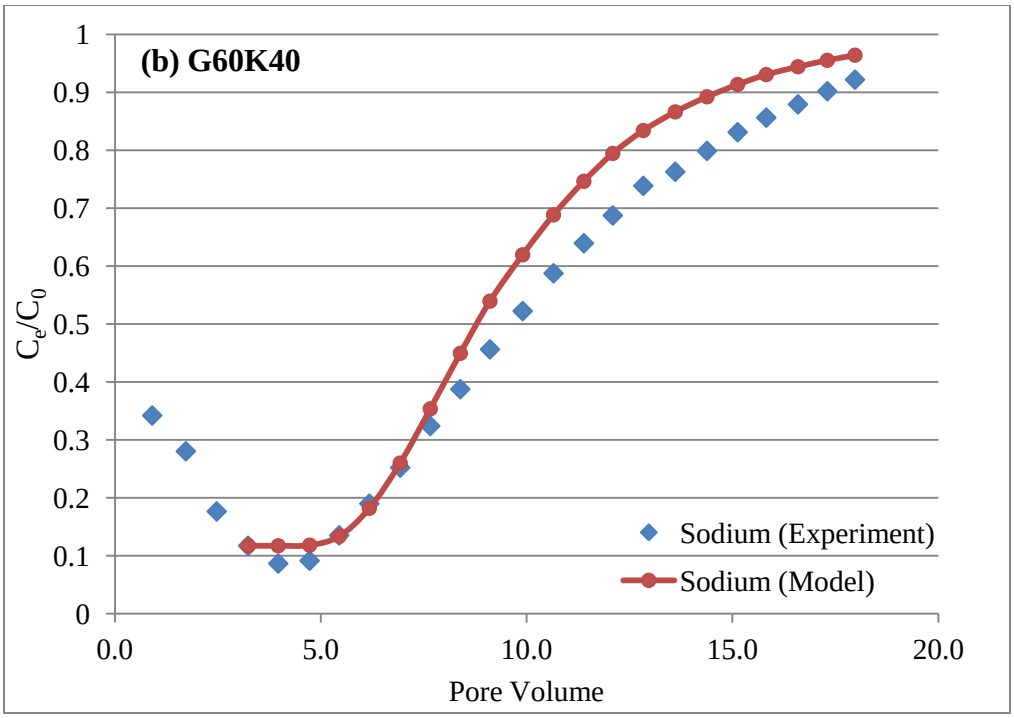

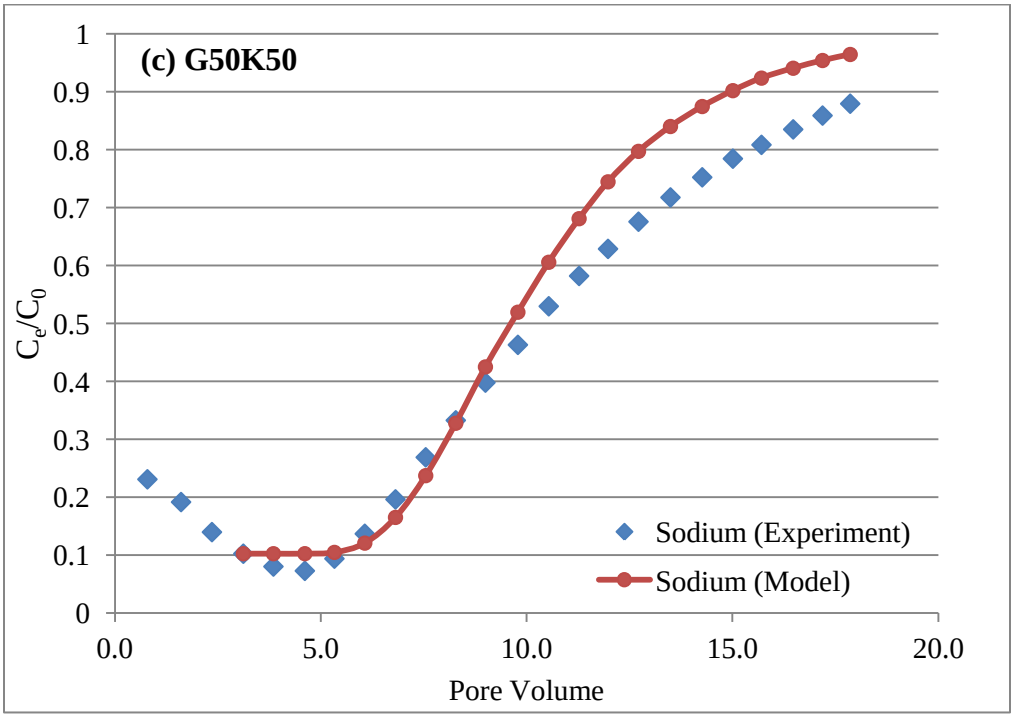

Figure 4.15: Sodium breakthrough curves

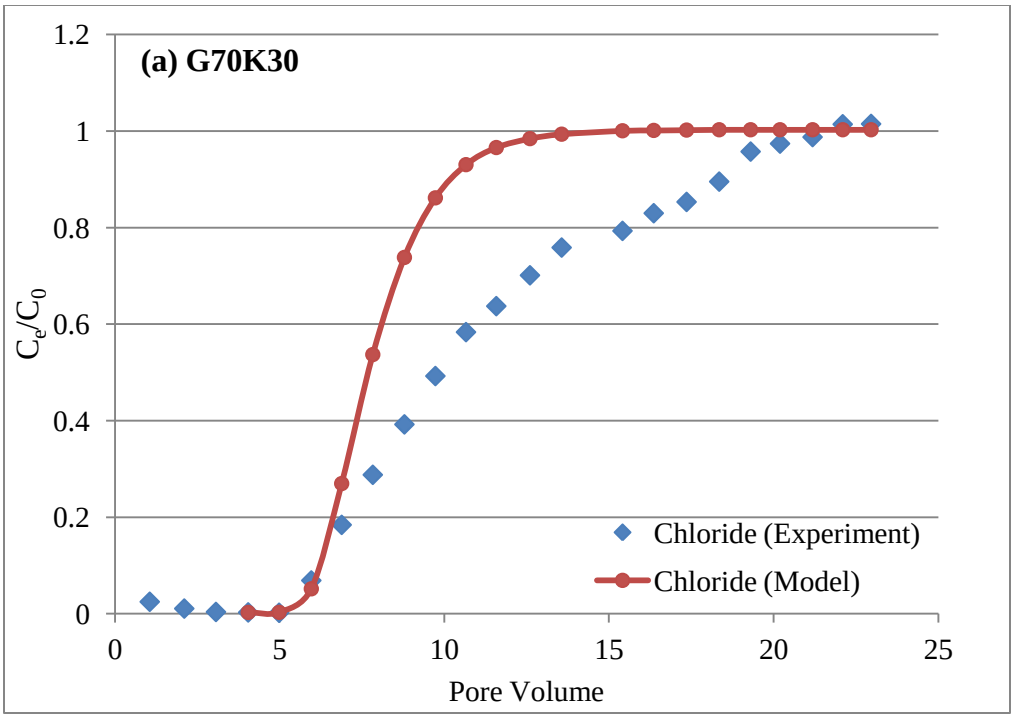
(a) G70K30
1.2
1
0.8
0.6
0.4
0.2
0
C_e/C_0
0
5
10
15
20
25
Pore Volume
Chloride (Experiment)
Chloride (Model)

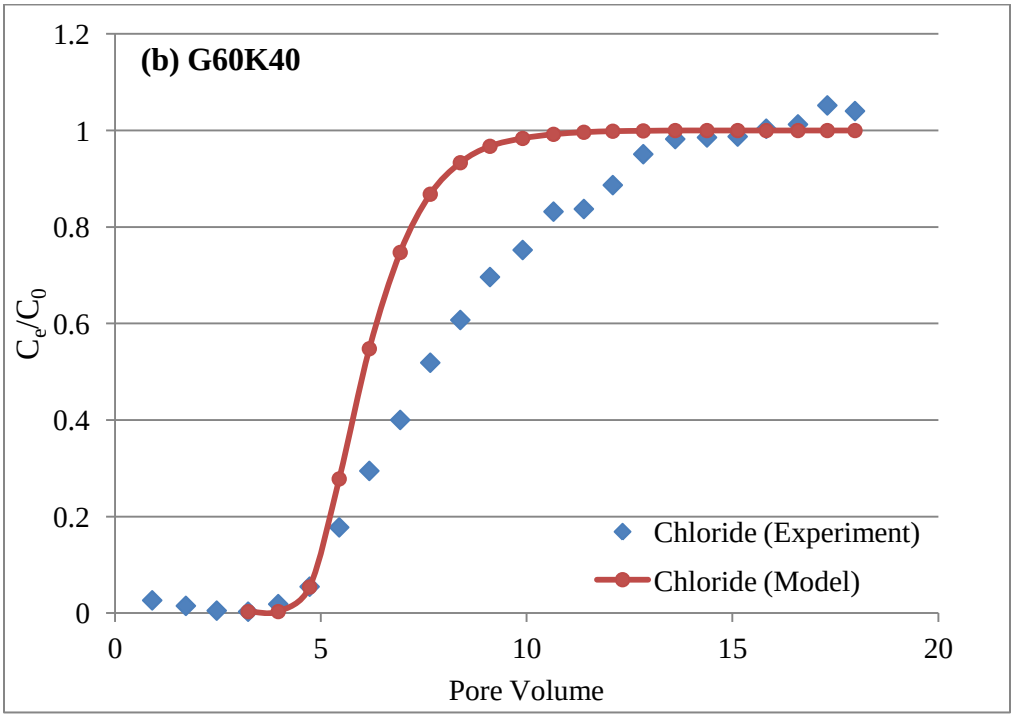
(b) G60K40
1.2
1
0.8
0.6
0.4
0.2
0
C_e/C_0
0
5
10
15
20
Pore Volume
Chloride (Experiment)
Chloride (Model)

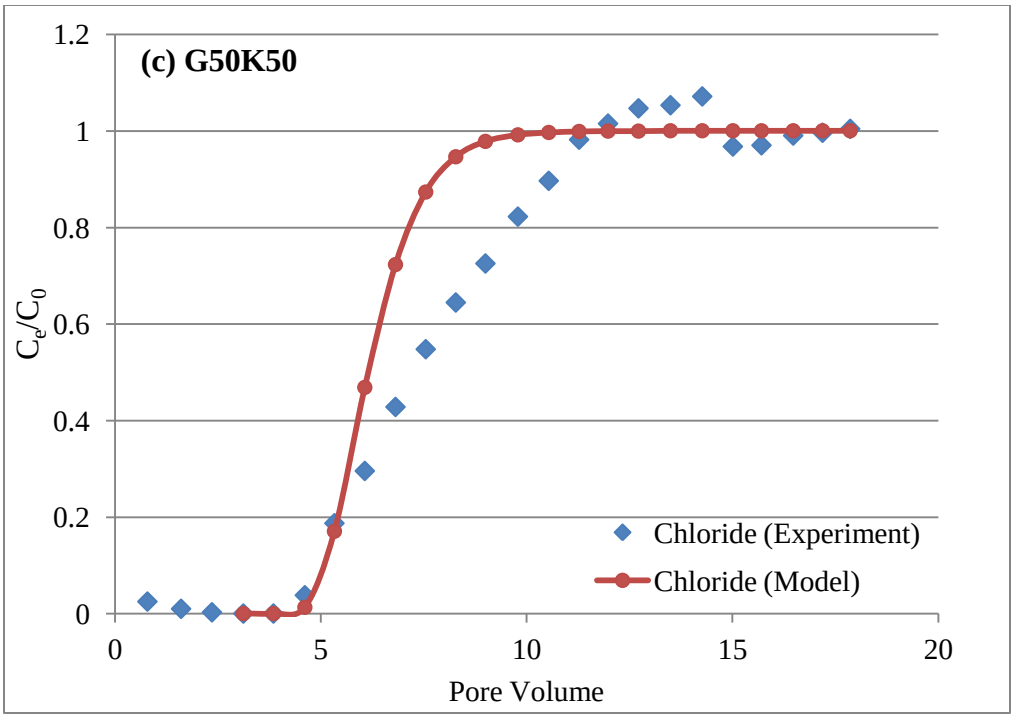

Figure 4.16: Chloride breakthrough curves

4.8. Mercury Porosimetry Analysis

The cumulative intrusion versus pore diameter is presented in Figures 4.17 (a) to 4.17 (c) and the detailed MIP test results are in Appendix B.

According to the results, the total intrusion of mercury in G70K30 decreased from 0.1124 mL/g to 0.0847 mL/g after permeation and the measured porosity decreased from 29.3% to 22.2%. The same trend was observed for G60K40 and G50K50 with initial intrusions of 0.1230 mL/g and 0.1379 mL/g relative to final values of 0.1087 mL/g and 0.1239 mL/g, respectively. The porosity of these two samples also decreased from 31.9% to 27.7% for G60K40 and from 35% to 30.7% for G50K50. Figures 4.18 (a) to 4.18 (c) show the modelling based on the adjusted porosity, as it can be observed change in porosity value did not affect the breakthrough curves considerably. While these results do not directly indicate a specific change in Darcy velocity or other controlling parameters in the model, they definitely suggest a decrease in Darcy velocity. Therefore, to evaluate how it could affect the model output, the same reduction in intruded mercury volume, 25%, 12% and 10% for G70K30, G60K40 and G50K50 respectively, was applied to the Darcy velocity. Two time periods were considered in re-modelling of the breakthrough curves; the initial Darcy velocity was assigned to the first period, while the decreased Darcy velocity (for the afore mentioned percentage change) was considered to be the value for the second period. The results for sodium are illustrated in Figures 4.19 (a) to 4.19 (c). As change in Darcy velocity value did not affect the chloride breakthrough curves noticeably, they are not shown. The modelling with a constant Darcy velocity is also shown on the same graphs.

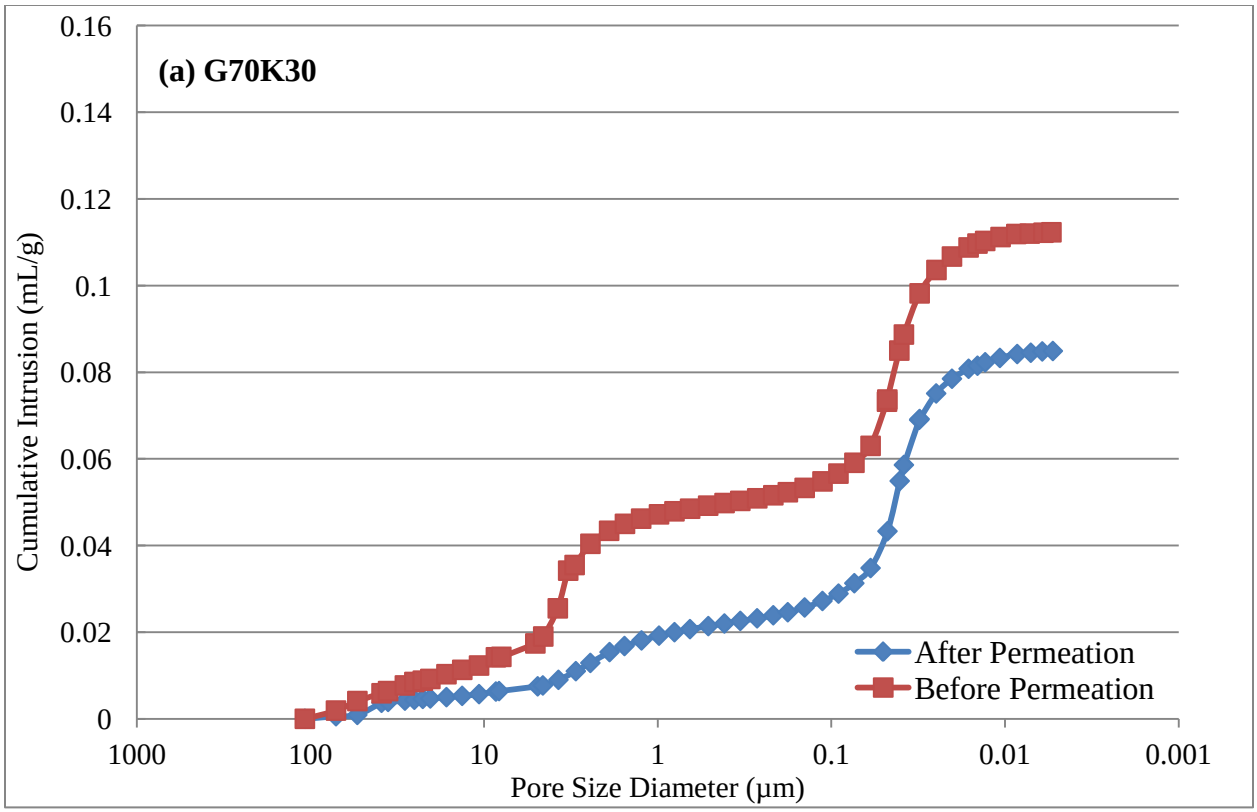
(a) G70K30
Cumulative Intrusion (mL/g)
0.16
0.14
0.12
0.1
0.08
0.06
0.04
0.02
0
1000
100
10
1
0.1
0.01
0.001
Pore Size Diameter (μm)
After Permeation
Before Permeation

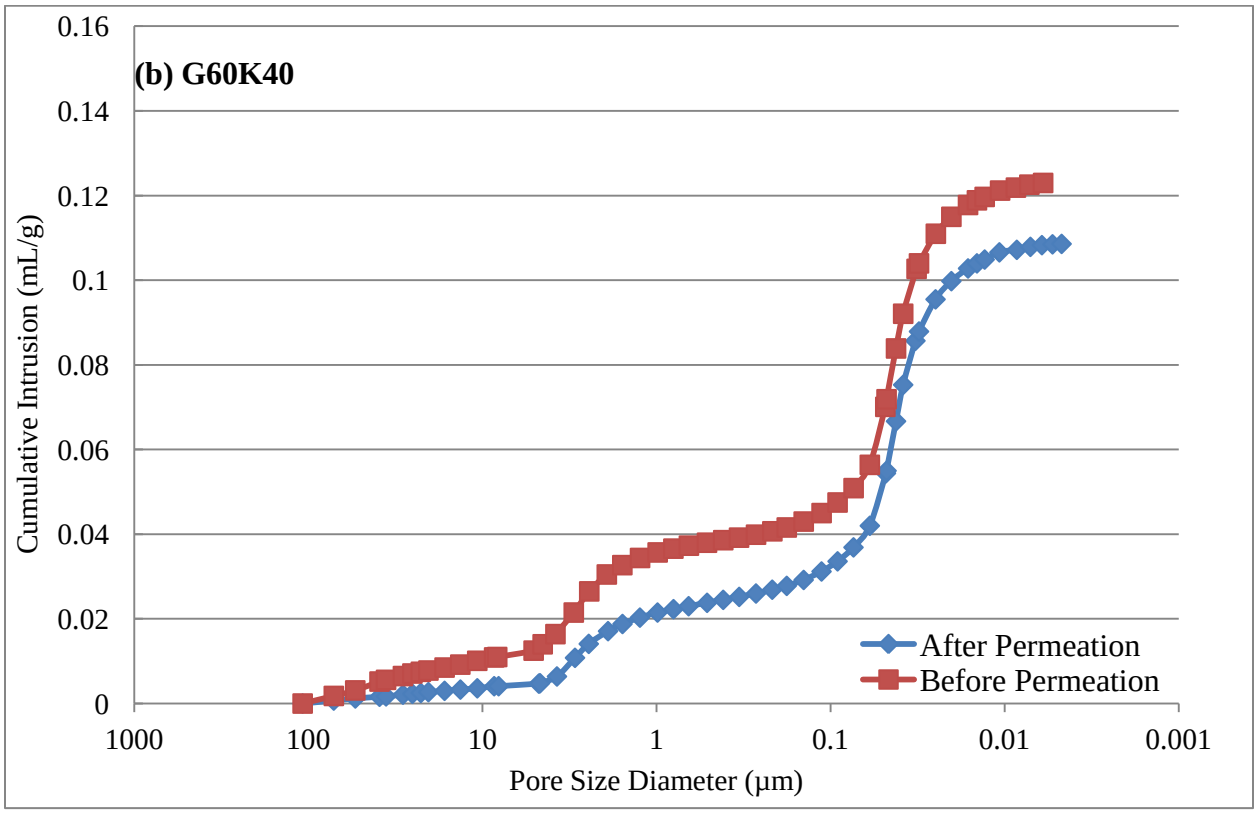
(b) G60K40
Cumulative Intrusion (mL/g)
0.16
0.14
0.12
0.1
0.08
0.06
0.04
0.02
0
1000
100
10
1
0.1
0.01
0.001
Pore Size Diameter (μm)
After Permeation
Before Permeation

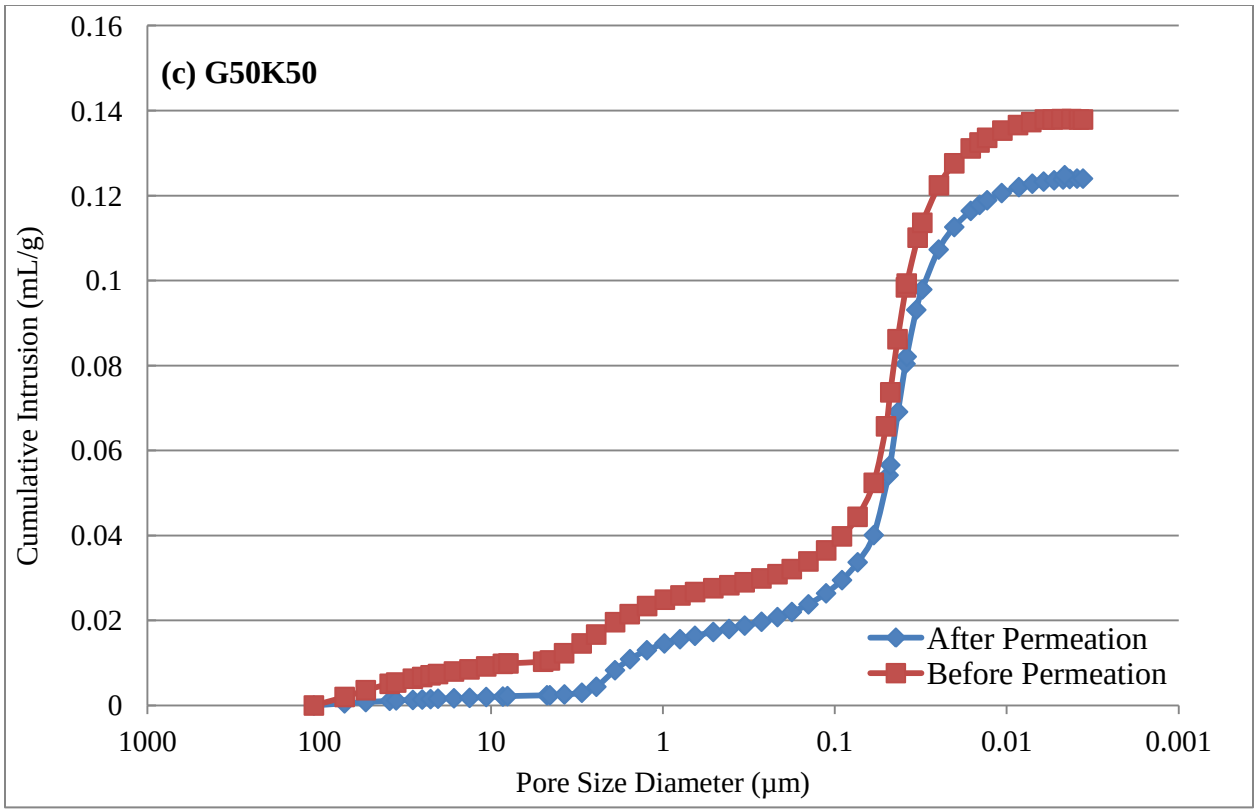

Figure 4.17: Cumulative Intrusion versus Pore size

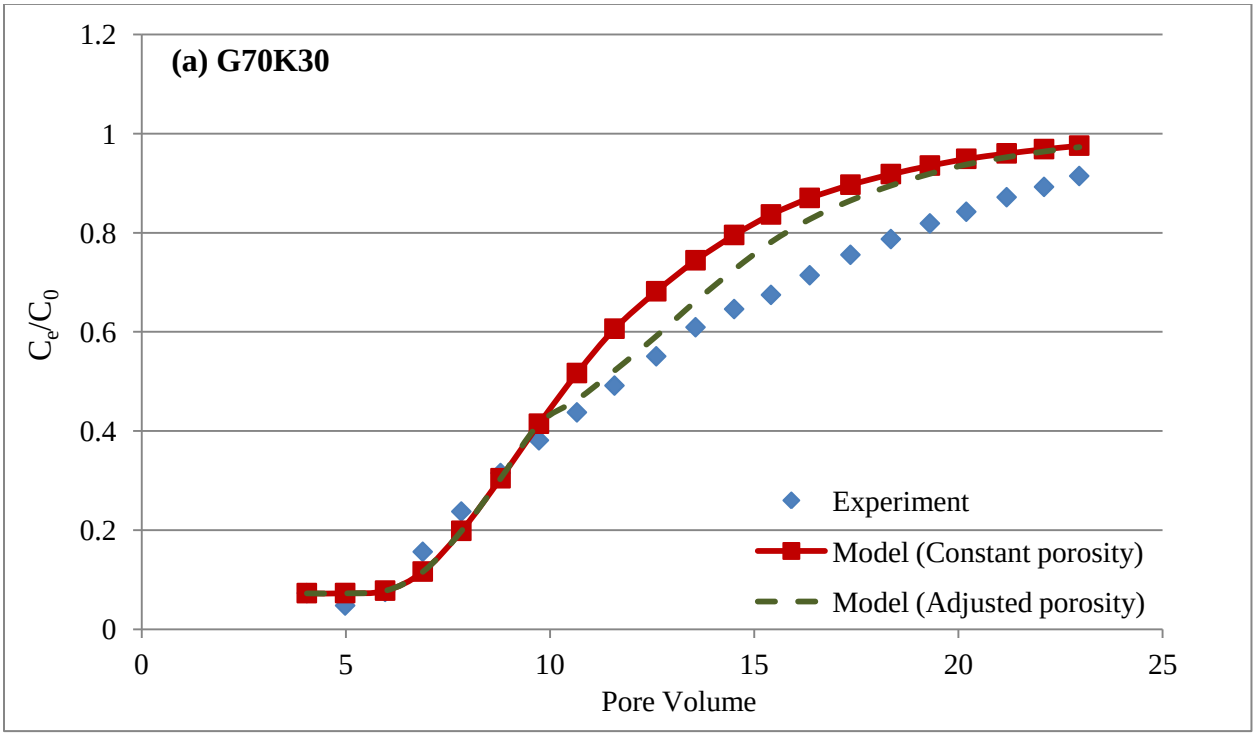

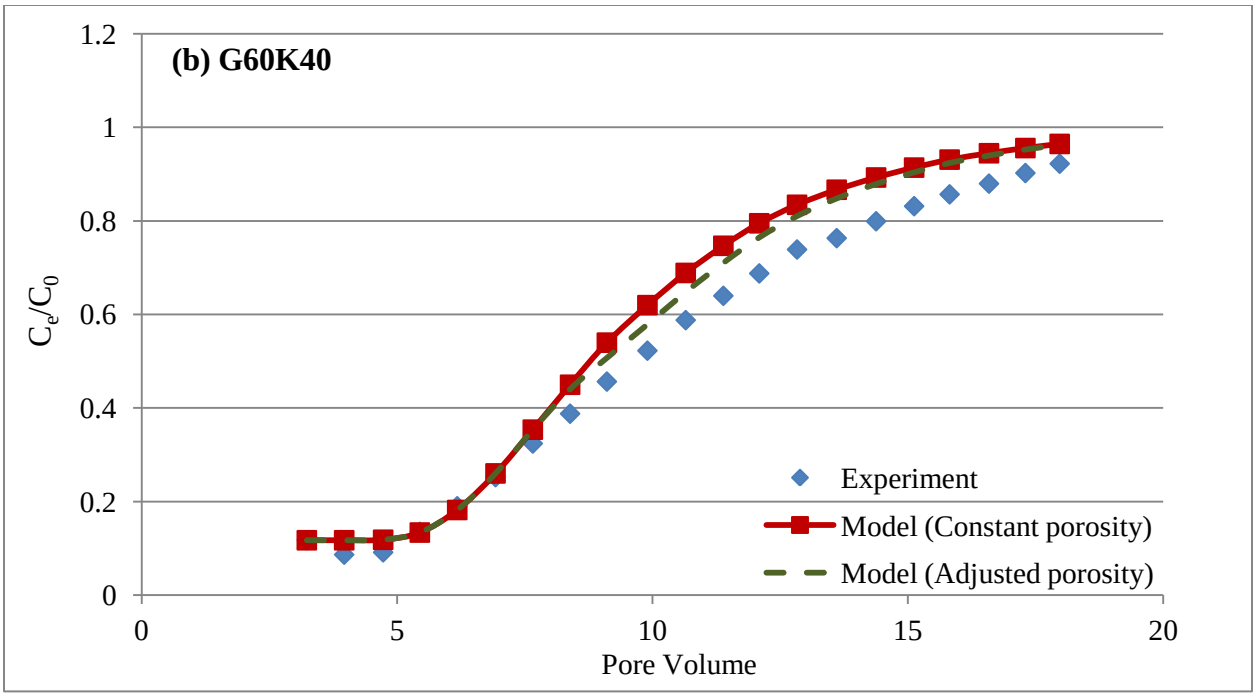

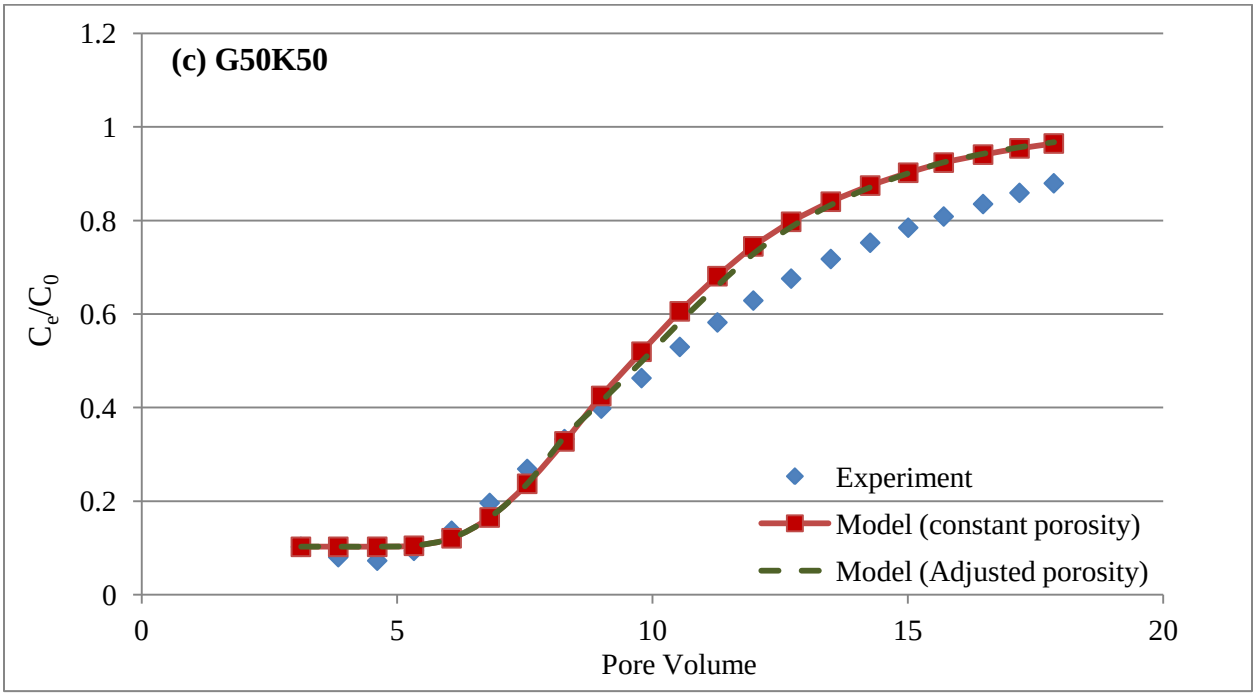

Figure 4.18: Sodium breakthrough curves (Adjusted porosity)

The results indicate that the discrepancy between experimental relative concentrations and model output decreased by considering variable Darcy velocity but they still did not match perfectly, suggesting that there could be some other parameters besides porosity and hence Darcy velocity governing the model results. These parameters may include change in the diffusion coefficient and distribution coefficient or the existence of different diffusion coefficient or distribution coefficient in different soil layers, which were considered constant throughout the sample thickness and test duration. Figure 4.20 shows sensitivity analysis based on change in diffusion coefficient and distribution coefficient; according to the result the model is noticeably sensitive to these two parameters. Further studies may be required to determine if each effective parameter used in the modelling remains constant during landfill operation or it changes and if it changes, how the model can be affected by variability in this parameter. It is very important to consider the field condition as much as possible in modelling to have a good estimation of contaminant concentration as the overestimation of solute loadings could result in a costly design. On the other hand, the effects of under estimation could have greater consequences beyond financial issues and can have serious effect on local environment and human health.

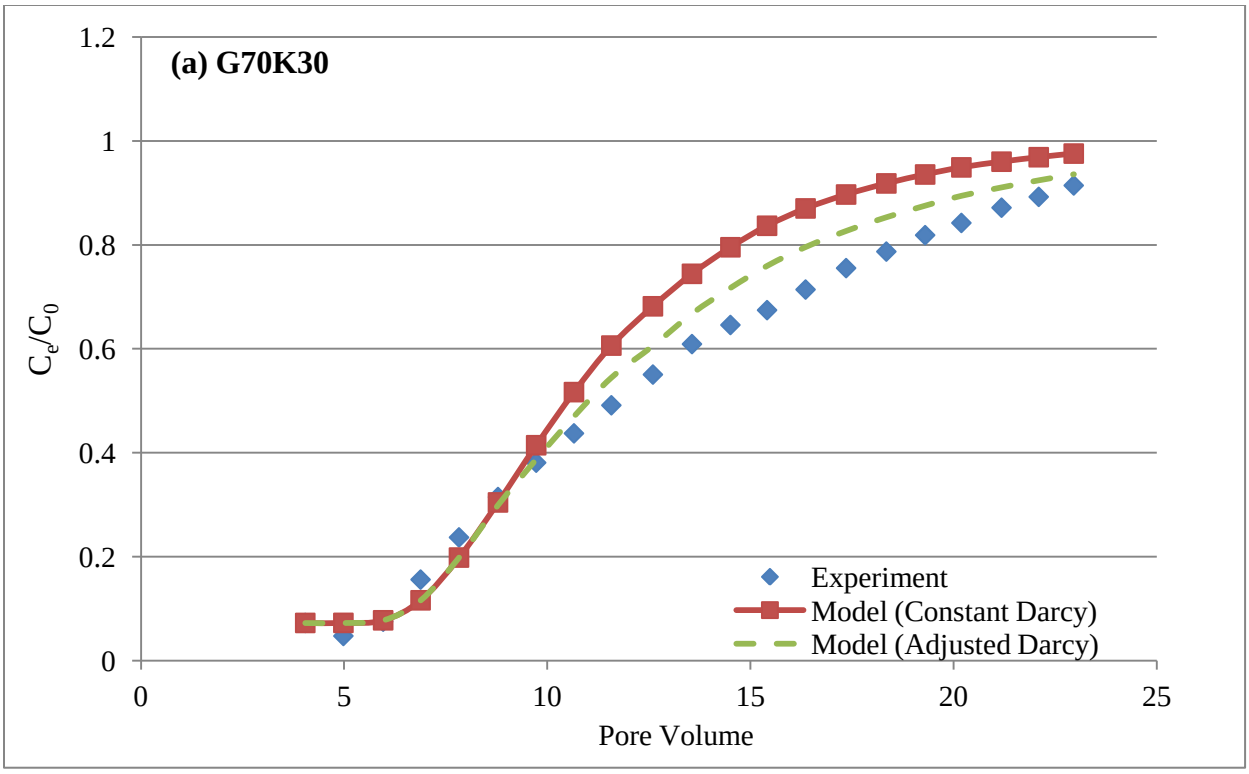
(a) G70K30
1.2
1
0.8
0.6
0.4
0.2
0
C_e/C_0
0
5
10
15
20
25
Pore Volume
Experiment
Model (Constant Darcy)
Model (Adjusted Darcy)

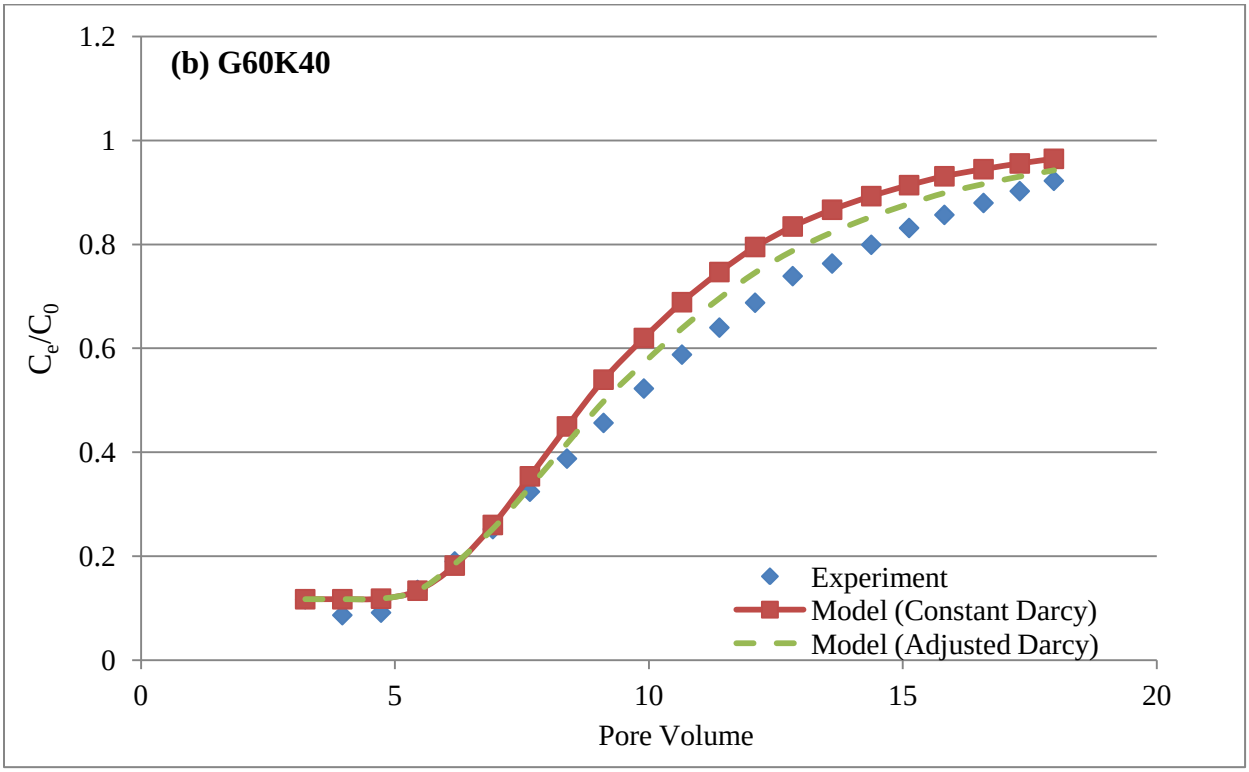
(b) G60K40
1.2
1
0.8
0.6
0.4
0.2
0
C_e/C_0
0
5
10
15
20
Pore Volume
Experiment
Model (Constant Darcy)
Model (Adjusted Darcy)

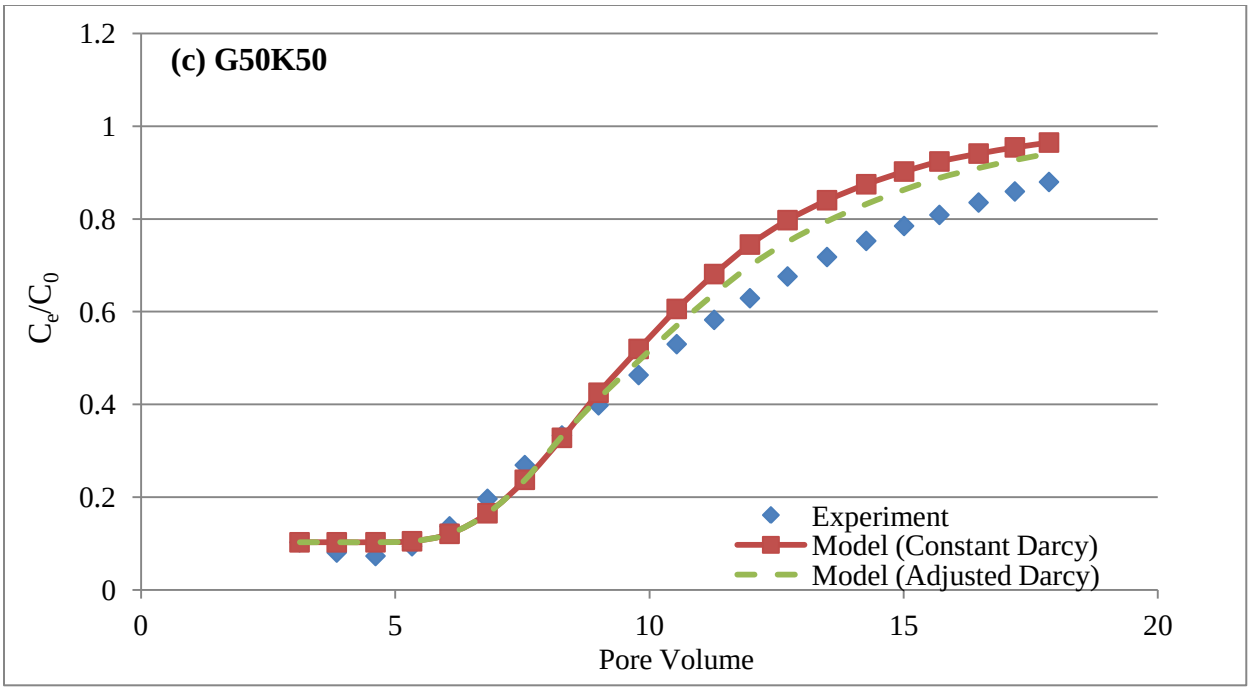

Figure 4.19: Sodium Breakthrough Curves (Adjusted Darcy velocity)

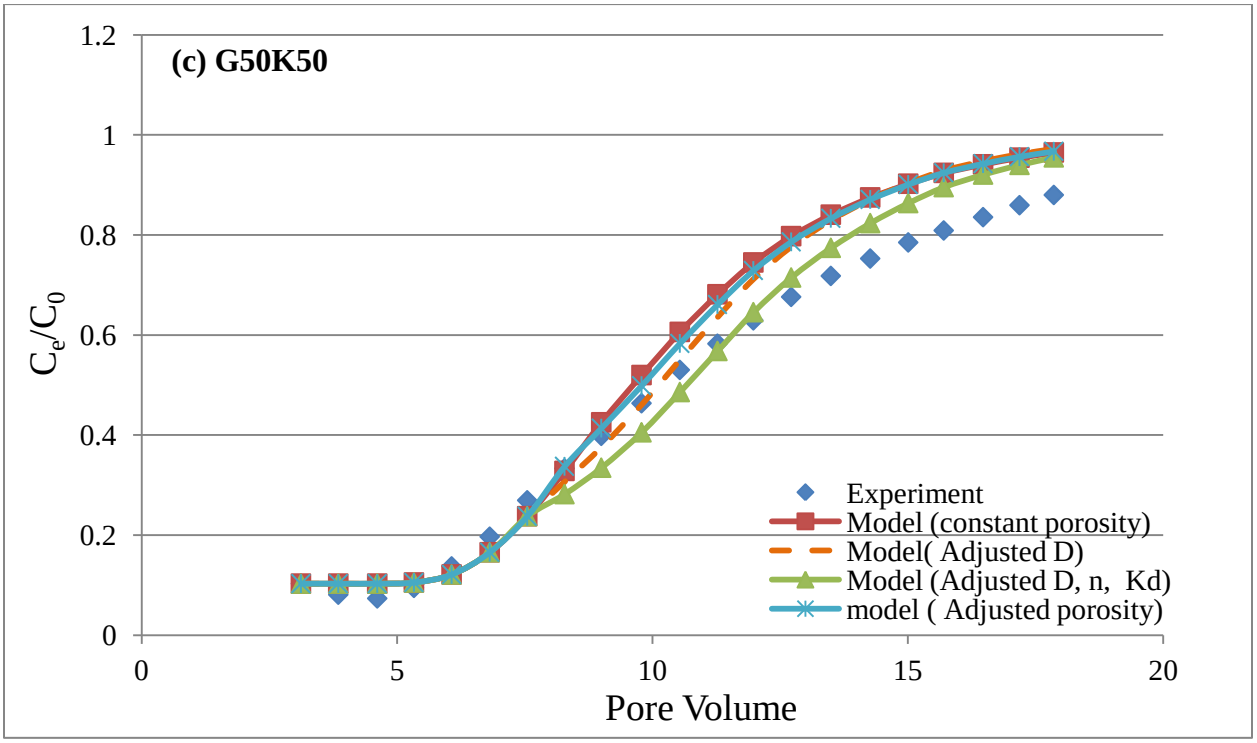

Figure 4. 20: Sodium breakthrough curves (Sensitivity analysis)

Chapter 5

Conclusion and Recommendations

5.1. Conclusion

This study aimed to evaluate the porosity of compacted glass beads-kaolinite soil samples before and after hydraulic conductivity testing. Hydraulic conductivity was considered to be one of the effective parameters used in modelling of solute breakthrough curves in an attempt order to assess part of the discrepancy between experimental results and modelling outputs observed in previous studies.

The results of mercury intrusion porosimetry (MIP) tests showed a decrease in the porosity of soil samples after permeation with sodium chloride solution. Initial porosity obtained from the MIP test was also less than calculated values from samples, properties which were probably as a result of voids that were totally enclosed within solid materials and had no exchange with the pore space that had continuity to boundaries of the medium. These kinds of pores were not accounted for in the MIP result since no mercury was intruded into them. Three different mixtures of glass beads and kaolinite were tested to evaluate the effect of clay size percentage in the pore size distribution change but according to the results, no clear relationship was found between the fraction of clay and change in porosity. In other words, more clay did not lead to a greater decrease in porosity. The decrease in porosity results in less pores available for solution flow and, therefore, in a lower Darcy velocity; therefore, additional modelling was performed using a variable Darcy velocity instead of a constant value and the output was found to be closer to experimental results. It can be concluded from the results that the Darcy velocity should not be considered to be constant and that a proper time period must be defined with different Darcy

velocity values specified for various times. However, there was still an overestimation of solute concentrations by the model showing that there were other processes that occurred during testing that were not accounted for in the model.

More studies are required to monitor other effective parameters that could influence the modelling, such as distribution coefficient and diffusion coefficient of the solutes during test and throughout the sample thickness.

It is very important to select the input parameters that are as close to real-life conditions as possible in order to approximate field values to prevent unrealistic predictions of contaminant concentrations and loadings, which could lead to costly monitoring and remediation.

5.2. Recommendations for Future Studies

Modelling of solute breakthrough curves with variable properties is an evolving concept and more research needed to improve applications for industry application. The following recommendations may be considered in future studies:

1) Hydraulic conductivity tests can be run on the same samples in different cells and mercury intrusion porosimetry test may be performed at different times to monitor changes in the pore size distribution structure.

2) The distribution coefficient and diffusion coefficient of solutes during hydraulic conductivity testing and in different layers of compacted samples should be monitored.

3) Perform tests with natural soil and real leachate to evaluate the effect of processes such as mineral dissolution, chemical and mineral precipitation.

References

- Aarne Vesilind p., W. Worrell, D. Reinhart, "*Solid waste engineering*", copyright 2002
- Ahmed, A. M. and Sulaiman, W. N., *"Evaluation of Groundwater and Soil Pollution in a Landfill Area Using Electrical Resistivity Imaging Survey"*, Environ. Manage. 28, 655–663, (2001).
- Anderson, D., Brown, K., Thomas, J., *"Conductivity of compacted clay soils to water and organic liquids",* Waste Management & Research 3 (4), 339–349, (1985).
- Aziz, H.A., M.S. Yussff, M.N. Adlan, N.H. Adnan, S. Alias, "*Physico-chemical removal of iron from semi-aerobic leachate by limestone filter*", Waste Manage., 24, 353–358 (2004).
- Baig S., I. Coulomb, P. Courant, P. Liechti, "*Treatment of landfill leachates: Lapeyrouse and Satrod case studies*", Ozone Sci. Eng. 21, 1–22 (1999).
- Baker, E., E. Bournay, A. Harayama, P. Rekacewicz, *"Vital Waste Statistics",* UNEP (2004).
- Barlaz, M. A. and R. K. Ham, *"Leachate and gas generation, in Geotechnical Practice for Waste Disposal"*, D. E. Daniel, Ed., Chapman and Hall, London, 113, 1993.
- Barlaz, M. A., R. K. Ham, and D. M. Schaefer, *"Mass balance analysis of decomposed refuse in laboratory scale lysimeters"*, ASCE J. Environ. Eng., 115, 1088, 1989b.
- Barlaz, M. A., R. K. Ham, and D. M. Schaefer, *"Methane Production from Municipal Refuse: A Review of Enhancement Techniques and Microbial Dynamics"*, CRC Crit. Rev. Environ. Contr., 19, 6, 557, 1990.
- Barlaz, M.A., D. M. Schaefer, and R. K. Ham, *"Bacterial Population Development and Chemical Characteristics of Refuse Decomposition in a Simulated Sanitary Landfill"*, Appl. Environ. Microbiol., 55, 55, 1989a.
- Barone, F.S., R. K. Rowe, and R. M. Quigley, *"A laboratory estimation of diffusion and adsorption coefficients for several volatile organics in a natural clayey soil"*. Journal of Contaminant Hydrology, 10: 225-250, (1992).
- Batchelder M, G. Cressey and J. B. Joseph *"Assessing mineral proportions in mudrock barriers"* Proc Sardinia 97, Sixth Int'l Landfill Symposium, S. Margherita di Pula, Cagliari, Italy; III, 25-32; Oct (1997a).
- Batchelder M., G. Cressey and J. B. Joseph *"Clay mineral transformation reactions within landfills and their implications for landfill containment"*, Special Publication of the Journal of the Geological Society, (1997b).
- Baumgarten G., C.F. Seyfried, "*Experiences and new developments in biological pretreatment and physical post-treatment of landfill leachate*", Water Sci. Technol., 34, 445–453(1996).
- Baun A., L. A. Reitzel, A. Ledin, T. H. Christensen, P. L. Bjerg, *"Natural attenuation of xenobiotic organic compounds in a landfill leachate plume (Vejen, Denmark)".* J Contam Hydrol, 65:269–91, (2003).
- Berger, W., U. Kalbe, J. Goebbels, "*Fabric studies on con-Fig. 6. Transport of toluene in three composite liners-cumulative mass discharged (adapted from Foose et al., 2002)"* , T.B. Edil /Waste Management 23, 561–571 569 taminated minerals layers in composite liners. Applied Clay Science 21, 89–98, (2003).
- Bjerg, P. L., K. Rugge, J. K. Pedersen, and T. H. Christensen, *"Distribution of Redox-Sensitive Groundwater Quality Parameters Downgradient of a Landfill (Grindsted, Denmark)"*, Environ.Sci. Technol. 29, 1387–1394, (1995).
- Blight, G.E., A. B. Fourie, J. Shamrock, C. Mbande, and J. W. F. Morris, *"The effect of waste composition on leachate and gas quality: a study in South Africa*", Waste Management Research, 17, 124-140, (1999).
- Bohdziewicz J., M. Bodzek, J. Gorska, "*Application of pressure-driven membrane techniques to biological treatment of landfillleachate",* Process Biochem., 36, 641–646 (2001).

- Bookter, T.J. and R. K. Ham, *"Stabilization of solid waste in landfills",* ASCE J. Environ. Eng., 108, 1089 (1982).
- Bou-Zeid, E., M. El-Fadel, *"Parametric sensitivity analysis of leachate transport simulations at landfill*s", Waste Management 24, 681–689, (2004).
- Bowders, J., D. Daniel,. *"Hydraulic conductivity of compacted clay to dilute organic chemicals",* J. Geotech. Engr. 113 (12), 1432–1449 (1987).
- Bozkurt, S., L. Moreno, and I. Neretnieks, *"Long-Term Processes in Waste Deposits",* Sci. Total Environ., 250, 101, (2000).
- Britz, T.J. "*Landfill leachate treatment*". In Microbiology of landfill sites. 2nd Edition. Edited by E. Senior. 2nd Edition. CRC Press Inc., Boca Raton, Florida, USA. 131-164, (1995).
- Brown, K., J. Thomas, "*A comparison of the convective and diffusive flux of organic contaminants through landfill liner systems*", Waste Management Research, 16 (3), 296–301 (1998).
- Cancelli, A., R. Cossu, F. Malpei, and A. Offresi, "*Effects of leachates on the permeability of sand-bentonite mixtures",* In Hydraulic barriers in soil and rock. ASTM STP 874. Edited by A.I. Johnson, R.K. Frobel, N.J. Cavalli and C.B. Pettersson. American Society for Testing and Materials, Philadelphia. 259-295, (1995).
- Cariera, C. and C. Masciopinto, "*Assessment of Groundwater after Leachate Release from Landfills"*, Annali di Chimica 88, 811–818 (1998).
- Carrier W.D., "*Goodbye, Hazen; Hello, Kozeny-Car- man*", Journal of Geotechnical and Geoenvironmental Engineering, Vol. 129, No. 11, 1054-1056 (2003).
- Ceçen, F., O. Aktas, *"Aerobic co-treatment of landfill leachate with domestic wastewater",* Environ. Eng. Sci., 21, 303–312, (2004).
- Chalermtanant T, S. Arrykul, N. Charoenthaisong, *"Potential use of lateritic and marine soils as landfill liners to retain heavy metals".* Waste Manag., 29:117–27, (2009).
- Cherry, J. A., R. J. Gillham, J. F. Braker, "Contaminants in groundwater: chemical processes.", Studies in geophysics, groundwater contamination, National Academy Press, Washington, D. C., 46-64, (1984).
- Chian, E. S. K., F. B. DeWalle, *"Sanitary landfill leachates and their treatment"*, J. Environ. Eng. Div. 411–431, (1976).
- Chianese, A., R. Ranauro, N. Verdone, *"Treatment of landfill leachate by reverse osmosis",* Water Res., 33, 647–652, (1999).
- Cho S.P., S.C. Hong, S. Hong, "*Photocatalytic degradation of the landfill leachate containing refractory matters and nitrogen compounds*", Appl. Catal. B: Environ., 39, 125–133 (2002).
- Cho, W. J., J.O. Lee, K.S. Chun, "The temperature effects on hydraulic conductivity of compacted bentonite", Applied Clay Science, Volume 14, Issues 1–3, 47–58, February (1999)
- Christensen, T.H. and P. Kjeldsen, *"Basic biochemical processes in landfills".* Chapter 2.1 in Sanitary Landfilling: Process, Technology and Environmental Impact, Christensen, T.H., Cossu, R., and Stegmann, R., Eds., Academic Press, London, UK, 29, (1989).
- Christensen, T.H. and P. Kjeldsen, *"Landfill emissions and environmental impact: An introduction",* in SARDINIA '95*",* Fifth International Landfill Symposium, Proceedings, Volume III, Christensen,T.H., Cossu, R., and Stegmann, R., Eds., CISA, Cagliari, Italy, (1995).
- Christensen, T.H., P. Kjeldsen, and R. Stegmann, *"Effects of landfill management procedures on landfill stabilization and leachate and gas quality",* Chapter 2.7 in Landfilling of Waste:Leachate, Christensen, T.H., Cossu, R., and Stegmann, R., Eds., Elsevier Applied Science,London, UK, 119, (1992).
- Crittenden B. and S. Kolaczkowski, *"Waste minimization: a practical guide"*, Institution of Chemical Engineers, Rugby, (1995).
- Crooks, V. E., R. M. Quigley, *"Saline leachate migration through clay: a comparative laboratory and field investigation".* Canadian Geotechnical Journal 21, 349–362, (1984).
- Daniel, D., *"Predicting hydraulic conductivity of clay liners",* J. Geotech. Engr. 110 (2), 285–300, (1984).

- Di Palma L., P. Ferrantelli, C. Merli, E. Petrucci, "*Treatment of industrial landfill leachate by means of evaporation and reverse osmosis*", Waste Manage., 22, 951‑955 (2002).
- Dodson, J. R., A. J. Hunt, H. L. Parker, Y. Yang, J. H. Clark, *"Elemental sustainability: Towards the total recovery of scarce metals"*, Chemical Engineering and Processing: Process Intensification, 51, 69-78, (2012).
- ECLAC Subregional Headquarters for the Caribbean, Port of Spain, December 2011, http://www.eclac.cl/publicaciones/xml/3/45473/LCARL.349.pdf
- Edil T. B., *"A review of aqueous-phase VOC transport in modern landfill liners".* Waste Manage, 23(7), 561–71, (2003).
- Ehrig, H.-J., *"Water and element balances of Landfills"*, in the landfill, Baccini, P., Ed., Springer Verlag, Berlin, Germany, 83. (Lecture Notes in Earth Sciences, Vol. 20), (1988).
- El-Fadel, M., A. Findikakis, J. Leckie, "*Modeling leachate generation and transport an solid waste landfills"*. Environmental Technology 18, 669–686, (1997b).
- El-Fadel, M., A. N. Findikakis & J. O. Leckie, "*Modeling Leachate Generation and Management of Municipal Solid Waste*", (1997).
- El-Fadel, M., A. N. Findikakis and J. O. Leckie, *"Environmental Impacts of Solid Waste Landfilling"* Department of Civil Engineering, Stanford University, Stanford, California, (1995).
- Emberton, J.R, "*The biological and chemical charactization of landfills*". In: Energy from landfill gas, Emberton, J.R. and Emberton, R.F. (eds.), Solihull, UK, 150-163 (1986).
- Environmentalists Every Day, *"History of Solid Waste Management"*, (2011).
- Environmentalists Every Day, *"solid waste management, components of a landfill",* (2012).
- EPA, "*Municipal Solid Waste Generation, Recycling and Disposal in the United States: Facts and Figures for 2008*", Washington, (2009).
- Eurostat, *"Treatment of municipal waste (Landfill, incineration)"*, European Commission, 1997–2010.
- Farquhar, G.J., F. A. Rovers, "*Gas production during refuse decomposition*". Water, Air and Soil Pollution, 2(10): 483-489, (1973).
- Fatta, D., A. Papadopoulos, and M. Loizidou, "*A Study on the Landfill Leachate and its Impact on the Groundwater Quality of the Greater Area*", Environ. Geochem. Health 21, 175–190 (1999).
- Fernandez, F., and R.M. Quigley, "*Hydraulic conductivity of natural clays permeated with simple liquid hydrocarbons*" Can. Geotech. J., 22, 205–214 (1985).
- Fernandez, F., R. Quigley, "*Viscosity and dielectric constant controls on the hydraulic conductivity of clayey soils permeated with water-soluble organics*". Can. Geotech. J. 25, 582–589 (1988).
- Foose G.J., C.H. Benson, T.B. Edil, "*Analytical methods for predicting concentration and mass flux from composite landfill liners*", Geosynthetics International, 8 (6), pp. 551–575 (2001).
- Foose G.J., C.H.Benson, T.B. Edil, "*Comparison of solute transport in three composite liners"*, J Geotech Geoenviron, 128(5):391–403 (2002).
- Foose, G. J., "*Leakage rates and chemical transport through composite liners*". PhD dissertation, Deparment of Civil and Environmental Engineering, University of Wisconsin Madison (1997).
- Foose, G.J., C.H. Benson, T.B. Edil, "*Comparison of solute transport in three composite liners*". Journal of Geotechnical and Geoenvironmental Engineering, ASCE 128 (5), 391–403 (2002).
- Frascari, D., F. Bronzini, G. Giordano, G. Tedioli, M. Nocentini, *"Long-term characterization, lagoon treatment and migration potential of landfillleachate: a case study in an active Italian landfill",* Chemosphere, 54, 335–343, (2004).
- Freeze, R. A., and J. A. Cherry, "Groundwater", Prentice-Hall, Englewood Cliffs, N.J., (1979).
- Frempong, E.M., M. Asce, E.K. Yanful, "*Interactions between Three Tropical Soils and Municipal Solid Waste Landfill Leachate*", 134(3), 379-396 (2008).

- Friedman, F. A., *"Volatile Organic Compounds in Groundwater and Leachate at Wisconsin Landfills"*, Wisconsin Department of Natural Resources, Rep. PUBL-WR-192-88, Madison, WI (1988).
- Gallorini, M., M. Pesavento, A. Profumo, and C. Riolo, C, "Analytical Related Problems in Metal and Trace Elements Determination in Industrial Waste Landfill Leachates", Sci. Total Environ. 133, 285–298 (1993).
- Ghosh, D., G. K. Bhattacharyya, "Adsorption of methylene blue on kaolinite", Applied Clay Science, Volume 20, Issue 6, 295–300, February (2002).
- Giroud, J.P., and R. Bonaparte, "*Leakage through liners constructed with geomembranes – Part II*". Composite liners. Geotextiles and Geomembranes, 8(2): 71-111 (1989).
- Haijian X, C. Yunmin, K. Han, T. Xiaowu, C. Renpeng, "*Analysis of diffusion–adsorption equivalency of landfill liner systems for organic contaminants*", J Environ Sci, 21, 552–60 (2009).
- Halvadakis C.P., A.p. Robertson and J.O. Leckie, "Landfill methanogenesis; literature review and critique", Tech. Rep. 271 Dept.Civ.Engrg, Stanford university, CA (1983).
- Harmsen, J., "Identification of organic compounds in leachate from a waste tip", Water Res., 17, 699(1983).
- Haxo, H.E., T.P. Lahey, "*Transport of dissolved organics from dilute aqueous solutions through flexible membrane liners*", Hazardous Waste and Hazardous Materials, 5 (4), 275–294 (1988).
- Head, K.H., "Manual of soil laboratory testing Vol. 1 – Soil classification and compaction tests". John Wiley & Sons, Toronto (1980).
- Henry J.G., D. Prasad, H. Young, "*Removal of organics from leachates by anaerobic filter*", Water Res., 21, 1395–1399 (1987).
- Hoeks, J. and J. Harmsen, "Methane gas and leachate from sanitary landfills". In Research Digest,(E. W. Schierbeek, ed.), Wageningen, Netherlands: ICW, pp. 32 (1980).
- Hoilijoki T.H., R.H. Kettunen, J.A. Rintala, "*Nitrification of anaerobically pretreated municipal landfill leachate at low temperature*", Water Res., 34, 1435–1446 (2000).
- Holtz R.D., and W. D. Kovacs, *"An Introduction to Geo- technical Engineering,"* Prentice-Hall, Englewood Cliffs, (1981).

http://www.epa.gov/osw/nonhaz/municipal/landfill.htm [Cited 9 July 2012]

- http://www.oecd.org/officialdocuments/displaydocumentpdf/?cote=env/epoc/wgwpr/se(2004)1/final&doclanguage=en
- Ikem, A., O. Osibanjo, M.K.C. Sridhar, and A. Sobande, *"Evaluation of Groundwater Quality Characteristics near Two waste Sites in Ibadan and Lagos, Nigeria"*, Water, Air, and Soil Poll, 140: 307–333. Kluwer Academic Publishers, the Netherlands, (2002).
- Im J.H., H.-J. Woo, M.-W. Choi, K.-B. Han, C.-W. Kim, "*Simultaneous organic and nitrogen removal from municipal landfill leachate using an anaerobic–aerobic system*", Water Res., 35, 2403–2410 (2001).
- Joseph J.B., Styles J R, S T S YUEN AND G CRESSEY, "*Variation in clay mineral perfomance in the presence of leachates "*, CISA Environmental Sanitary Engineering Centre, volume 3, 255-264 (2001).
- Joseph, J.B., J.R. Styles, S.T.S. Yuen, and G. Cressey, "*Variations in clay mineral performance in the presence of leachates*". In Proceedings of the Eigth International Landfill Symposium, Sardinia 2001, Italy, October 2001 [online]. Available from http://www.civag.unimelb.edu.au/~syu/others/papers/sardic01.pdf. [cited 15 February 2003].
- Kalbe U, W. Muller, W. Berger, J. Eckardt, "*Transport of organic contaminants within composite liner systems*". Appl Clay Sci;21, 67–76 (2002).
- Kargi, F., M. Pamukoglu, *"Simultaneous adsorption and biological treatment of pre-treated landfill leachate by fed-batch operation",* Process Biochem., 38, 1413–1420, (2003).

- Kennedy, K.J., E.M. Lentz, "*Treatment of landfill leachate using sequencing batch and continuous flow upflow anaerobic sludge blanket (UASB) reactors*", Water Res., 34, 3640–3656 (2000).
- Khan, R., T. Husain, H. U. Khan, S.M. Khan and A. Hoda, A, "*Municipal Solid Waste Management – A Case Study*', Municipal Engin. 7, 109–116 (1990).
- Kile, D. E., C.T. Chiou, H. Zhou, H. Li, O. Xu, *"Partitioning of nonpolar organic pollutants from water to soil and sediment organic matters",* Environ. Sci. & Technol., 29 (5), 1401–1406, (1995).
- Kim, J.Y., T.B. Edil, J.K. Park, "*Volatile organic compound (VOC) transport through compacted clay*". Journal of Geotechnical and Geoenvironmental Engineering, ASCE 127 (2), 126–134 (2001).
- Kjeldsen P, M. A. Barlaz, A.P. Rooker, A. Baun, A. Ledin & T.H. Christensen, "*Present and Long-Term Composition of MSW Landfill Leachate*", A Review, Critical Reviews in Environmental Science and Technology, 32 (4), 297-336 (2002).
- Kunkle, G. R. and J.W. Shade, "*Monitoring Groundwater Quality Near a Sanitary Landfill*", Groundwater 14, 11–20 (1976).
- Lacoste E., and P. Chalmin, "*From Waste to Resource – An Abstract of the 2006 World Waste Survey*" Economica, Paris (2007).
- Lau I.W.C., P. Wang, H.H.P. Fang, "*Organic removal of anaerobically treated leachate by Fenton coagulation*", J. Environ. Eng. Sci., pp. 666–669 (2001).
- Leckie J.O., J.G. Pacey and Halvadakis C.p., "*Landfill management with moisture control*", J.Env.Eng.Div., ASCE, 105, 337-355 (1979).
- Lema J.M., R. Mendez, R. Blazquez, "*Characteristics of landfill leachates and alternatives for their treatment*", a review Water Air Soil Pollut., 40, 223–250 (1988).
- Li X.Z., Q.L. Zhao, "*Efficiency of biological treatment affected by high strength of ammonium-nitrogen inleachate and chemical precipitation of ammonium-nitrogen as pretreatment*", Chemosphere, 44, 37–43 (2001).
- Lo I., *"Characteristics and treatment of leachates from domestic landfills",* Environ. Int., 22, pp. 433–442 (1996).
- Lo I.M.C., A.F.T. Luk, X. Yang, "*Migration of heavy metals in saturated sand and bentonite/soil admixture*". J Environ Eng., 130(8), 906–9 (2004).
- Loizidou, M. and E.G. Kapetanios, "*Effect of Leachate from Landfills on Groundwater Quality*" , Sci. Total Environ. 128, 69–81(1993).
- Lopez, A., M. Pagano, A. Volpe, A. Di Pinto, *"Fenton's pre-treatment of mature landfill leachate",* Chemosphere, 54, 1005–1010, (2004).
- Lu HJ, M.T. Luan, J.L. Zhang, "*Study on transport of Cr(IV) through the landfill liner composed of two layer soils*". Desalination, 266(1–3), 87–92 (2011).
- Lu, J.C.S., B. Einchenberger, and R.J. Steams, "*Leachate from municipal landfills – production and management*. Pollution Review Technology, 119, 259-289 (1985).
- Marttinen S.K., R.H. Kettunen, K.M. Sormunen, R.M. Soimasuo, J.A. Rintala, "*Screening of physical–chemical methods for removal of organic material, nitrogen and toxicity from low strength landfill leachates*", Chemosphere, 46, 851–858 (2002).
- Mitchell, J. K., "Fundamentals of soil behavior" 2nd Ed., John Wiley and sons. Inc., New York. N. Y., (1993).
- Mitchell, J.K., "*Fundamentals of soil behaviour*". Second Edition. John Wiley and Sons, Inc., New York. 400 (1993).
- Mueller, W., R. Jakob, R. Tatzky-Gerth,, "*Solubilities, diffusion and partition coefficients of organic pollutants in HDPE geomembranes: experimental results and calculations*". In: Proceedings of the Sixth

International Conference on Geosynthetics, Atlanta, Industrial Fabrics Association International, St. Paul, MN, 239‑248 (August 1998).

- Myrand, D., R.W. Gillham, E.A. Sudicky, S.F. O'Hannesin and R.L. Johnson, "*Diffusion of volatile organic compounds in natural clay deposits: laboratory tests*", Journal of Contaminant Hydrology, 10, 159-177 (1992).
- OECD Environmental Data: Compendium 2006–2008, OECD, (2008).
- OECD Environmental Outlook to 2030: Consequences of Policy Inaction, OECD, (2008).
- OECD, "*Addressing the economics of wastes, organisation of economic cooperation and development,ECD*", Paris (2004).

- OECD, Sector case studies, "*household energy and water consumption and waste generation: trends, environmental impacts and policy responses, (ENV/EPOC/WPNEP15/FINAL)".* Organisation for Economic Cooperation and Development Environment Directorate 1999–2001 Programme on Sustainable Development, OECD, Paris, France, 56–83 (2001).
- Orupold, K., T. Tenno, T. Henrysson, "*Biological lagooning of phenols-containing oil shale ash heaps leachate*", Water Res., 34, 4389–4396 (2000).
- Ozturk I., M. Altinbas, I. Koyuncu, O. Arikan, C. Gomec-Yangin, "Advanced physico-chemical treatment experiences on young municipal landfill leachates", Waste Manage., 23, pp. 441–446 (2003).
- Park J.K., J.P. Sakti, J.A. Hoopes, "Transport of organic compounds in thermoplastic geomembranes Imathematical model", Journal of Environmental Engineering, ASCE, 122 (9), pp. 800–806 (1996).
- Park, J.K., M. Nibras, "Mass flux of organic chemicals through polyethylene geomembranes", Water Environment Research, Washington, DC, 65 (3), 227–237 (1993).
- Parker, A. and G.M. Williams. "*Landfill site selection and operation from municipal and hazardous waste disposal*". In Developments in Environmental Control and Public Health, (A. Porteous, ed.), London,UK: Applied Science Publishers, 1–37 (1981).
- Pohland, F. G. and S.R. Harper, "*Critical review and summary of leachate and gas production from landfills*", EPA/600/2-86/073, PB86–240181 (1986).
- Pohland, F.G., and S.R.Harper, "*Critical review and summary of leachate and gas production from landfills".* USEPA Report No. EPA/600/2-86/073. USEPA, Cincinnati (1985).
- Porter R.C., "*The Economics of Waste" Resources for the Future"*, Washington DC (2002).
- Public Administration Service, "*Municipal refuse disposal*", Prepared for the Institute for Solid Wastes of America Public Works Association (1970).
- Qasim, S.R., and W. Chiang, "*Sanitary landfill leachate*", Technomic Publishing Co., Inc., Lancaster, USA (1994).
- Quigley R.M, F. Fernandez and R.K. Rowe, "*Clayey barrier assessment for impoundment of domestic waste leachate (southern Ontario) including clay/leachate compatibility by hydraulic conductivity*", Canadian Geotechnical Journal, 25, 574-581(1988).
- R. Gourdon , C. Comel, P. Vermande, J. Veron, "*Fractionation of the organic matter of a landfill leachate before and after aerobic or anaerobic biological treatment*", Water Res., 23, 167–173(1989).
- Reinhart, D.R. and C.J. Grosh, "*Analysis of Florida MSW landfill leachate quality*", Florida Center for Solid and Hazardous Management, Gainesville, FL, (1998).
- Reinhart, D.R., "*A review of recent studies on the sources of hazardous compounds emitted from solid waste landfills: a US experience*", Waste Management Research, 11, 257-268 (1993).
- Reinhart, D.R., and Grosh, C.J., "*Analysis of Florida MSW landfill leachate quality*", Florida Center for Solid and Hazardous Waste Management Report #97-3, 14-21 (July 1988).
- Renoua, S., J.G. Givaudana, S. Poulaina, F. Dirassouyanb, P. "Moulinc Landfill leachate treatment: Review and opportunity", Journal of Hazardous Materials 150, 468–493 (2008).

- Rivas, F. J., F. Beltran, O. Gimeno, B. Acedo, F. Carvalho, *"Stabilized leachates: ozone-actived carbon treatment and kinetics"*, Water Res., 37, 4823–4834, (2003).
- Robinson, H. and J. Gronow, J., "*Groundwater Protection in the U.K.: Assessment of the Landfill Leachate Source-Term*", Institute of Water Engineers and Managers 6, 229–236 (1992).
- Robinson, H.D., "*A review of the composition of leachates from domestic wastes in landfill sites".* A report prepared by Aspinwall Company for the Department of the Environment, UK., 511(1995).
- Robinson, H.D., "The technical aspects of controlled waste management". A review of the composition of leachates from domestic wastes in landfill sites. Report for the UK Department of the Environment. Waste Science and Research, Aspinwall & Company, Ltd., London, UK, (1995).
- Rowe R.K., "*Pollutant Transport through Barriers*". Proceedings of the Geotechnical Practice for Waste Disposal, Special Publication, 13, (Ed. R D Woods), ASCE, 159-184 (1987).
- Rowe, R.K., "*Geosynthetics and the minimization of contaminant migration through barrier systems beneath solid waste"*. In: Proceedings of the Sixth International Conference on Geosynthetics, Atlanta, Industrial Fabrics Association International, St. Paul, MN, pp. 27–102 (1998).
- Rowe, R.K., "*Long-term performance of contaminant barrier systems*" ,Geotechnique 55, No. 9, 631–678 (2005).
- Rowe, R.K., Hrapovic, L., Kosaric, N., "*Diffusion of chloride and dichloromethane through an HDPE geomembrane*". Geosynthetics International 2 (3), 507–536 (1995).
- Rowe, R.K., R.M. Quigley, and J.R. Booker, "*Clayey barrier systems for waste disposal facilities*". E & FN Spon, London. 390 (1995).
- Rowe, R.K., R.M. Quigley, and J.R. Booker, "*Clay-leachate compatibility by measurement of hydraulic conductivity*" Clay barrier systems for waste disposal facilities, Chap. 4, E & FN Spon,London (1995).
- Rowe, R.K., R.M. Quigley, R.W.I. Brachman & J.R. Booker, "*Barrier systems for waste disposal facilities*". London:Taylor & Francis (E & FN Spon), (2004).
- Shackelford, C.D., "*Transit-time design of earthen barriers*".Engineering Geology, Elsevier Publishing, Amsterdam 29, 79–94 (1990).
- Shackelford, C.D., and Redmond, L.R., "Solute breakthrough curves for processed kaolin at low flow rates", Journal of Geotechnical Engineering, 121(1), 17-32 (1995).
- Shakelford, C. D., "Waste-soil interactions that alter hydraulic conductivity". Hydraulic Conductivity and Waste Contaminant Transport in Soil, ASTM STP 1142, D. E. Daniel and Stephen J. Trautwein. Eds., ASTM, (1994a).
- Shakelford, C. D., Redmond P. L., "Solute breakthrough curves for processed Kaolin at low flow rates".
- Silva, A. C., M. Dezotti, G.L. Sant'Anna Jr., *"Treatment and detoxication of a sanitary landfill leachate",* Chemosphere, 55, 207–214, (2004).
- Sivapullaiah, P. V. and A. Sridharan, "Liquid Limit of Soll Mixtures" Geotechnieal Testing Journal, GTJODJ, Vol. 8, No. 3, 111-116, Sept. (1985).
- Slack, R. J., J.R. Gronow, and N. Voulvoulis, "*Household hazardous waste in municipal landfills: contaminants in leachate*". Science of the Total Environment, 337, 419-445 (2005).
- Slacka R.J., J.R. Gronowb, N. Voulvoulisa, "*Household hazardous waste in municipal landfills: contaminants in leachate*". Science of The Total Environment,Volume 337, Issues 1–3, 119–137 (January 2005).
- Tabet K., P. Moulin, J.D. Vilomet, A. Amberto, F. Charbit, "*Purification of landfill leachate with membrane processes*": preliminary studies for an industrial plant, Sep. Sci. Technol., 37, 1041–1063 (2002).

- Tatsi, A. A., A. I. Zouboulis, *"A field investigation of the quantity and quality of leachate from a municipal solid waste landfill in a Mediterranean climate (Thessaloniki, Greece)*", Division of Chemical Technology, Department of Chemistry, Aristotle University, GR-54006 Thessaloniki, Greece, 9 July (2002).
- Tatsi, A. A., A.I Zouboulis, "A field investigation of the quantity and quality of leachate from a municipal solid waste landfill in a Mediterranean climate (Thessaloniki, Greece)", Advances in Environmental Research 6, 207_219, (2002). http://www.sciencedirect.com/science/article/pii/S1093019101000521
- Tatsi, A. A., I. Zouboulis, K.A. Matis, P. Samaras, *"Coagulation–flocculation pretreatment of sanitary landfill leachates",* Chemospher, 53, 737–744, (2003).
- Thorton, S. F., J.H. Tellam, and D.N. Lerner, "*Attenuation of landfill leachate by UK Triassic sandstone aquifer materials. I: Fate of inorganic pollutant in laboratory column.*" J. Contam. Hydrol., 43, 327–354 (2000).
- Timur H., I. Ozturk, "Anaerobic sequencing batch reactor treatment of landfill leachate", Water Res., 33, pp. 3225–3230 (1999).
- Trebouet, D., J.P. Schlumpf, P. Jaouen, J.P. Maleriat, F. Quemeneur, *"Effect of operating conditions on the nano filtration of landfill leachates: pilot-scale studies",* Environ. Technol., 20, 587–596, (1999).
- Tuncer B. Edil, "*A review of aqueous-phase VOC transport in modern landfill liners",* Waste Management 23, 561–571(2003).
- United States Environmental Protection Agency. "*Municiple solid waste generation, landfill section*" (2012).
- United States Environmental Protection Agency. Wastes, Municiple solid waste section, Available from http://www.epa.gov/wastes/nonhaz/municipal/(2012) [Cited 15 July 2012]
- Uygur A., F. Kargi, *"Biological nutrient removal from pre-treated landfill leachate in a sequencing batch reactor"*, J. Environ. Manage, 71, 9–14, (2004).
- Van Dijk, L., G.C.G. Roncken, "*Membrane bioreactors for wastewater treatment: the state of the art and new developments*", Water Sci. Technol., 35, 35–41 (1997).
- Van Impe, W.F., "*Environmental Geotechnics: ITC 5 Activities – state-of-the-art*". In Proceedings of the Third International. Congress on Environmental Geotechnics, Lisboa, Portugal, 7-11 September 1998. A.A. Balkema, Rotterdam, Netherlands, 4, 1163–1187 (1998).
- Wang Z.P., Z. Zhang, Y.-J. Lin, N.-S. Deng, T. Tao, K. Zhuo, "*Landfill leachate treatment by a coagulation–photooxidation process*", J. Hazard. Mater., B95, 153–159 (2002).
- Wang, B., Y. Shen, *"Performance of an anaerobic baffled reactor (ABR) as a hydrolysis–acidogenesis unit in treating landfill leachate mixed with municipal sewage*", Water Sci. Technol., 42, 115–121, (2000).
- Wu J.J., C. Wu, H. Ma, C.C. Chang, "*Treatment of landfill leachate by ozone-based advanced oxidation processes*", Chemosphere, 54, 997–1003 (2004).
- Yanful, E., M. Haug, L. Wong,"*The impact of synthetic leachate on the hydraulic conductivity of a smectitic till underlying a landfill near Saskatoon, Saskatchewan*", Canadian Geotech. J. 27, 507–519 (1990).
- Zacarias-Farah, A., E. Geyer-Allely, *"Household consumption patterns in OECD countries: trends and figures",* J. Clean. Prod., 11, pp. 819–827, (2003).

Appendix A

Pressure Transducer Calibration

A.1.

Date: Feb 20/2008

Model No: Dynisco APT311JA-1C Serial No: 230426

Range: 0-689.5 kPa Inventory No 017-310

Volts.Exec.: 10 Output: 3.959 mV/V

Offset: 344

Deadweight Tester Reading	Transducer Reading
0	0
22	21
100	100
200	201
400	402
600	599

Notes: Calibrated using Chandler Deadweight Tester (017-95) Transducer read on KTest Sciemetrics DA Serial No G8098

A.2.

Date: Feb 20/2008

Model No: Dynisco APT311JA-1C Serial No: 279498

Range: 0-689.5 kPa Inventory No 017-351

Volts.Exec.: 10 Output: 3.453 mV/V

Offset: 1190

Deadweight Tester Reading	Transducer Reading
0	0
22	23
100	100
200	201
400	402
600	596

Notes: Calibrated using Chandler Deadweight Tester (017-95) Transducer read on KTest Sciemetrics DA Serial No G8098

A.3.

Date: Feb 20/2008

Model No: Dynisco APT311JA-1C Serial No: 230428

Range: 0-689.5 kPa Inventory No 017-312

Volts.Exec.: 10 Output: 3.898 mV/V

Offset: 202

Deadweight Tester Reading	Transducer Reading
0	0
22	22
100	101
200	201
400	401
600	600

Notes: Calibrated using Chandler Deadweight Tester (017-95) Transducer read on KTest Sciemetrics DA Serial No G8098

A.4.

Date: Feb 20/2008

Model No: Dynisco APT311JA-1C Serial No: 461719

Range: 0-689.5 kPa Inventory No 017-429

Volts.Exec.: 10 Output: 3.555 mV/V

Offset: 98

Deadweight Tester Reading	Transducer Reading
0	0
22	22
100	101
200	201
400	401
600	600

Notes: Calibrated using Chandler Deadweight Tester (017-95) Transducer read on KTest Sciemetrics DA Serial No G8098

Appendix B

Mercury Intrusion Porosimetry Report

Geotechnical Research Centre - Poresize Analysis

AutoPore IV 9500 V1.07 Serial: 689 Port: 1/1 Page 1

Sample ID: 30%-center
Operator: sarakarimi
Submitter: dr.yanful
File: C:\9500\DATA\30%-MIP.SMP

LP Analysis Time: 11/6/2012 1:27:55PM
HP Analysis Time: 11/6/2012 2:53:39PM
Report Time: 11/6/2012 3:36:27PM

Sample Weight: 1.3300 g
Correction Type: None
Show Neg. Int: Yes

Summary Report

Penetrometer parameters

Penetrometer:	13-00570606 3 ml, 0.39, Solid		
Pen. Constant:	11.007 µL/pF	Pen. Weight:	61.9700 g
Stem Volume:	0.3900 mL	Max. Head Pressure:	4.6800 psia
Pen. Volume:	3.3900 mL	Assembly Weight:	102.2900 g

Hg Parameters

Adv. Contact Angle:	140.000 degrees	Rec. Contact Angle:	140.000 degrees
Hg Surface Tension:	480.000 dynes/cm	Hg Density:	13.5369 g/mL

User Parameters

Param 1:	0.000	Param 2:	0.000	Param 3:	0.000

Low Pressure:

Evacuation Pressure:	50 µmHg
Evacuation Time:	5 mins
Mercury Filling Pressure:	1.98 psia
Equilibration Time:	10 secs
Maximum Intrusion Volume:	0.010 mL/g

High Pressure:

Equilibration Time:	10 secs
Maximum Intrusion Volume:	0.010 mL/g

No Blank Correction

Intrusion Data Summary

Total Intrusion Volume =	0.1124	mL/g
Total Pore Area =	6.555	m²/g
Median Pore Radius (Volume) =	496	A
Median Pore Radius (Area) =	176	A
Average Pore Radius (2V/A) =	343	A
Bulk Density at 1.98 psia =	2.6093	g/mL
Apparent (skeletal) Density =	3.6923	g/mL
Porosity =	29.3329	%
Stem Volume Used =	40	%

Pore Structure Summary

Threshold Pressure:	2.79	psia (Calculated)
Characteristic length =	382511	A
Conductivity formation factor =	0.010	
Permeability constant =	0.00442	
Permeability =	264.3938	mdarcy
BET Surface Area =	200.0000	m²/g
Pore shape exponent =	1.00	
Tortuosity factor =	1.899	
Tortuosity =	2.6831	
Percolation Fractal dimension =	2.682	
Backbone Fractal dimension =	N/A	

Mayer Stowe Summary

Interstitial porosity =	29.3329	%
Breakthrough pressure ratio =	8.7463	

Sample ID: 30%-center
Operator: sarakarimi
Submitter: dr.yanful
File: C:\9500\DATA\30%-MIP.SMP

LP Analysis Time: 11/6/2012 1:27:55PM
HP Analysis Time: 11/6/2012 2:53:39PM
Report Time: 11/6/2012 3:36:27PM

Sample Weight: 1.3300 g
Correction Type: None
Show Neg. Int: Yes

Material Compressibility

Linear Coefficient = -2.2382e-05 1/psia
Quadratic Coefficient = 3.1491e-10 1/psia²

Sample ID: 30%-center
Operator: sarakarimi
Submitter: dr.yanful
File: C:\9500\DATA\30%-MIP.SMP

LP Analysis Time: 11/6/2012 1:27:55PM
HP Analysis Time: 11/6/2012 2:53:39PM
Report Time: 11/6/2012 3:36:27PM

Sample Weight: 1.3300 g
Correction Type: None
Show Neg. Int: Yes

Tabular Report

Pore Radius (A)	Mean Radius (A)	Incremental Pore Volume (mL/g)	% Incremental Intrusion Volume	Mayer-Stowe Cumulative Volume finer % (%)	Cumulative Pore Area (m^2/g)
538217	538217	0.0000	0.0000	100.0000	0.000
356206	447212	0.0019	1.6871	98.3129	0.000
268300	312253	0.0022	1.9833	96.3295	0.000
194683	231492	0.0018	1.6356	94.6939	0.000
178537	186610	0.0005	0.4765	94.2174	0.000
142849	160693	0.0013	1.1977	93.0197	0.001
125960	134405	0.0008	0.7083	92.3113	0.001
112670	119315	0.0003	0.2705	92.0409	0.001
101967	107318	0.0004	0.3220	91.7189	0.001
82317	92142	0.0011	1.0174	90.7015	0.001
66752	74534	0.0010	0.9015	89.8000	0.001
53430	60091	0.0010	0.9144	88.8856	0.002
42715	48073	0.0019	1.6485	87.2371	0.002
39770	41242	0.0001	0.0743	87.1628	0.003
25330	32550	0.0031	2.7695	84.3933	0.004
22807	24068	0.0016	1.4478	82.9454	0.006
18804	20805	0.0065	5.7777	77.1677	0.012
16385	17594	0.0087	7.7695	69.3982	0.022
15043	15714	0.0013	1.1587	68.2394	0.024
12197	13620	0.0049	4.3801	63.8593	0.031
9522	10860	0.0030	2.6988	61.1605	0.036
7718	8620	0.0016	1.4414	59.7191	0.040
6226	6972	0.0012	1.0892	58.6299	0.044
4913	5570	0.0010	0.9226	57.7073	0.047
4003	4458	0.0007	0.6509	57.0564	0.051
3253	3628	0.0006	0.5609	56.4956	0.054
2560	2906	0.0007	0.6065	55.8891	0.059
2060	2310	0.0006	0.5032	55.3858	0.064
1672	1866	0.0005	0.4826	54.9033	0.070
1335	1504	0.0006	0.5512	54.3520	0.078
1079	1207	0.0007	0.6066	53.7454	0.089
890	984	0.0007	0.6295	53.1160	0.104
712	801	0.0010	0.9274	52.1886	0.130
562	637	0.0015	1.3076	50.8810	0.176
455	508	0.0018	1.5884	49.2927	0.246
368	411	0.0025	2.1880	47.1047	0.365
297	333	0.0039	3.5091	43.5956	0.603
239	268	0.0102	9.1125	34.4831	1.367
238	238	0.0005	0.4760	34.0071	1.412
203	220	0.0113	10.0131	23.9939	2.434
191	197	0.0037	3.3231	20.6708	2.814
155	173	0.0095	8.4730	12.1978	3.915
124	140	0.0054	4.8096	7.3883	4.689
101	113	0.0031	2.7805	4.6077	5.244
81	91	0.0021	1.8389	2.7688	5.699
72	77	0.0009	0.7697	1.9991	5.925

Sample ID: 30%-center
Operator: sarakarimi
Submitter: dr.yanful
File: C:\9500\DATA\30%-MIP.SMP

LP Analysis Time: 11/6/2012 1:27:55PM
HP Analysis Time: 11/6/2012 2:53:39PM
Report Time: 11/6/2012 3:36:27PM

Sample Weight: 1.3300 g
Correction Type: None
Show Neg. Int: Yes

Tabular Report

Pore Radius (A)	Mean Radius (A)	Incremental Pore Volume (mL/g)	% Incremental Intrusion Volume	Mayer-Stowe Cumulative Volume finer % (%)	Cumulative Pore Area (m^2/g)
65	69	0.0006	0.5382	1.4610	6.101
53	59	0.0009	0.8292	0.6318	6.416
43	48	0.0007	0.6396	-0.0078	6.715
36	39	0.0001	0.0667	-0.0745	6.754
30	33	0.0002	0.1450	-0.2195	6.852
27	29	0.0001	0.0906	-0.3100	6.924
24	25	0.0000	0.0314	-0.3415	6.952
21	23	0.0000	0.0136	-0.3551	6.965
19	20	-0.0002	-0.1851	-0.1700	6.761
18	19	-0.0002	-0.1700	-0.0000	6.555
23	20	0.0013	1.1763	-1.1763	7.848
30	27	0.0009	0.8178	-1.9942	8.539
39	35	0.0007	0.6378	-2.6319	8.954
51	45	0.0004	0.3718	-3.0037	9.141
67	59	0.0002	0.1873	-3.1910	9.212
86	76	-0.0000	-0.0290	-3.1620	9.204
111	98	-0.0003	-0.2417	-2.9203	9.149
146	128	-0.0006	-0.5020	-2.4183	9.061
187	166	-0.0007	-0.6507	-1.7676	8.973
247	217	-0.0011	-1.0184	-0.7492	8.867
323	285	-0.0015	-1.3151	0.5659	8.763
410	366	-0.0016	-1.3871	1.9530	8.678
533	471	-0.0021	-1.8539	3.8069	8.590
710	622	-0.0027	-2.4384	6.2454	8.502
887	799	-0.0027	-2.4074	8.6527	8.434
1183	1035	-0.0039	-3.4355	12.0882	8.359
1519	1351	-0.0040	-3.5339	15.6221	8.301
2123	1821	-0.0055	-4.9176	20.5396	8.240
2659	2391	-0.0040	-3.6000	24.1396	8.206
3527	3093	-0.0043	-3.7825	27.9222	8.178
4427	3977	-0.0030	-2.6869	30.6091	8.163
5576	5001	-0.0022	-1.9494	32.5585	8.155
7230	6403	-0.0016	-1.4122	33.9707	8.150
9452	8341	-0.0010	-0.9015	34.8722	8.147
12001	10727	-0.0005	-0.4860	35.3581	8.146
15859	13930	-0.0004	-0.3823	35.7404	8.146
19987	17923	-0.0003	-0.2661	36.0065	8.145
31174	25581	-0.0003	-0.2555	36.2619	8.145

Geotechnical Research Centre - Poresize Analysis

AutoPore IV 9500 V1.07 Serial: 689 Port: 1/1 Page 5

Sample ID: 30%-center
Operator: sarakarimi
Submitter: dr.yanful
File: C:\9500\DATA\30%-MIP.SMP

LP Analysis Time: 11/6/2012 1:27:55PM
HP Analysis Time: 11/6/2012 2:53:39PM
Report Time: 11/6/2012 3:36:27PM

Sample Weight: 1.3300 g
Correction Type: None
Show Neg. Int: Yes

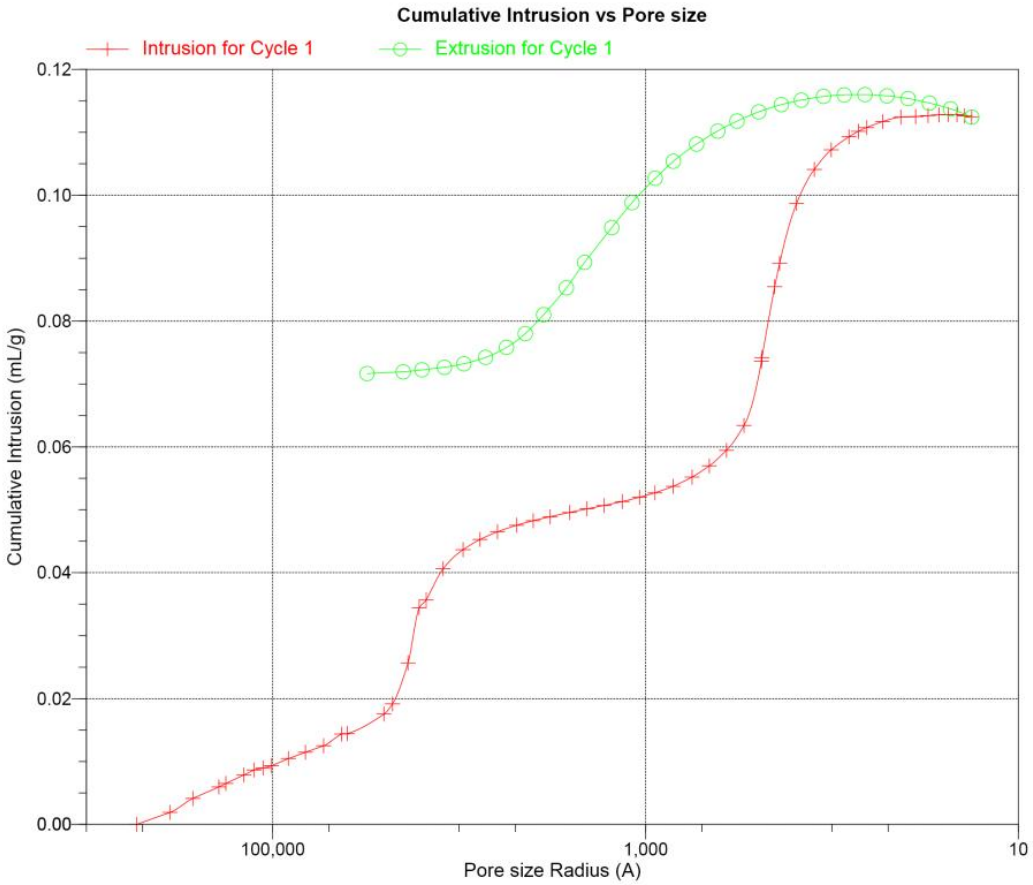

Figure A.1: Cumulative Intrusion vs Pore Size (G70K30)

Geotechnical Research Centre - Poresize Analysis

AutoPore IV 9500 V1.07 Serial: 689 Port: 1/1 Page 6

Sample ID: 30%-center
Operator: sarakarimi
Submitter: dr.yanful
File: C:\9500\DATA\30%-MIP.SMP

LP Analysis Time: 11/6/2012 1:27:55PM
HP Analysis Time: 11/6/2012 2:53:39PM
Report Time: 11/6/2012 3:36:27PM

Sample Weight: 1.3300 g
Correction Type: None
Show Neg. Int: Yes

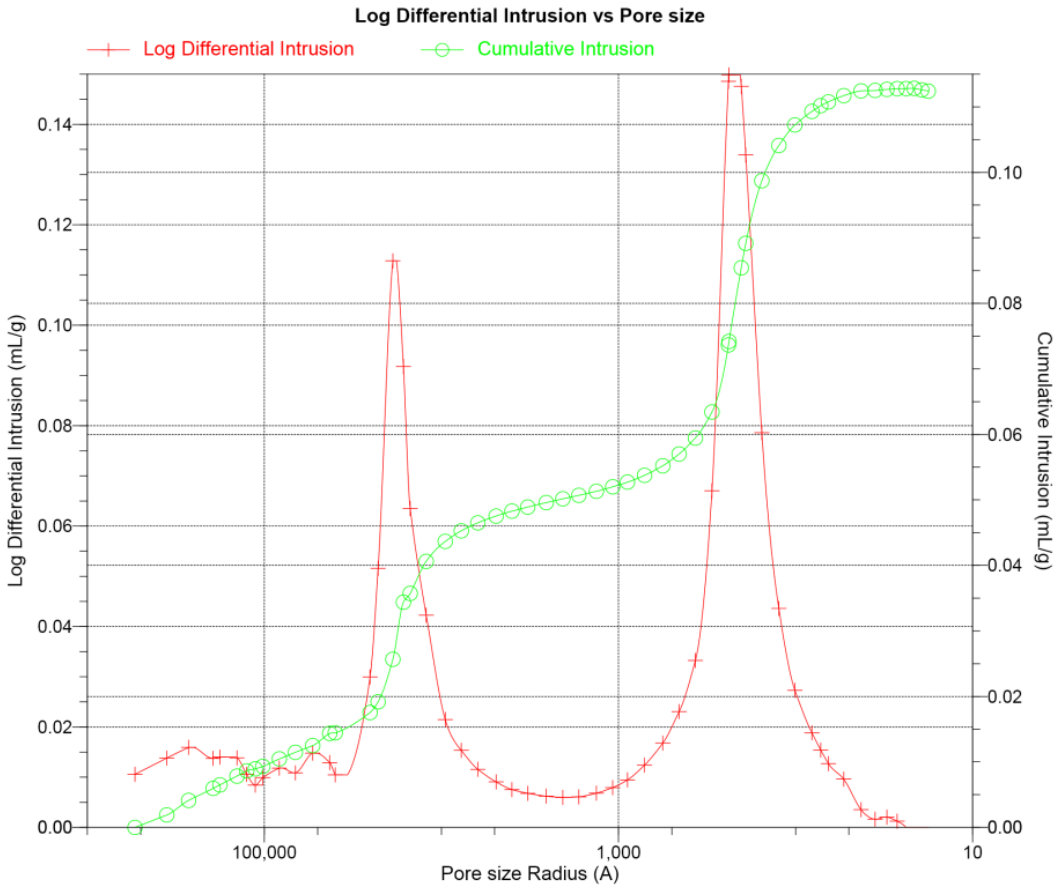

Figure A.2: Log Differential Intrusion vs Pore Size (G70K30)

Geotechnical Research Centre - Poresize Analysis

Sample ID: 30%-center-f
Operator: sarakarimi
Submitter: dryanful
File: C:\9500\DATA\FCENTERA.SMP

LP Analysis Time: 11/20/2012 11:57:41AM
HP Analysis Time: 11/20/2012 1:53:01PM
Report Time: 11/20/2012 2:52:38PM

Sample Weight: 1.4000 g
Correction Type: None
Show Neg. Int: Yes

Summary Report

Penetrometer parameters

Penetrometer:	13-00570606 3 ml, 0.39, Solid				
Pen. Constant:	11.007	µL/pF	Pen. Weight:	61.7300	g
Stem Volume:	0.3900	mL	Max. Head Pressure:	4.6800	psia
Pen. Volume:	3.3900	mL	Assembly Weight:	101.7800	g

Hg Parameters

Adv. Contact Angle:	140.000	degrees	Rec. Contact Angle:	140.000	degrees
Hg Surface Tension:	480.000	dynes/cm	Hg Density:	13.5369	g/mL

User Parameters

Param 1:	0.000	Param 2:	0.000	Param 3:	0.000

Low Pressure:

Evacuation Pressure:	50	µmHg
Evacuation Time:	5	mins
Mercury Filling Pressure:	1.98	psia
Equilibration Time:	10	secs
Maximum Intrusion Volume:	0.010	mL/g

High Pressure:

Equilibration Time:	10	secs
Maximum Intrusion Volume:	0.010	mL/g

No Blank Correction

Intrusion Data Summary

Total Intrusion Volume =	0.0847	mL/g
Total Pore Area =	7.232	m²/g
Median Pore Diameter (Volume) =	0.0483	µm
Median Pore Diameter (Area) =	0.0321	µm
Average Pore Diameter (4V/A) =	0.0469	µm
Bulk Density at 1.98 psia =	2.6176	g/mL
Apparent (skeletal) Density =	3.3638	g/mL
Porosity =	22.1837	%
Stem Volume Used =	31	%

Pore Structure Summary

Threshold Pressure:	3.82	psia (Calculated)
Characteristic length =	55.8614	µm
Conductivity formation factor =	0.009	
Permeability constant =	0.00442	
Permeability =	123.1860	mdarcy
BET Surface Area =	200.0000	m²/g
Pore shape exponent =	1.00	
Tortuosity factor =	1.979	
Tortuosity =	2.6357	
Percolation Fractal dimension =	2.624	
Backbone Fractal dimension =	N/A	

Mayer Stowe Summary

Interstitial porosity =	25.9500	%
Breakthrough pressure ratio =	9.4600	

Sample ID: 30%-center-f
Operator: sarakarimi
Submitter: dryanful
File: C:\9500\DATA\FCENTERA.SMP

LP Analysis Time: 11/20/2012 11:57:41AM
HP Analysis Time: 11/20/2012 1:53:01PM
Report Time: 11/20/2012 2:52:38PM

Sample Weight: 1.4000 g
Correction Type: None
Show Neg. Int: Yes

Material Compressibility

Linear Coefficient = -1.7287e-05 1/psia
Quadratic Coefficient = 2.3897e-10 1/psia²

Sample ID: 30%-center-f
Operator: sarakarimi
Submitter: dryanful
File: C:\9500\DATA\FCENTERA.SMP

LP Analysis Time: 11/20/2012 11:57:41AM
HP Analysis Time: 11/20/2012 1:53:01PM
Report Time: 11/20/2012 2:52:38PM

Sample Weight: 1.4000 g
Correction Type: None
Show Neg. Int: Yes

Tabular Report

Pore Diameter (µm)	Mean Diameter (µm)	Incremental Pore Volume (mL/g)	% Incremental Intrusion Volume	Mayer-Stowe Cumulative Volume finer % (%)	Cumulative Pore Area (m^2/g)
107.5434	107.5434	0.0000	0.0000	100.0000	0.000
71.2477	89.3956	0.0006	0.6979	99.3021	0.000
53.6914	62.4696	0.0003	0.3895	98.9126	0.000
38.9476	46.3195	0.0028	3.3108	95.6018	0.000
35.7040	37.3258	0.0002	0.1948	95.4070	0.000
28.5590	32.1315	0.0003	0.4057	95.0013	0.000
25.2017	26.8803	0.0002	0.1785	94.8227	0.000
22.5341	23.8679	0.0002	0.1785	94.6442	0.000
20.3960	21.4650	0.0001	0.1461	94.4981	0.000
16.4630	18.4295	0.0003	0.3571	94.1411	0.000
13.3739	14.9184	0.0003	0.3571	93.7840	0.001
10.6853	12.0296	0.0004	0.4220	93.3621	0.001
8.5486	9.6170	0.0006	0.6654	92.6967	0.001
8.1961	8.3724	0.0001	0.1405	92.5562	0.001
4.9115	6.5538	0.0011	1.3088	91.2474	0.002
4.5857	4.7486	0.0002	0.2788	90.9686	0.002
3.7297	4.1577	0.0013	1.5210	89.4477	0.003
2.9610	3.3453	0.0020	2.3621	87.0856	0.005
2.4424	2.7017	0.0019	2.1862	84.8994	0.008
1.8931	2.1678	0.0025	2.9087	81.9907	0.013
1.5532	1.7232	0.0014	1.6944	80.2962	0.016
1.2395	1.3964	0.0013	1.5921	78.7041	0.020
0.9827	1.1111	0.0011	1.2948	77.4093	0.024
0.8004	0.8915	0.0008	0.9452	76.4641	0.028
0.6519	0.7261	0.0007	0.8104	75.6538	0.031
0.5112	0.5816	0.0007	0.8707	74.7831	0.036
0.4129	0.4621	0.0006	0.7154	74.0677	0.042
0.3344	0.3737	0.0006	0.6776	73.3901	0.048
0.2676	0.3010	0.0006	0.7377	72.6525	0.056
0.2160	0.2418	0.0007	0.8309	71.8215	0.068
0.1782	0.1971	0.0007	0.8230	70.9986	0.082
0.1425	0.1604	0.0011	1.2612	69.7374	0.109
0.1125	0.1275	0.0015	1.7346	68.0028	0.155
0.0909	0.1017	0.0017	2.0380	65.9647	0.223
0.0737	0.0823	0.0024	2.7918	63.1730	0.338
0.0594	0.0665	0.0035	4.1618	59.0112	0.550
0.0475	0.0535	0.0085	10.0142	48.9970	1.185
0.0404	0.0440	0.0116	13.7027	35.2943	2.241
0.0382	0.0393	0.0037	4.3254	30.9689	2.613
0.0312	0.0347	0.0104	12.2230	18.7459	3.808
0.0310	0.0311	0.0002	0.2926	18.4533	3.839
0.0249	0.0279	0.0059	6.9269	11.5265	4.680
0.0202	0.0225	0.0034	4.0114	7.5151	5.284
0.0162	0.0182	0.0023	2.7498	4.7653	5.797
0.0144	0.0153	0.0007	0.8597	3.9056	5.987
0.0130	0.0137	0.0008	0.9437	2.9619	6.220

Sample ID: 30%-center-f
Operator: sarakarimi
Submitter: dryanful
File: C:\9500\DATA\FCENTERA.SMP

LP Analysis Time: 11/20/2012 11:57:41AM
HP Analysis Time: 11/20/2012 1:53:01PM
Report Time: 11/20/2012 2:52:38PM

Sample Weight: 1.4000 g
Correction Type: None
Show Neg. Int: Yes

Tabular Report

Pore Diameter (µm)	Mean Diameter (µm)	Incremental Pore Volume (mL/g)	% Incremental Intrusion Volume	Mayer-Stowe Cumulative Volume finer % (%)	Cumulative Pore Area (m^2/g)
0.0107	0.0119	0.0010	1.2367	1.7252	6.574
0.0085	0.0096	0.0009	1.0063	0.7189	6.929
0.0071	0.0078	0.0003	0.3426	0.3763	7.077
0.0061	0.0066	0.0003	0.3171	0.0592	7.240
0.0053	0.0057	0.0001	0.1657	-0.1065	7.338
0.0047	0.0050	0.0000	0.0560	-0.1625	7.376
0.0043	0.0045	0.0000	0.0107	-0.1732	7.384
0.0039	0.0041	-0.0001	-0.0701	-0.1030	7.326
0.0036	0.0037	-0.0001	-0.1030	-0.0000	7.232
0.0046	0.0041	0.0011	1.2834	-1.2834	8.295
0.0060	0.0053	0.0008	0.8967	-2.1801	8.867
0.0078	0.0069	0.0005	0.6363	-2.8163	9.179
0.0102	0.0090	0.0003	0.3451	-3.1615	9.309
0.0133	0.0117	0.0000	0.0404	-3.2019	9.321
0.0172	0.0153	-0.0002	-0.2312	-2.9706	9.269
0.0222	0.0197	-0.0004	-0.5119	-2.4588	9.181
0.0292	0.0257	-0.0008	-0.9088	-1.5499	9.061
0.0373	0.0332	-0.0010	-1.1700	-0.3799	8.942
0.0495	0.0434	-0.0014	-1.6317	1.2519	8.814
0.0646	0.0570	-0.0018	-2.0735	3.3253	8.691
0.0820	0.0733	-0.0019	-2.2288	5.5542	8.588
0.1065	0.0942	-0.0024	-2.8598	8.4140	8.485
0.1420	0.1243	-0.0031	-3.6767	12.0907	8.385
0.1776	0.1598	-0.0030	-3.5128	15.6035	8.310
0.2366	0.2071	-0.0041	-4.8267	20.4301	8.231
0.3041	0.2703	-0.0039	-4.6382	25.0683	8.173
0.4259	0.3650	-0.0051	-5.9953	31.0636	8.117
0.5312	0.4785	-0.0034	-4.0015	35.0651	8.089
0.7069	0.6190	-0.0034	-3.9838	39.0489	8.067
0.8825	0.7947	-0.0022	-2.5883	41.6373	8.056
1.1144	0.9985	-0.0018	-2.1182	43.7555	8.049
1.4457	1.2801	-0.0014	-1.6846	45.4401	8.045
1.9008	1.6733	-0.0011	-1.2639	46.7039	8.042
2.4285	2.1647	-0.0007	-0.8448	47.5487	8.041
3.1417	2.7851	-0.0005	-0.6158	48.1645	8.040
4.0538	3.5977	-0.0004	-0.4373	48.6018	8.039
6.6281	5.3409	-0.0004	-0.5291	49.1309	8.039

Geotechnical Research Centre - Poresize Analysis

AutoPore IV 9500 V1.07 Serial: 689 Port: 1/1 Page 5

Sample ID: 30%-center-f
Operator: sarakarimi
Submitter: dryanful
File: C:\9500\DATA\FCENTERA.SMP

LP Analysis Time: 11/20/2012 11:57:41AM
HP Analysis Time: 11/20/2012 1:53:01PM
Report Time: 11/20/2012 2:52:38PM

Sample Weight: 1.4000 g
Correction Type: None
Show Neg. Int: Yes

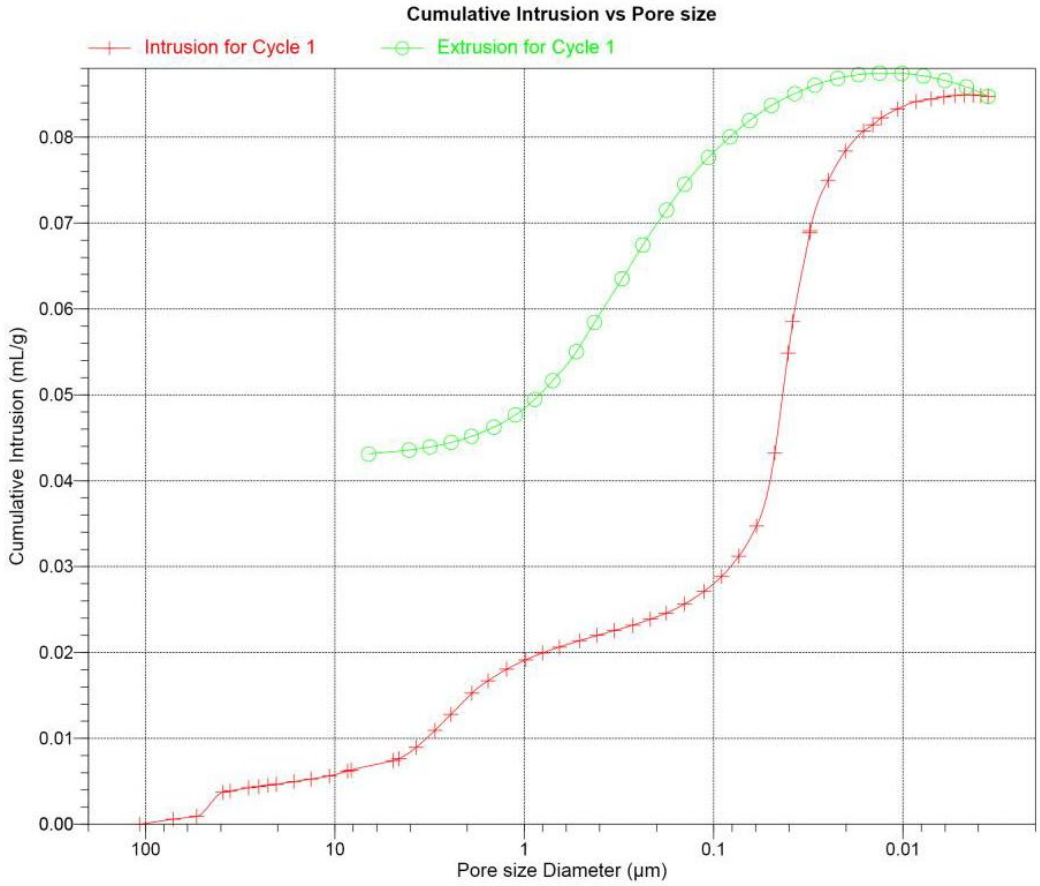

Figure A.3: Cumulative Intrusion vs Pore Size (G70K30-Final)

Geotechnical Research Centre - Poresize Analysis

AutoPore IV 9500 V1.07 Serial: 689 Port: 1/1 Page 6

Sample ID: 30%-center-f
Operator: sarakarimi
Submitter: dryanful
File: C:\9500\DATA\FCENTERA.SMP

LP Analysis Time: 11/20/2012 11:57:41AM
HP Analysis Time: 11/20/2012 1:53:01PM
Report Time: 11/20/2012 2:52:38PM

Sample Weight: 1.4000 g
Correction Type: None
Show Neg. Int: Yes

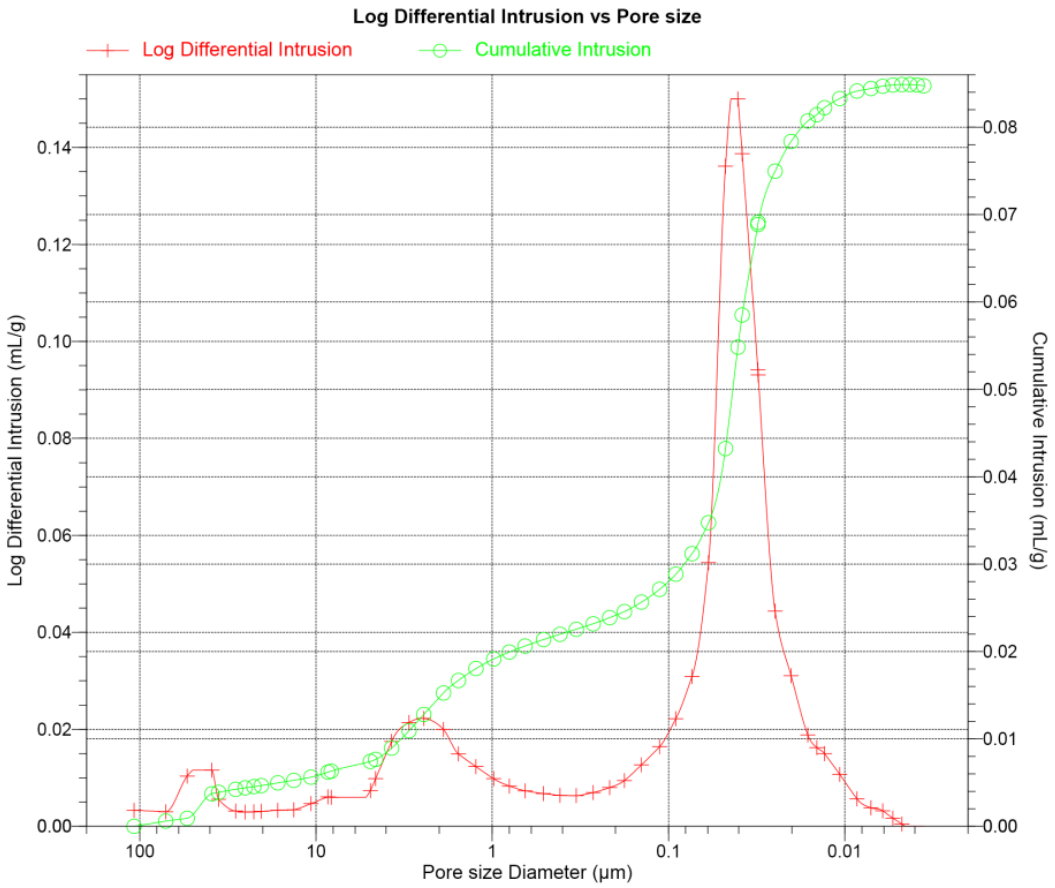

Figure A. 4: Log Differential Intrusion vs Pore Size (G70K30-Final)

Geotechnical Research Centre - Poresize Analysis

AutoPore IV 9500 V1.07 Serial: 689 Port: 1/1 Page 1

Sample ID: 40%-center
Operator: sara karimi
Submitter: Dr.Yanful
File: C:\9500\DATA\40%-MIP.SMP

LP Analysis Time: 11/6/2012 5:29:24PM
HP Analysis Time: 11/6/2012 6:18:13PM
Report Time: 11/6/2012 6:45:07PM

Sample Weight: 1.2700 g
Correction Type: None
Show Neg. Int: Yes

Summary Report

Penetrometer parameters

Penetrometer:	13-00570606 3 ml, 0.39, Solid				
Pen. Constant:	11.007	µL/pF	Pen. Weight:	61.9900	g
Stem Volume:	0.3900	mL	Max. Head Pressure:	4.6800	psia
Pen. Volume:	3.3900	mL	Assembly Weight:	102.5100	g

Hg Parameters

Adv. Contact Angle:	140.000	degrees	Rec. Contact Angle:	140.000	degrees
Hg Surface Tension:	480.000	dynes/cm	Hg Density:	13.5369	g/mL

User Parameters

Param 1:	0.000	Param 2:	0.000	Param 3:	0.000

Low Pressure:

Evacuation Pressure:	50	µmHg
Evacuation Time:	5	mins
Mercury Filling Pressure:	1.98	psia
Equilibration Time:	10	secs
Maximum Intrusion Volume:	0.010	mL/g

High Pressure:

Equilibration Time:	10	secs
Maximum Intrusion Volume:	0.010	mL/g

No Blank Correction

Intrusion Data Summary

Total Intrusion Volume =	0.1230	mL/g
Total Pore Area =	9.537	m²/g
Median Pore Radius (Volume) =	269	A
Median Pore Radius (Area) =	167	A
Average Pore Radius (2V/A) =	258	A
Bulk Density at 1.98 psia =	2.5891	g/mL
Apparent (skeletal) Density =	3.7990	g/mL
Porosity =	31.8485	%
Stem Volume Used =	41	%

Pore Structure Summary

Threshold Pressure:	6.84	psia (Calculated)
Characteristic length =	155972	A
Conductivity formation factor =	0.020	
Permeability constant =	0.00442	
Permeability =	84.7470	mdarcy
BET Surface Area =	200.0000	m²/g
Pore shape exponent =	1.00	
Tortuosity factor =	1.870	
Tortuosity =	4.2831	
Percolation Fractal dimension =	2.665	
Backbone Fractal dimension =	N/A	

Mayer Stowe Summary

Interstitial porosity =	31.8485	%
Breakthrough pressure ratio =	7.9001	

Sample ID: 40%-center
Operator: sara karimi
Submitter: Dr.Yanful
File: C:\9500\DATA\40%-MIP.SMP

LP Analysis Time: 11/6/2012 5:29:24PM
HP Analysis Time: 11/6/2012 6:18:13PM
Report Time: 11/6/2012 6:45:07PM

Sample Weight: 1.2700 g
Correction Type: None
Show Neg. Int: Yes

Material Compressibility

Linear Coefficient = -2.7490e-05 1/psia
Quadratic Coefficient = 3.8561e-10 1/psia²

Sample ID: 40%-center
Operator: sara karimi
Submitter: Dr.Yanful
File: C:\9500\DATA\40%-MIP.SMP

LP Analysis Time: 11/6/2012 5:29:24PM
HP Analysis Time: 11/6/2012 6:18:13PM
Report Time: 11/6/2012 6:45:07PM

Sample Weight: 1.2700 g
Correction Type: None
Show Neg. Int: Yes

Tabular Report

Pore Radius (A)	Mean Radius (A)	Incremental Pore Volume (mL/g)	% Incremental Intrusion Volume	Mayer-Stowe Cumulative Volume finer % (%)	Cumulative Pore Area (m^2/g)
538157	538157	0.0000	0.0000	100.0000	0.000
356302	447230	0.0018	1.4791	98.5209	0.000
268340	312321	0.0013	1.0354	97.4855	0.000
194652	231496	0.0021	1.6763	95.8092	0.000
178606	186629	0.0004	0.2958	95.5133	0.000
142783	160695	0.0009	0.7149	94.7984	0.000
125991	134387	0.0006	0.4561	94.3424	0.001
112657	119324	0.0004	0.3451	93.9972	0.001
101937	107297	0.0003	0.2588	93.7384	0.001
82307	92122	0.0007	0.5300	93.2084	0.001
66858	74582	0.0007	0.5547	92.6537	0.001
53421	60139	0.0009	0.7272	91.9265	0.001
42744	48082	0.0008	0.6656	91.2608	0.002
41050	41897	0.0001	0.0718	91.1891	0.002
25350	33200	0.0015	1.2211	89.9680	0.003
22490	23920	0.0015	1.2242	88.7438	0.004
18995	20743	0.0024	1.9545	86.7893	0.006
14909	16952	0.0051	4.1630	82.6262	0.012
12145	13527	0.0050	4.0414	78.5849	0.020
9630	10887	0.0040	3.2149	75.3700	0.027
7842	8736	0.0022	1.7686	73.6014	0.032
6203	7023	0.0017	1.3963	72.2051	0.037
4915	5559	0.0013	1.0190	71.1861	0.041
3991	4453	0.0009	0.6971	70.4890	0.045
3251	3621	0.0007	0.5782	69.9108	0.049
2559	2905	0.0007	0.5969	69.3139	0.054
2064	2312	0.0006	0.4952	68.8187	0.059
1675	1870	0.0006	0.5096	68.3090	0.066
1338	1507	0.0007	0.5972	67.7119	0.076
1078	1208	0.0008	0.6908	67.0210	0.090
891	985	0.0009	0.7564	66.2646	0.109
712	802	0.0014	1.1281	65.1365	0.143
562	637	0.0020	1.6349	63.5016	0.206
455	508	0.0025	2.0098	61.4918	0.304
368	412	0.0034	2.7584	58.7335	0.469
297	333	0.0055	4.5004	54.2330	0.802
242	270	0.0137	11.1215	43.1115	1.816
238	240	0.0018	1.4584	41.6532	1.966
210	224	0.0120	9.7458	31.9074	3.036
191	201	0.0082	6.6599	25.2475	3.852
160	176	0.0106	8.6205	16.6270	5.060
155	158	0.0013	1.0786	15.5484	5.229
124	140	0.0070	5.6624	9.8860	6.226
101	113	0.0040	3.2858	6.6002	6.944
81	91	0.0028	2.2964	4.3038	7.566
72	77	0.0011	0.9072	3.3966	7.857

Sample ID: 40%-center
Operator: sara karimi
Submitter: Dr.Yanful
File: C:\9500\DATA\40%-MIP.SMP

LP Analysis Time: 11/6/2012 5:29:24PM
HP Analysis Time: 11/6/2012 6:18:13PM
Report Time: 11/6/2012 6:45:07PM

Sample Weight: 1.2700 g
Correction Type: None
Show Neg. Int: Yes

Tabular Report

Pore Radius (A)	Mean Radius (A)	Incremental Pore Volume (mL/g)	% Incremental Intrusion Volume	Mayer-Stowe Cumulative Volume finer % (%)	Cumulative Pore Area (m^2/g)
65	69	0.0008	0.6870	2.7096	8.103
53	59	0.0015	1.1856	1.5240	8.596
43	48	0.0007	0.5454	0.9785	8.875
36	39	0.0007	0.5511	0.4274	9.222
30	33	0.0004	0.2922	0.1352	9.439
27	29	0.0002	0.1595	-0.0243	9.577
24	25	0.0001	0.0527	-0.0770	9.628
21	23	-0.0000	-0.0238	-0.0532	9.602
19	20	-0.0001	-0.0471	-0.0061	9.545
18	19	-0.0000	-0.0061	0.0000	9.537
23	20	0.0011	0.8902	-0.8902	10.607
30	27	0.0009	0.7267	-1.6169	11.280
39	35	0.0006	0.4940	-2.1109	11.631
51	45	0.0003	0.2617	-2.3725	11.775
67	59	0.0000	0.0264	-2.3989	11.786
86	76	-0.0003	-0.2055	-2.1934	11.719
111	98	-0.0005	-0.4172	-1.7762	11.615
146	128	-0.0009	-0.7060	-1.0702	11.480
187	166	-0.0011	-0.8720	-0.1982	11.351
248	217	-0.0016	-1.3067	1.1084	11.203
323	285	-0.0020	-1.6090	2.7174	11.064
410	366	-0.0021	-1.6973	4.4148	10.950
533	471	-0.0027	-2.2352	6.6499	10.833
710	622	-0.0037	-2.9712	9.6211	10.716
888	799	-0.0035	-2.8570	12.4781	10.628
1183	1035	-0.0054	-4.3995	16.8776	10.523
1522	1353	-0.0056	-4.5682	21.4459	10.440
2131	1827	-0.0081	-6.5498	27.9957	10.352
2651	2391	-0.0059	-4.7631	32.7587	10.303
3523	3087	-0.0061	-4.9203	37.6790	10.264
4421	3972	-0.0039	-3.1513	40.8303	10.244
5552	4986	-0.0025	-2.0009	42.8312	10.234
7233	6392	-0.0017	-1.3538	44.1850	10.229
9476	8355	-0.0009	-0.7424	44.9273	10.227
12187	10831	-0.0006	-0.4553	45.3826	10.226
15699	13943	-0.0004	-0.3092	45.6918	10.225
19977	17838	-0.0003	-0.2354	45.9272	10.225
31918	25948	-0.0003	-0.2310	46.1581	10.225

Geotechnical Research Centre - Poresize Analysis

AutoPore IV 9500 V1.07 Serial: 689 Port: 1/1 Page 5

Sample ID: 40%-center
Operator: sara karimi
Submitter: Dr.Yanful
File: C:\9500\DATA\40%-MIP.SMP

LP Analysis Time: 11/6/2012 5:29:24PM
HP Analysis Time: 11/6/2012 6:18:13PM
Report Time: 11/6/2012 6:45:07PM

Sample Weight: 1.2700 g
Correction Type: None
Show Neg. Int: Yes

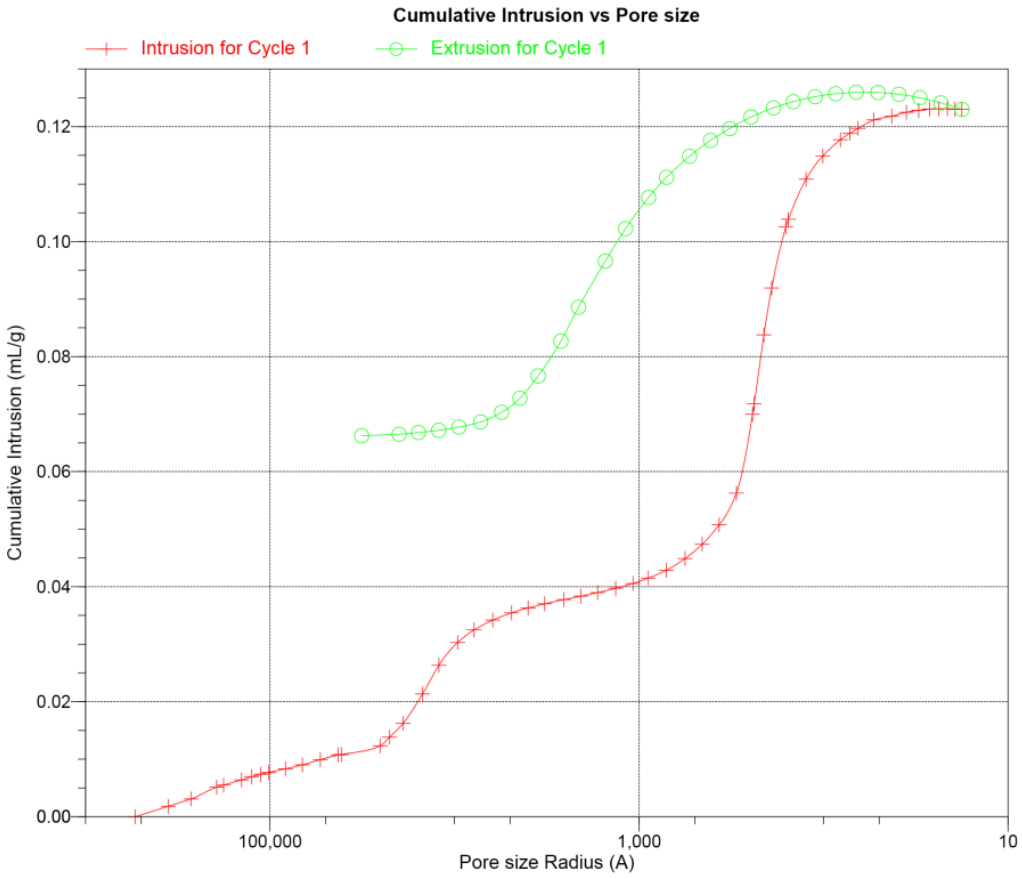

Figure A.5: Cumulative Intrusion vs Pore Size (G60K40)

Geotechnical Research Centre - Poresize Analysis

AutoPore IV 9500 V1.07 Serial: 689 Port: 1/1 Page 6

Sample ID: 40%-center
Operator: sara karimi
Submitter: Dr.Yanful
File: C:\9500\DATA\40%-MIP.SMP

LP Analysis Time: 11/6/2012 5:29:24PM
HP Analysis Time: 11/6/2012 6:18:13PM
Report Time: 11/6/2012 6:45:07PM

Sample Weight: 1.2700 g
Correction Type: None
Show Neg. Int: Yes

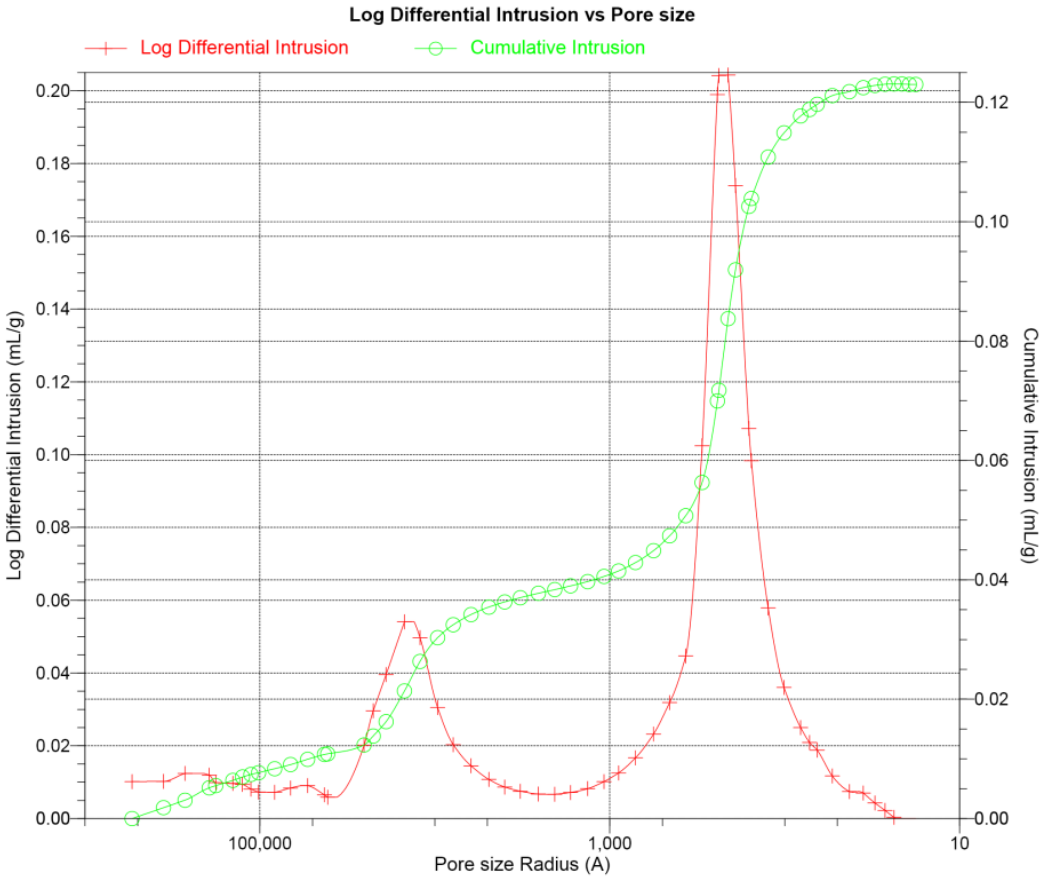

Figure A.6: Log Differential Intrusion vs Pore Size (G60K40)

Geotechnical Research Centre - Poresize Analysis

Sample ID: 40%-center-f
Operator: sarakarimi
Submitter: dr.yanful
File: C:\9500\DATA\FCENTERB.SMP

LP Analysis Time: 11/20/2012 3:56:19PM
HP Analysis Time: 11/20/2012 5:01:45PM
Report Time: 11/20/2012 5:37:53PM

Sample Weight: 1.4600 g
Correction Type: None
Show Neg. Int: Yes

Summary Report

Penetrometer parameters

Penetrometer:	13-00570606 3 ml, 0.39, Solid				
Pen. Constant:	11.007	µL/pF	Pen. Weight:	61.7500	g
Stem Volume:	0.3900	mL	Max. Head Pressure:	4.6800	psia
Pen. Volume:	3.3900	mL	Assembly Weight:	101.3400	g

Hg Parameters

Adv. Contact Angle:	140.000	degrees	Rec. Contact Angle:	140.000	degrees
Hg Surface Tension:	480.000	dynes/cm	Hg Density:	13.5369	g/mL

User Parameters

Param 1:	0.000	Param 2:	0.000	Param 3:	0.000

Low Pressure:

Evacuation Pressure:	50	µmHg
Evacuation Time:	5	mins
Mercury Filling Pressure:	1.98	psia
Equilibration Time:	10	secs
Maximum Intrusion Volume:	0.010	mL/g

High Pressure:

Equilibration Time:	10	secs
Maximum Intrusion Volume:	0.010	mL/g

No Blank Correction

Intrusion Data Summary

Total Intrusion Volume =	0.1087	mL/g
Total Pore Area =	9.827	m²/g
Median Pore Diameter (Volume) =	0.0479	µm
Median Pore Diameter (Area) =	0.0322	µm
Average Pore Diameter (4V/A) =	0.0443	µm
Bulk Density at 1.98 psia =	2.5469	g/mL
Apparent (skeletal) Density =	3.5225	g/mL
Porosity =	27.6963	%
Stem Volume Used =	42	%

Pore Structure Summary

Threshold Pressure:	71.91	psia (Calculated)
Characteristic length =	2.9665	µm
Conductivity formation factor =	0.047	
Permeability constant =	0.00442	
Permeability =	1.8421	mdarcy
BET Surface Area =	200.0000	m²/g
Pore shape exponent =	1.00	
Tortuosity factor =	1.917	
Tortuosity =	16.6918	
Percolation Fractal dimension =	2.645	
Backbone Fractal dimension =	N/A	

Mayer Stowe Summary

Interstitial porosity =	27.6963	%
Breakthrough pressure ratio =	9.1062	

Sample ID: 40%-center-f
Operator: sarakarimi
Submitter: dr.yanful
File: C:\9500\DATA\FCENTERB.SMP

LP Analysis Time: 11/20/2012 3:56:19PM
HP Analysis Time: 11/20/2012 5:01:45PM
Report Time: 11/20/2012 5:37:53PM

Sample Weight: 1.4600 g
Correction Type: None
Show Neg. Int: Yes

Material Compressibility

Linear Coefficient = -2.3890e-05 1/psia
Quadratic Coefficient = 3.3179e-10 1/psia²

Sample ID: 40%-center-f
Operator: sarakarimi
Submitter: dr.yanful
File: C:\9500\DATA\FCENTERB.SMP

LP Analysis Time: 11/20/2012 3:56:19PM
HP Analysis Time: 11/20/2012 5:01:45PM
Report Time: 11/20/2012 5:37:53PM

Sample Weight: 1.4600 g
Correction Type: None
Show Neg. Int: Yes

Tabular Report

Pore Diameter (µm)	Mean Diameter (µm)	Incremental Pore Volume (mL/g)	% Incremental Intrusion Volume	Mayer-Stowe Cumulative Volume finer % (%)	Cumulative Pore Area (m^2/g)
107.6369	107.6369	0.0000	0.0000	100.0000	0.000
71.3234	89.4802	0.0007	0.6064	99.3936	0.000
53.6173	62.4704	0.0005	0.4245	98.9691	0.000
38.9263	46.2718	0.0004	0.4124	98.5567	0.000
35.7179	37.3221	0.0001	0.0728	98.4840	0.000
28.5566	32.1372	0.0004	0.3638	98.1201	0.000
25.1944	26.8755	0.0002	0.1698	97.9503	0.000
22.5386	23.8665	0.0002	0.1455	97.8048	0.000
20.3918	21.4652	0.0002	0.1698	97.6350	0.000
16.4652	18.4285	0.0003	0.2426	97.3924	0.000
13.3525	14.9089	0.0003	0.2789	97.1135	0.000
10.6840	12.0183	0.0003	0.2547	96.8588	0.000
8.5438	9.6139	0.0005	0.4366	96.4222	0.001
8.0560	8.2999	0.0000	0.0226	96.3996	0.001
4.7320	6.3940	0.0006	0.5823	95.8173	0.001
4.6575	4.6948	0.0001	0.0889	95.7284	0.001
3.7253	4.1914	0.0016	1.4796	94.2488	0.003
2.9331	3.3292	0.0044	4.0519	90.1969	0.008
2.4456	2.6894	0.0033	3.0165	87.1804	0.013
1.8948	2.1702	0.0030	2.7713	84.4090	0.018
1.5653	1.7301	0.0017	1.5449	82.8641	0.022
1.2431	1.4042	0.0015	1.3522	81.5119	0.026
0.9845	1.1138	0.0012	1.0800	80.4319	0.031
0.7971	0.8908	0.0008	0.7756	79.6563	0.035
0.6527	0.7249	0.0007	0.6805	78.9758	0.039
0.5111	0.5819	0.0008	0.7163	78.2595	0.044
0.4130	0.4621	0.0007	0.6241	77.6353	0.050
0.3344	0.3737	0.0007	0.6272	77.0082	0.057
0.2677	0.3010	0.0008	0.7183	76.2898	0.067
0.2160	0.2418	0.0009	0.8222	75.4676	0.082
0.1783	0.1971	0.0009	0.8714	74.5963	0.102
0.1425	0.1604	0.0014	1.3145	73.2818	0.137
0.1125	0.1275	0.0020	1.8401	71.4417	0.200
0.0910	0.1017	0.0024	2.2206	69.2211	0.295
0.0737	0.0823	0.0033	3.0498	66.1714	0.456
0.0594	0.0665	0.0051	4.6916	61.4797	0.763
0.0480	0.0537	0.0124	11.3830	50.0968	1.685
0.0476	0.0478	0.0006	0.5523	49.5445	1.736
0.0420	0.0448	0.0117	10.7308	38.8137	2.777
0.0382	0.0401	0.0086	7.9097	30.9040	3.635
0.0325	0.0354	0.0107	9.8818	21.0222	4.850
0.0310	0.0318	0.0022	2.0374	18.9848	5.129
0.0249	0.0279	0.0076	6.9910	11.9937	6.218
0.0202	0.0225	0.0043	3.9799	8.0138	6.987
0.0162	0.0182	0.0030	2.7458	5.2681	7.644
0.0144	0.0153	0.0012	1.0745	4.1936	7.949

Sample ID: 40%-center-f
Operator: sarakarimi
Submitter: dr.yanful
File: C:\9500\DATA\FCENTERB.SMP

LP Analysis Time: 11/20/2012 3:56:19PM
HP Analysis Time: 11/20/2012 5:01:45PM
Report Time: 11/20/2012 5:37:53PM

Sample Weight: 1.4600 g
Correction Type: None
Show Neg. Int: Yes

Tabular Report

Pore Diameter (µm)	Mean Diameter (µm)	Incremental Pore Volume (mL/g)	% Incremental Intrusion Volume	Mayer-Stowe Cumulative Volume finer % (%)	Cumulative Pore Area (m^2/g)
0.0130	0.0137	0.0009	0.8266	3.3669	8.211
0.0107	0.0119	0.0017	1.5812	1.7857	8.792
0.0085	0.0096	0.0006	0.5346	1.2511	9.034
0.0071	0.0078	0.0007	0.6286	0.6226	9.383
0.0061	0.0066	0.0004	0.3485	0.2740	9.613
0.0053	0.0057	0.0002	0.1902	0.0838	9.757
0.0047	0.0050	0.0001	0.0973	-0.0135	9.841
0.0043	0.0045	-0.0000	-0.0028	-0.0108	9.839
0.0039	0.0041	-0.0000	-0.0058	-0.0049	9.833
0.0036	0.0037	-0.0000	-0.0049	0.0000	9.827
0.0046	0.0041	0.0009	0.8571	-0.8571	10.738
0.0060	0.0053	0.0007	0.6840	-1.5411	11.297
0.0078	0.0069	0.0005	0.4419	-1.9830	11.575
0.0102	0.0090	0.0002	0.1884	-2.1714	11.667
0.0133	0.0117	-0.0001	-0.0784	-2.0930	11.638
0.0172	0.0153	-0.0003	-0.3205	-1.7725	11.546
0.0222	0.0197	-0.0007	-0.5983	-1.1742	11.414
0.0292	0.0257	-0.0010	-0.9460	-0.2281	11.254
0.0373	0.0332	-0.0012	-1.1325	0.9043	11.106
0.0495	0.0434	-0.0018	-1.6725	2.5768	10.938
0.0646	0.0570	-0.0023	-2.1004	4.6772	10.778
0.0819	0.0733	-0.0024	-2.1882	6.8654	10.648
0.1065	0.0942	-0.0031	-2.8913	9.7566	10.515
0.1420	0.1243	-0.0041	-3.7939	13.5505	10.382
0.1776	0.1598	-0.0039	-3.5910	17.1415	10.284
0.2367	0.2071	-0.0056	-5.1498	22.2913	10.176
0.3042	0.2704	-0.0056	-5.1178	27.4091	10.094
0.4249	0.3645	-0.0073	-6.7063	34.1153	10.014
0.5311	0.4780	-0.0047	-4.3014	38.4167	9.974
0.7064	0.6188	-0.0047	-4.3243	42.7411	9.944
0.8847	0.7956	-0.0028	-2.6119	45.3529	9.930
1.1085	0.9966	-0.0022	-2.0592	47.4121	9.921
1.4464	1.2774	-0.0017	-1.5849	48.9970	9.915
1.8945	1.6704	-0.0012	-1.0838	50.0808	9.913
2.4443	2.1694	-0.0007	-0.6803	50.7610	9.911
3.1477	2.7960	-0.0005	-0.4761	51.2371	9.910
4.0523	3.6000	-0.0004	-0.3711	51.6082	9.910
6.5411	5.2967	-0.0004	-0.4125	52.0207	9.910

Geotechnical Research Centre - Poresize Analysis

AutoPore IV 9500 V1.07 Serial: 689 Port: 1/1 Page 5

Sample ID: 40%-center-f
Operator: sarakarimi
Submitter: dr.yanful
File: C:\9500\DATA\FCENTERB.SMP

LP Analysis Time: 11/20/2012 3:56:19PM
HP Analysis Time: 11/20/2012 5:01:45PM
Report Time: 11/20/2012 5:37:53PM

Sample Weight: 1.4600 g
Correction Type: None
Show Neg. Int: Yes

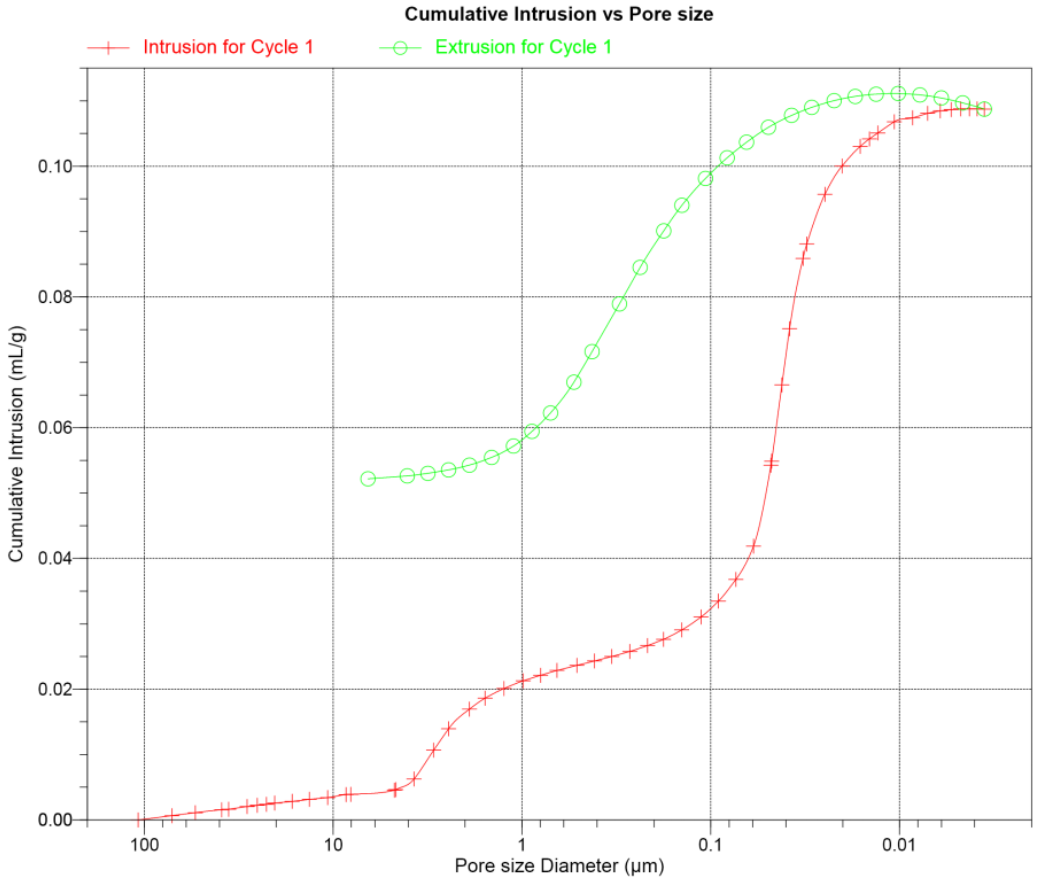

Figure A.7: Cumulative Intrusion vs Pore Size (G60K40-Final)

Geotechnical Research Centre - Poresize Analysis

AutoPore IV 9500 V1.07 Serial: 689 Port: 1/1 Page 6

Sample ID: 40%-center-f
Operator: sarakarimi
Submitter: dr.yanful
File: C:\9500\DATA\FCENTERB.SMP

LP Analysis Time: 11/20/2012 3:56:19PM
HP Analysis Time: 11/20/2012 5:01:45PM
Report Time: 11/20/2012 5:37:53PM

Sample Weight: 1.4600 g
Correction Type: None
Show Neg. Int: Yes

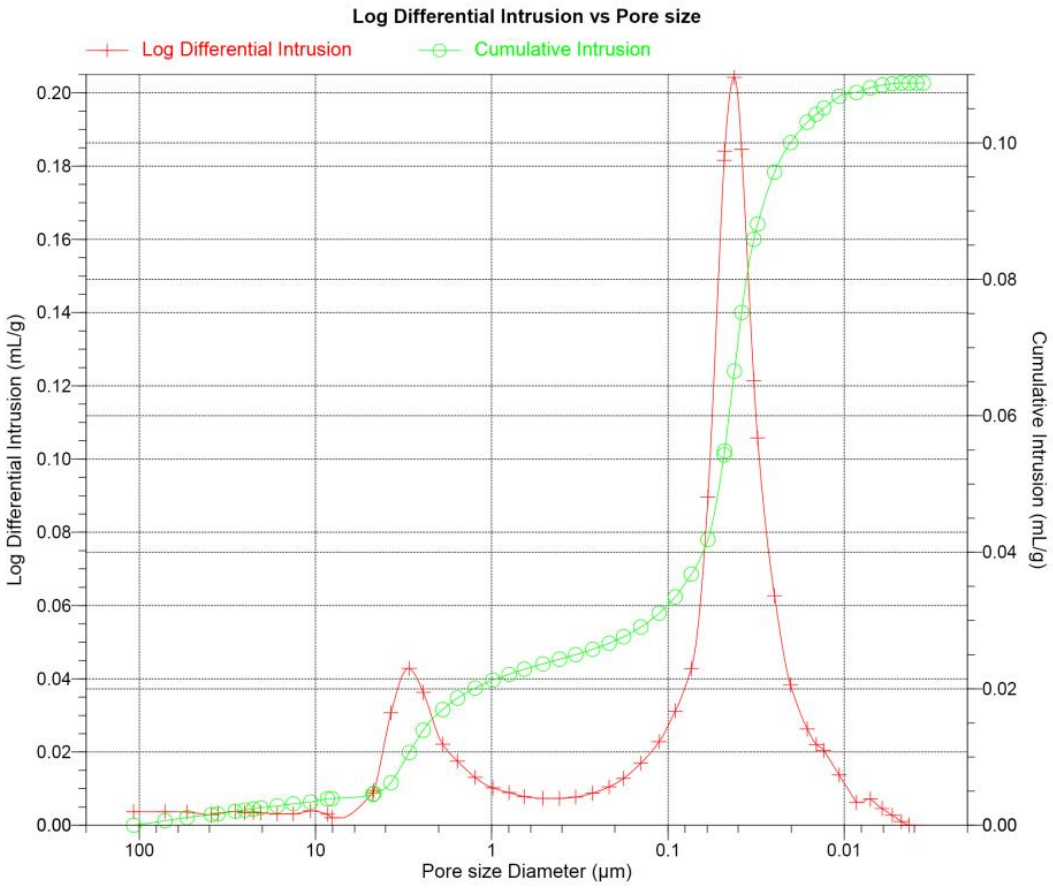

Figure A.8: Log Differential Intrusion vs Pore Size (G60K40-Final)

Geotechnical Research Centre - Poresize Analysis

Sample ID: 50%-center
Operator: sara karimi
Submitter: Dr.Yanful
File: C:\9500\DATA\50%-MIP.SMP

LP Analysis Time: 11/6/2012 7:45:46PM
HP Analysis Time: 11/6/2012 8:31:57PM
Report Time: 11/6/2012 8:34:45PM

Sample Weight: 1.2000 g
Correction Type: None
Show Neg. Int: Yes

Summary Report

Penetrometer parameters

Penetrometer:	13-00570606 3 ml, 0.39, Solid				
Pen. Constant:	11.007	µL/pF	Pen. Weight:	61.9800	g
Stem Volume:	0.3900	mL	Max. Head Pressure:	4.6800	psia
Pen. Volume:	3.3900	mL	Assembly Weight:	102.6600	g

Hg Parameters

Adv. Contact Angle:	140.000	degrees	Rec. Contact Angle:	140.000	degrees
Hg Surface Tension:	480.000	dynes/cm	Hg Density:	13.5369	g/mL

User Parameters

Param 1:	0.000	Param 2:	0.000	Param 3:	0.000

Low Pressure:

Evacuation Pressure:	50	µmHg
Evacuation Time:	5	mins
Mercury Filling Pressure:	1.98	psia
Equilibration Time:	10	secs
Maximum Intrusion Volume:	0.010	mL/g

High Pressure:

Equilibration Time:	10	secs
Maximum Intrusion Volume:	0.010	mL/g

No Blank Correction

Intrusion Data Summary

Total Intrusion Volume =	0.1379	mL/g
Total Pore Area =	12.179	m²/g
Median Pore Radius (Volume) =	246	A
Median Pore Radius (Area) =	170	A
Average Pore Radius (2V/A) =	226	A
Bulk Density at 1.98 psia =	2.5342	g/mL
Apparent (skeletal) Density =	3.8955	g/mL
Porosity =	34.9459	%
Stem Volume Used =	43	%

Pore Structure Summary

Threshold Pressure:	18.37	psia (Calculated)
Characteristic length =	58053	A
Conductivity formation factor =	0.029	
Permeability constant =	0.00442	
Permeability =	17.0785	mdarcy
BET Surface Area =	200.0000	m²/g
Pore shape exponent =	1.00	
Tortuosity factor =	1.835	
Tortuosity =	9.5042	
Percolation Fractal dimension =	2.622	
Backbone Fractal dimension =	N/A	

Mayer Stowe Summary

Interstitial porosity =	34.9459	%
Breakthrough pressure ratio =	6.6658	

Sample ID: 50%-center
Operator: sara karimi
Submitter: Dr.Yanful
File: C:\9500\DATA\50%-MIP.SMP

LP Analysis Time: 11/6/2012 7:45:46PM
HP Analysis Time: 11/6/2012 8:31:57PM
Report Time: 11/6/2012 8:34:45PM

Sample Weight: 1.2000 g
Correction Type: None
Show Neg. Int: Yes

Material Compressibility

Linear Coefficient = -3.3492e-05 1/psia
Quadratic Coefficient = 4.6934e-10 1/psia²

Geotechnical Research Centre - Poresize Analysis

Sample ID: 50%-center
Operator: sara karimi
Submitter: Dr.Yanful
File: C:\9500\DATA\50%-MIP.SMP

LP Analysis Time: 11/6/2012 7:45:46PM
HP Analysis Time: 11/6/2012 8:31:57PM
Report Time: 11/6/2012 8:34:45PM

Sample Weight: 1.2000 g
Correction Type: None
Show Neg. Int: Yes

Tabular Report

Pore Radius (A)	Mean Radius (A)	Incremental Pore Volume (mL/g)	% Incremental Intrusion Volume	Mayer-Stowe Cumulative Volume finer % (%)	Cumulative Pore Area (m^2/g)
537773	537773	0.0000	0.0000	100.0000	0.000
356035	446904	0.0020	1.4313	98.5687	0.000
268335	312185	0.0016	1.1869	97.3818	0.000
194708	231522	0.0015	1.0938	96.2879	0.000
178461	186584	0.0003	0.2327	96.0552	0.000
142765	160613	0.0009	0.6284	95.4268	0.000
125981	134373	0.0004	0.2909	95.1359	0.001
112663	119322	0.0004	0.3142	94.8217	0.001
101944	107304	0.0003	0.2095	94.6123	0.001
82330	92137	0.0006	0.4422	94.1701	0.001
66869	74600	0.0005	0.3840	93.7860	0.001
53422	60145	0.0007	0.4887	93.2973	0.001
42713	48067	0.0006	0.4538	92.8435	0.001
39677	41195	0.0001	0.0575	92.7860	0.001
24910	32294	0.0004	0.2860	92.5000	0.002
22750	23830	0.0003	0.2072	92.2928	0.002
18824	20787	0.0017	1.2283	91.0646	0.004
14871	16847	0.0023	1.6535	89.4110	0.006
12242	13557	0.0021	1.5291	87.8819	0.009
9506	10874	0.0029	2.0863	85.7957	0.015
7812	8659	0.0019	1.3929	84.4027	0.019
6190	7001	0.0019	1.3732	83.0295	0.025
4880	5535	0.0015	1.0866	81.9429	0.030
3958	4419	0.0010	0.7255	81.2174	0.034
3253	3605	0.0008	0.5685	80.6489	0.039
2549	2901	0.0009	0.6212	80.0277	0.045
2056	2303	0.0007	0.5257	79.5020	0.051
1675	1865	0.0007	0.4945	79.0074	0.058
1338	1506	0.0009	0.6471	78.3603	0.070
1079	1208	0.0010	0.7545	77.6058	0.087
891	985	0.0012	0.8498	76.7560	0.111
713	802	0.0018	1.3292	75.4269	0.157
562	637	0.0026	1.9042	73.5227	0.239
455	509	0.0033	2.3859	71.1368	0.369
369	412	0.0046	3.3032	67.8336	0.590
297	333	0.0080	5.7843	62.0493	1.070
252	274	0.0133	9.6749	52.3745	2.042
238	245	0.0080	5.7658	46.6086	2.692
216	227	0.0125	9.0734	37.5353	3.795
193	204	0.0122	8.8425	28.6927	4.989
191	192	0.0009	0.6847	28.0081	5.087
165	178	0.0108	7.8653	20.1428	6.305
155	160	0.0035	2.5148	17.6279	6.738
124	140	0.0088	6.4046	11.2234	8.003
101	113	0.0052	3.7944	7.4290	8.933
81	91	0.0035	2.5135	4.9154	9.696

Sample ID: 50%-center
Operator: sara karimi
Submitter: Dr.Yanful
File: C:\9500\DATA\50%-MIP.SMP

LP Analysis Time: 11/6/2012 7:45:46PM
HP Analysis Time: 11/6/2012 8:31:57PM
Report Time: 11/6/2012 8:34:45PM

Sample Weight: 1.2000 g
Correction Type: None
Show Neg. Int: Yes

Tabular Report

Pore Radius (A)	Mean Radius (A)	Incremental Pore Volume (mL/g)	% Incremental Intrusion Volume	Mayer-Stowe Cumulative Volume finer % (%)	Cumulative Pore Area (m^2/g)
72	77	0.0014	1.0349	3.8805	10.068
65	69	0.0011	0.7730	3.1076	10.379
53	59	0.0017	1.2227	1.8849	10.948
43	48	0.0013	0.9230	0.9619	11.478
36	39	0.0007	0.5436	0.4183	11.861
30	33	0.0006	0.4252	-0.0069	12.216
27	29	0.0000	0.0158	-0.0227	12.232
24	25	0.0001	0.0682	-0.0909	12.306
21	23	0.0000	0.0190	-0.1100	12.330
19	20	-0.0001	-0.0964	-0.0136	12.199
18	19	-0.0000	-0.0136	-0.0000	12.179
23	20	0.0013	0.9279	-0.9279	13.430
30	27	0.0010	0.6932	-1.6211	14.149
39	35	0.0006	0.4468	-2.0678	14.505
51	45	0.0003	0.2198	-2.2877	14.640
67	59	-0.0000	-0.0345	-2.2532	14.624
86	76	-0.0004	-0.2754	-1.9778	14.524
111	98	-0.0007	-0.5015	-1.4764	14.384
146	128	-0.0011	-0.8077	-0.6687	14.210
187	166	-0.0014	-0.9900	0.3213	14.046
247	217	-0.0020	-1.4722	1.7936	13.859
323	285	-0.0025	-1.8047	3.5983	13.685
410	366	-0.0026	-1.8957	5.4940	13.542
533	471	-0.0035	-2.5207	8.0147	13.394
711	622	-0.0046	-3.3637	11.3784	13.245
888	799	-0.0047	-3.3970	14.7753	13.128
1183	1036	-0.0069	-4.9964	19.7718	12.995
1520	1351	-0.0076	-5.5298	25.3016	12.882
2087	1804	-0.0127	-9.2438	34.5454	12.741
2122	2105	-0.0016	-1.1959	35.7414	12.725
2647	2385	-0.0055	-3.9576	39.6990	12.679
3532	3090	-0.0074	-5.3382	45.0372	12.631
4402	3967	-0.0045	-3.2516	48.2888	12.609
5553	4977	-0.0030	-2.1858	50.4746	12.597
7303	6428	-0.0018	-1.3144	51.7890	12.591
9502	8403	-0.0009	-0.6777	52.4667	12.589
12122	10812	-0.0006	-0.4403	52.9070	12.588
16135	14129	-0.0004	-0.3262	53.2332	12.587
20388	18262	-0.0003	-0.2150	53.4482	12.587
31971	26179	-0.0003	-0.2183	53.6665	12.587

Geotechnical Research Centre - Poresize Analysis

AutoPore IV 9500 V1.07 Serial: 689 Port: 1/1 Page 5

Sample ID: 50%-center
Operator: sara karimi
Submitter: Dr.Yanful
File: C:\9500\DATA\50%-MIP.SMP

LP Analysis Time: 11/6/2012 7:45:46PM
HP Analysis Time: 11/6/2012 8:31:57PM
Report Time: 11/6/2012 8:34:45PM

Sample Weight: 1.2000 g
Correction Type: None
Show Neg. Int: Yes

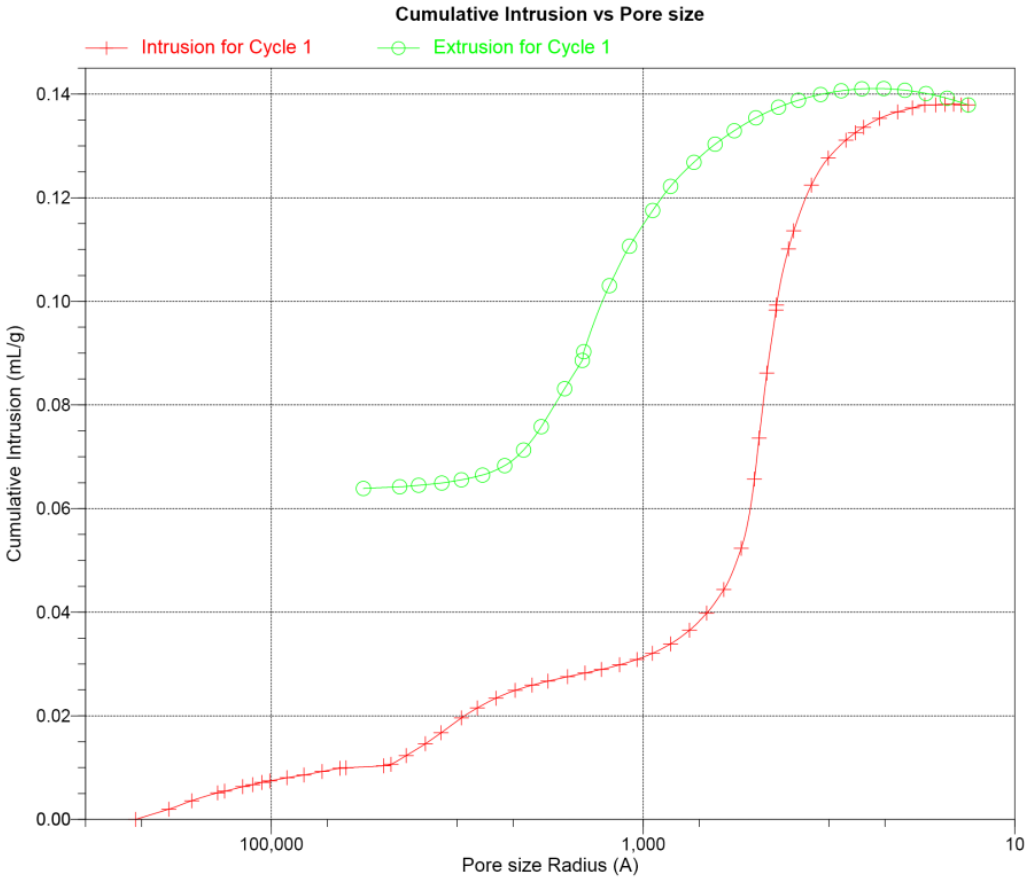

Figure A.9: Cumulative Intrusion vs Pore Size (G50K50)

Geotechnical Research Centre - Poresize Analysis

AutoPore IV 9500 V1.07 Serial: 689 Port: 1/1 Page 6

Sample ID: 50%-center
Operator: sara karimi
Submitter: Dr.Yanful
File: C:\9500\DATA\50%-MIP.SMP

LP Analysis Time: 11/6/2012 7:45:46PM
HP Analysis Time: 11/6/2012 8:31:57PM
Report Time: 11/6/2012 8:34:45PM

Sample Weight: 1.2000 g
Correction Type: None
Show Neg. Int: Yes

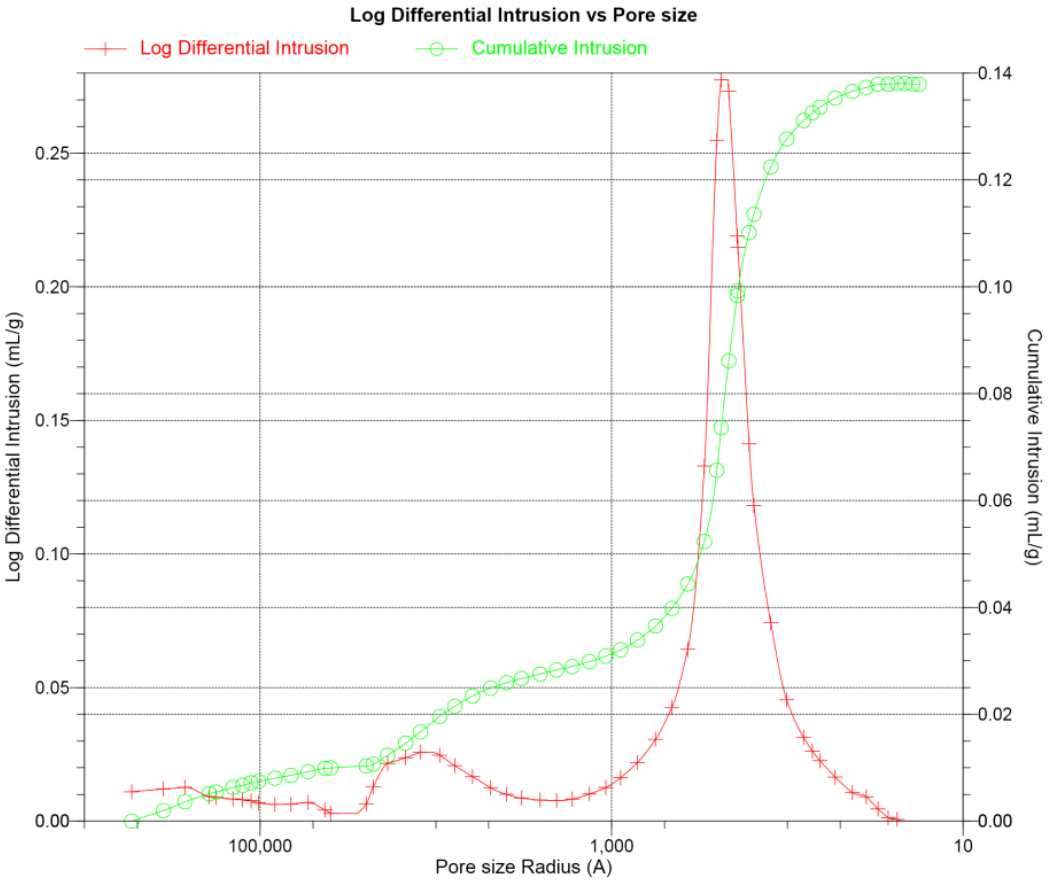

Figure A.10: Log Differential Intrusion vs Pore Size (G50K50)

Geotechnical Research Centre - Poresize Analysis

Sample ID: 50%-center-f
Operator: sarakarimi
Submitter: dr.yanful
File: C:\9500\DATA\FCENTERC.SMP

LP Analysis Time: 11/20/2012 6:32:51PM
HP Analysis Time: 11/20/2012 7:33:14PM
Report Time: 11/20/2012 7:56:19PM

Sample Weight: 1.4500 g
Correction Type: None
Show Neg. Int: Yes

Summary Report

Penetrometer parameters

Penetrometer:	13-00570606 3 ml, 0.39, Solid				
Pen. Constant:	11.007	µL/pF	Pen. Weight:	61.7300	g
Stem Volume:	0.3900	mL	Max. Head Pressure:	4.6800	psia
Pen. Volume:	3.3900	mL	Assembly Weight:	101.1400	g

Hg Parameters

Adv. Contact Angle:	140.000	degrees	Rec. Contact Angle:	140.000	degrees
Hg Surface Tension:	480.000	dynes/cm	Hg Density:	13.5369	g/mL

User Parameters

Param 1:	0.000	Param 2:	0.000	Param 3:	0.000

Low Pressure:

Evacuation Pressure:	50	µmHg
Evacuation Time:	5	mins
Mercury Filling Pressure:	1.98	psia
Equilibration Time:	10	secs
Maximum Intrusion Volume:	0.010	mL/g

High Pressure:

Equilibration Time:	10	secs
Maximum Intrusion Volume:	0.010	mL/g

No Blank Correction

Intrusion Data Summary

Total Intrusion Volume =	0.1239	mL/g
Total Pore Area =	12.461	m²/g
Median Pore Diameter (Volume) =	0.0455	µm
Median Pore Diameter (Area) =	0.0317	µm
Average Pore Diameter (4V/A) =	0.0398	µm
Bulk Density at 1.98 psia =	2.4752	g/mL
Apparent (skeletal) Density =	3.5702	g/mL
Porosity =	30.6709	%
Stem Volume Used =	47	%

Pore Structure Summary

Threshold Pressure:	99.09	psia (Calculated)
Characteristic length =	2.1528	µm
Conductivity formation factor =	0.029	
Permeability constant =	0.00442	
Permeability =	0.6011	mdarcy
BET Surface Area =	200.0000	m²/g
Pore shape exponent =	1.00	
Tortuosity factor =	1.883	
Tortuosity =	23.3483	
Percolation Fractal dimension =	2.535	
Backbone Fractal dimension =	N/A	

Mayer Stowe Summary

Interstitial porosity =	30.6709	%
Breakthrough pressure ratio =	8.4402	

Sample ID: 50%-center-f
Operator: sarakarimi
Submitter: dr.yanful
File: C:\9500\DATA\FCENTERC.SMP

LP Analysis Time: 11/20/2012 6:32:51PM
HP Analysis Time: 11/20/2012 7:33:14PM
Report Time: 11/20/2012 7:56:19PM

Sample Weight: 1.4500 g
Correction Type: None
Show Neg. Int: Yes

Material Compressibility

Linear Coefficient = -2.8744e-05 1/psia
Quadratic Coefficient = 3.9917e-10 1/psia²

Sample ID: 50%-center-f
Operator: sarakarimi
Submitter: dr.yanful
File: C:\9500\DATA\FCENTERC.SMP

LP Analysis Time: 11/20/2012 6:32:51PM
HP Analysis Time: 11/20/2012 7:33:14PM
Report Time: 11/20/2012 7:56:19PM

Sample Weight: 1.4500 g
Correction Type: None
Show Neg. Int: Yes

Tabular Report

Pore Diameter (µm)	Mean Diameter (µm)	Incremental Pore Volume (mL/g)	% Incremental Intrusion Volume	Mayer-Stowe Cumulative Volume finer % (%)	Cumulative Pore Area (m^2/g)
107.5517	107.5517	0.0000	0.0000	100.0000	0.000
71.3219	89.4368	0.0005	0.3965	99.6035	0.000
53.6625	62.4922	0.0003	0.2679	99.3355	0.000
38.9544	46.3084	0.0003	0.2036	99.1319	0.000
35.7096	37.3320	0.0001	0.0429	99.0890	0.000
28.5526	32.1311	0.0001	0.1072	98.9819	0.000
25.1909	26.8718	0.0001	0.0643	98.9176	0.000
22.5339	23.8624	0.0001	0.0536	98.8640	0.000
20.3889	21.4614	0.0001	0.0536	98.8104	0.000
16.4636	18.4263	0.0001	0.1072	98.7032	0.000
13.3497	14.9067	0.0001	0.0965	98.6068	0.000
10.6845	12.0171	0.0002	0.1393	98.4674	0.000
8.5494	9.6170	0.0001	0.1179	98.3495	0.000
8.0399	8.2947	0.0001	0.0477	98.3019	0.000
4.7325	6.3862	0.0002	0.2014	98.1004	0.000
4.5571	4.6448	0.0000	0.0210	98.0795	0.001
3.7467	4.1519	0.0002	0.1643	97.9152	0.001
2.9672	3.3570	0.0004	0.3419	97.5733	0.001
2.4433	2.7052	0.0014	1.1563	96.4170	0.003
1.9032	2.1733	0.0039	3.1835	93.2335	0.011
1.5566	1.7299	0.0026	2.1278	91.1058	0.017
1.2412	1.3989	0.0021	1.7063	89.3995	0.023
0.9816	1.1114	0.0016	1.2524	88.1471	0.028
0.7968	0.8892	0.0010	0.8402	87.3069	0.033
0.6521	0.7244	0.0008	0.6848	86.6221	0.038
0.5102	0.5812	0.0009	0.7394	85.8827	0.044
0.4128	0.4615	0.0007	0.6010	85.2818	0.050
0.3349	0.3739	0.0008	0.6280	84.6537	0.059
0.2672	0.3010	0.0009	0.7525	83.9012	0.071
0.2159	0.2415	0.0011	0.8743	83.0270	0.089
0.1780	0.1969	0.0012	0.9592	82.0678	0.113
0.1425	0.1602	0.0018	1.4830	80.5848	0.159
0.1125	0.1275	0.0026	2.0674	78.5174	0.240
0.0909	0.1017	0.0031	2.5247	75.9927	0.363
0.0737	0.0823	0.0042	3.3662	72.6265	0.565
0.0594	0.0665	0.0064	5.1341	67.4923	0.948
0.0487	0.0540	0.0141	11.3748	56.1175	1.991
0.0476	0.0482	0.0024	1.9135	54.2040	2.188
0.0429	0.0452	0.0125	10.0814	44.1226	3.293
0.0388	0.0409	0.0113	9.1239	34.9986	4.399
0.0382	0.0385	0.0017	1.3431	33.6555	4.572
0.0336	0.0359	0.0110	8.8879	24.7676	5.799
0.0310	0.0323	0.0048	3.8957	20.8718	6.397
0.0249	0.0279	0.0094	7.5997	13.2722	7.746
0.0202	0.0225	0.0053	4.2665	9.0056	8.685
0.0162	0.0182	0.0038	3.0295	5.9762	9.512

Sample ID: 50%-center-f
Operator: sarakarimi
Submitter: dr.yanful
File: C:\9500\DATA\FCENTERC.SMP

LP Analysis Time: 11/20/2012 6:32:51PM
HP Analysis Time: 11/20/2012 7:33:14PM
Report Time: 11/20/2012 7:56:19PM

Sample Weight: 1.4500 g
Correction Type: None
Show Neg. Int: Yes

Tabular Report

Pore Diameter (µm)	Mean Diameter (µm)	Incremental Pore Volume (mL/g)	% Incremental Intrusion Volume	Mayer-Stowe Cumulative Volume finer % (%)	Cumulative Pore Area (m²/g)
0.0144	0.0153	0.0014	1.1578	4.8183	9.886
0.0130	0.0137	0.0011	0.8885	3.9299	10.207
0.0107	0.0119	0.0017	1.3556	2.5742	10.774
0.0085	0.0096	0.0014	1.1174	1.4568	11.350
0.0071	0.0078	0.0008	0.6212	0.8356	11.744
0.0061	0.0066	0.0005	0.3874	0.4481	12.035
0.0053	0.0057	0.0003	0.2175	0.2307	12.223
0.0047	0.0050	0.0002	0.1499	0.0808	12.371
0.0043	0.0045	0.0001	0.0438	0.0370	12.419
0.0039	0.0041	0.0001	0.0613	-0.0243	12.494
0.0036	0.0037	-0.0000	-0.0243	-0.0000	12.461
0.0046	0.0041	0.0008	0.6640	-0.6640	13.265
0.0060	0.0053	0.0007	0.5728	-1.2368	13.799
0.0078	0.0069	0.0004	0.3630	-1.5998	14.060
0.0102	0.0090	0.0001	0.1168	-1.7166	14.124
0.0133	0.0117	-0.0003	-0.2637	-1.4529	14.013
0.0172	0.0153	-0.0004	-0.2950	-1.1579	13.917
0.0222	0.0197	-0.0008	-0.6704	-0.4875	13.748
0.0292	0.0257	-0.0013	-1.0736	0.5861	13.541
0.0373	0.0333	-0.0016	-1.2916	1.8777	13.348
0.0495	0.0434	-0.0024	-1.9069	3.7846	13.131
0.0646	0.0570	-0.0029	-2.3041	6.0887	12.931
0.0820	0.0733	-0.0030	-2.4171	8.5059	12.767
0.1066	0.0943	-0.0039	-3.1829	11.6887	12.600
0.1421	0.1243	-0.0051	-4.1315	15.8203	12.435
0.1775	0.1598	-0.0047	-3.7890	19.6092	12.317
0.2374	0.2074	-0.0068	-5.5196	25.1288	12.186
0.3039	0.2706	-0.0066	-5.3629	30.4917	12.087
0.4255	0.3647	-0.0091	-7.3529	37.8446	11.987
0.5321	0.4788	-0.0056	-4.5226	42.3672	11.941
0.7073	0.6197	-0.0059	-4.7370	47.1042	11.903
0.8784	0.7929	-0.0035	-2.8112	49.9153	11.885
1.1070	0.9927	-0.0027	-2.2027	52.1180	11.874
1.4506	1.2788	-0.0022	-1.7397	53.8577	11.867
1.9011	1.6759	-0.0014	-1.1260	54.9837	11.864
2.4404	2.1708	-0.0008	-0.6627	55.6464	11.862
3.1482	2.7943	-0.0006	-0.4852	56.1317	11.862
4.0353	3.5917	-0.0004	-0.3550	56.4867	11.861
6.5243	5.2798	-0.0005	-0.4113	56.8980	11.861

Geotechnical Research Centre - Poresize Analysis

AutoPore IV 9500 V1.07 Serial: 689 Port: 1/1 Page 5

Sample ID: 50%-center-f
Operator: sarakarimi
Submitter: dr.yanful
File: C:\9500\DATA\FCENTERC.SMP

LP Analysis Time: 11/20/2012 6:32:51PM
HP Analysis Time: 11/20/2012 7:33:14PM
Report Time: 11/20/2012 7:56:19PM

Sample Weight: 1.4500 g
Correction Type: None
Show Neg. Int: Yes

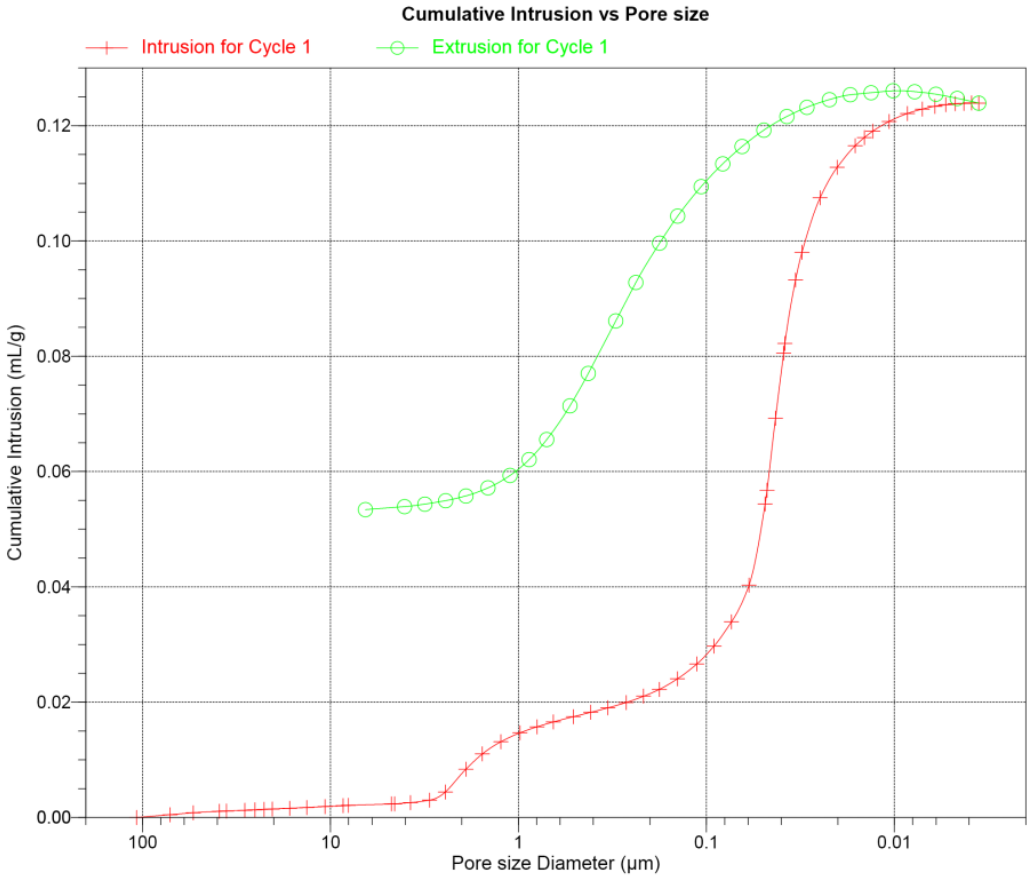

Figure A.11: Cumulative Intrusion vs Pore Size (G50K50-Final)

Geotechnical Research Centre - Poresize Analysis

AutoPore IV 9500 V1.07 Serial: 689 Port: 1/1 Page 6

Sample ID: 50%-center-f
Operator: sarakarimi
Submitter: dr.yanful
File: C:\9500\DATA\FCENTERC.SMP

LP Analysis Time: 11/20/2012 6:32:51PM
HP Analysis Time: 11/20/2012 7:33:14PM
Report Time: 11/20/2012 7:56:19PM

Sample Weight: 1.4500 g
Correction Type: None
Show Neg. Int: Yes

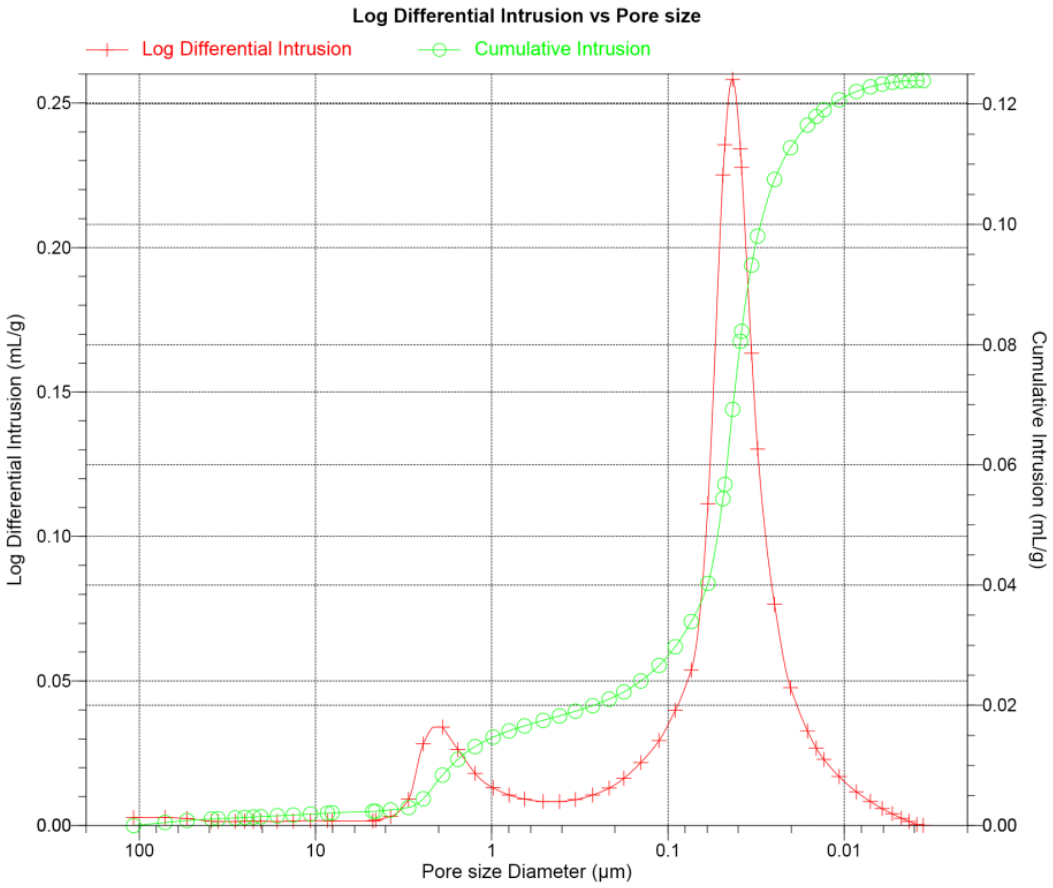

Figure A.12: Log Differential Intrusion vs Pore Size (G50K50-Final)

Sara Karimi

Career Objective

A highly talented, creative and motivated Civil Engineer with one year work experience, seeking for a junior level position in Geotechnical/Geoenvironmental Engineering with a reputed construction company

Employment History

Junior Civil Engineer **June 2009- August 2010**
Tablieh Construction Company (www.Tablieh.com), Tehran, Iran
Responsibilities:

- Gather timely and accurate progress data from subcontractors on a timely basis
- Writing weekly and monthly progress reports
- Preparing monthly oral presentation for client and consultant team
- Assisting project manager with typical project planning and scheduling tasks

Education

Master of Engineering Science- Geotechnical/Geoenvironmental Engineering
The University of Western Ontario, London, ON, Canada **September 2010- January 2013**

Bachelor of Engineering Science- Civil and Environmental Engineering
Amirkabir University of Technology, Tehran, Iran **September 2005-August 2009**

Skills

- Landfill design
- Shallow and deep foundation design
- Slope stability assessment
- Excellent POLLUTE knowledge
- Advance knowledge of geotechnical laboratory testing procedures
- Proficiency in AutoCAD
- Proven computer skills, MS office suits (Excel, PowerPoint, Word)
- Familiar with MS Project and Primavera
- Strong analytical skills
- Great skill in preparing reports and presentations
- Willing to take challenges and responsibility
- Ability and willingness to work on multiple projects and tasks
- Willing to travel

Graduate Courses

- ***Foundation Engineering:***

Design of foundation for all types of structures. Spread footings, raft and piled foundations, floated foundations, embankments with focus on methods of analysis, and their applications to real soil problems.

- ***Environmental Geotechnique:***

Geology, mineralogy, physico-chemistry and geotechnical properties of component soils. Erodibility of soils in relation to moisture content, mineralogy, climate and attack by moving water, mineral water interactions, multiphase flow, acid mine drainage, solution-mineral equilibrium, geochemical modeling.

- ***Groundwater Flow and Contaminant:***

Develop understanding of groundwater importance in the hydrologic cycle as well as understanding of the sources and characteristics of groundwater pollutants and applying scientific and engineering knowledge for contaminated site remediation design to meet specified needs and legislative.

- ***Water Quality and Treatment:***

Develops graduate level concepts for the examination of drinking water quality and discussion of state of art for treating drinking water, incorporates significant experimentation with the pilot plant at Walkerton Clean Water Center.

Academic Projects

Graduate:

- ***MEScThesis :*** Modelling of contaminant breakthrough curves through a landfill liner with POLLUTE and comparing the models with experimental results
- "Determination of clay minerals" ,Final project of Environmental geotechnique
- "Hydrogeology and simulation of ground water flow at superfund site in Woburn, Massachusetts", Final project of groundwater flow and contaminant transport
- "Designing compressor foundation for Amirkabir petrochemical complex in Iran" Final project of Foundation Engineering course

Undergraduate:

- Design of a 5-story reinforced concrete structure and a 8-story steel structure
- Loading analysis of a residential building
- Time history and respond spectrum analysis for a 8-story building in an earthquake

Certificates

- Technology demonstration hands-on training for operation of conventional treatment process (From Walkerton Clean Water Center)

References

References available on request